Infrastructure Scaling and Pricing

Fikret Caner Göçmen

Submitted in partial fulfillment of the
requirements for the degree of
Doctor of Philosophy
under the Executive Committee
of the Graduate School of Arts and Sciences

COLUMBIA UNIVERSITY

2014

ABSTRACT

Infrastructure Scaling and Pricing

Fikret Caner Göçmen

Infrastructure systems play a crucial role in our daily lives. They include, but are not limited to, the highways we take while we commute to work, the stadiums we go to watch games, and the power plants that provide the electricity we consume in our homes. In this thesis we study infrastructure systems from several different perspectives with a focus on pricing and scalability. The pricing aspect of our research focuses on two industries: toll roads and sports events. Afterwards, we analyze the potential impact of small modular infrastructure on a wide variety of industries.

We start by analyzing the problem of determining the tolls that maximize revenue for a managed lane operator – that is, an operator who can charge a toll for the use of some lanes on a highway while a number of parallel lanes remain free to use. Managing toll lanes for profit is becoming increasingly common as private contractors agree to build additional lane capacity in return for the opportunity to retain toll revenue. We start by modeling the lanes as queues and show that the dynamic revenue-maximizing toll is always greater than or equal to the myopic toll that maximizes expected revenue from each arriving vehicle. Numerical examples show that a dynamic revenue-maximizing toll scheme can generate significantly more expected revenue than either a myopic or a static toll scheme. An important implication is that the revenue-maximizing fee does not only depend on the current state, but also on anticipated future arrivals. We discuss the managerial implications and present several numerical examples.

Next, we relax the queueing assumption and model traffic propagation on a highway realistically by using simulation. We devise a framework that can be used to obtain revenue maximizing tolls in such a context. We calibrate our framework by using data from the SR-91 Highway in Orange County, CA and explore different tolling schemes. Our numerical experiments suggest that simple

dynamic tolling mechanisms can lead to substantial revenue improvements over myopic and time-of-use tolling policies.

In the third part, we analyze the revenue management of consumer options for tournaments. Sporting event managers typically only offer advance tickets which guarantee a seat at a future sporting event in return for an upfront payment. Some event managers and ticket resellers have started to offer call options under which a customer can pay a small amount now for the guaranteed option to attend a future sporting event by paying an additional amount later. We consider the case of tournament options where the event manager sells team-specific options for a tournament final, such as the Super Bowl, before the finalists are determined. These options guarantee a final game ticket to the bearer if his team advances to the finals. We develop an approach by which an event manager can determine the revenue maximizing prices and amounts of advance tickets and options to sell for a tournament final. Afterwards, for a specific tournament structure we show that offering options is guaranteed to increase expected revenue for the event. We also establish bounds for the revenue improvement and show that introducing options can increase social welfare. We conclude by presenting a numerical application of our approach.

Finally, we argue that advances made in automation, communication and manufacturing portend a dramatic reversal of the "bigger is better" approach to cost reductions prevalent in many basic infrastructure industries, e.g. transportation, electric power generation and raw material processing. We show that the traditional reductions in capital costs achieved by scaling up in size are generally matched by learning effects in the mass-production process when scaling up in numbers instead. In addition, using the U.S. electricity generation sector as a case study, we argue that the primary operating cost advantage of large unit scale is reduced labor, which can be eliminated by employing low-cost automation technologies. Finally, we argue that locational, operational and financial flexibilities that accompany smaller unit scale can reduce investment and operating costs even further. All these factors combined argue that with current technology, economies of numbers may well dominate economies of unit scale.

Table of Contents

List of Figures

List of Tables

Acknowledgments

This thesis resulted from collaborations with my advisors Prof. Garrett van Ryzin and Prof. Robert Phillips, my committee members Prof. Guillermo Gallego and Prof. Klaus Lackner, and fellow graduate students Santiago Balseiro and Eric Dahlgren. I have learned a lot from their assistance and constructive feedback. Writing this thesis would not have been possible without them.

I would like to thank my thesis advisors Prof. Garrett van Ryzin and Prof. Robert Phillips in particular for their invaluable guidance and extreme patience. They have spent countless hours meeting with me and going over my work. I will always be indebted to them.

Professor Guillermo Gallego has played a key role in writing Chapter 4. Together with Professor Robert Phillips, he has helped transition this work from a class project into a full fledged thesis chapter.

I am very happy and fortunate to have worked with Professor Klaus Lackner on the material in Chapter 5. His deep understanding of the problem and the vision he provided were instrumental in the development of the material in this chapter.

I would like to thank Professor Omar Besbes for agreeing to be one of my committee members. Throughout my time in the PhD program he has been of extraordinary help with his constructive feedback. I would also like to thank him for reading my thesis in depth and providing valuable suggestions.

I am very fortunate to have worked with Santiago on the 4th chapter of this thesis. Together with his wife they have been much more than just friends.

Working with Eric Dahlgren on the material in Chapter 5 has been both fun and rewarding. He has put a great deal of effort into improving the chapter into its current shape.

I am very happy to have met Professor Nelson Fraiman during my time here. I have learned a

great deal from him both personally and professionally. He was always there to help whenever I needed his advice. I would also like to thank Prof. Awi Federgruen for his assistance in Chapter 2. He has graciously donated his time to answer my questions about Dynamic Programming.

I have made great memories on the fourth floor of Uris thanks to a special group of people. I am very lucky that my time in the PhD program has overlapped with Nikhil Bhat, Deniz Çiçek, Juan Manuel Chaneton, Davide Crapis, Daniel Guetta, Yonatan Gur, Damla Güneş, Yunru Han, Cinar Kılcıoğlu, Sang Won Kim, Lijian Lu, Yina Lu, Daniela Saban, Mehmet Sağlam, Serdar Şimsek, John Yao and Hua Zheng.

My time in New York would not have been this fun without my friends! I am extremely lucky to have met Gökçe Akın Aras, Korhan Aras, Burak Başkurt, Soner Bilge, Berk Birand, Zeynep Boğa, Semra Çomu, Ezgi Demirdağ, Cem Dilmegani, Gökhan Dündar, Anna Gleyzer, Neşet Güner, Hakan Hekimoğlu, Gökhan Karapınar, Erdem Kaya, Derya Koç, Cathleen Murphy, Noam Ophir, Burak Öcal, Pamir Özbay, Erinç Tokluoğlu, Aslıhan Tuncer, Meriç Uzunoğlu and Michael Wang.

I would like to thank Clara, Dan, Elizabeth, Joyce, Karin and Winnie for providing all the assistance I needed throughout my time here. It made my life much easier and I appreciate it.

I would also like to thank Gündüz and Kezban Ateş for their support. Since my father passed away, you have been there whenever I needed. I am very lucky to have you in my life.

My last year in New York was very special thanks to an amazing person – Kristel. I am very luck to have her in my life. Without her extraordinary support reaching the light at the end of this tunnel would have been much more difficult.

Most importantly, I would like to thank my mother for her unconditional love, patience, and support. She has always been there for me, and hopefully one day I will be as good of a parent as she has been to me.

To my parents

Chapter 1

Introduction

Infrastructure is a widely used word that can take on drastically different meanings depending on the context in which it is used. The following is an accurate description of what it encompasses in the context of this thesis:

> Infrastructure systems or networks of interrelated components are the analogous arteries and veins attaching society to the essential commodities and services required to uphold or improve the standards of living. They are often monopolistic in terms of local or regional control of a good or service and typically involve substantial capital investment. (Fulmer, 2009)

In this thesis we analyze infrastructure from a very broad perspective. The next three chapters focus on its pricing and the last chapter focuses on investment strategies with a focus on small modular infrastructure.

Chapters 2 and 3 concentrate on the pricing of a *managed lanes* scheme in which some of the lanes on a highway have a usage toll while the other *unmanaged lanes* are always free to use[1]. This is typical of managed lane schemes in which the only alternative to the managed lanes is a set of parallel unmanaged lanes on the same expressway. This distinguishes managed lane projects from

[1]What we call a managed lane scheme is sometimes called a *high-occupancy and toll (HOT)* scheme in the literature. In this case, the lanes with a toll are called the *HOT* lanes and free lanes are called the *general purpose (GP)* lanes.

pure toll roads in which the alternative to paying a toll is to take a different route – e.g. to take surface roads. The motivation of an arriving driver to pay a toll to use the managed lanes is the possibility of less congestion – and hence a faster travel time – than if she took the unmanaged lanes. However, we note that there is no guarantee that taking the managed lanes will save the driver time. Over the past ten years, managed lanes have become an increasingly common part of new highway construction. In 2010, ten managed lane projects were already in operation with six more being either planned or in development (Chung and Recker, 2011).

In both of the chapters we will utilize a very simple model where cars entering a highway have to choose between two sets of parallel lanes, managed and unmanaged, based on the current toll and expected time savings. The goal of the toll setting entity is to maximize the expected revenue from the managed lanes. This objective is aligned with several recent projects where the managed lanes are constructed on pre-existing highways using a build-transfer-operate scheme. In this approach, a private company will take responsibility for building the managed lanes. In exchange, it is awarded the concession to set and retain the tolls from these newly built lanes. Examples of such projects include the 495 Express Lanes and the 95 Express Lanes in the Washington D.C. area, and the LBJ Freeway and North Tarrant Expressway in the Dallas-Forth Worth area.

Most of the newly built managed lanes come with dynamic tolling capability that enables the managed lanes operator to update the tolls as frequently as every five minutes (LBJ Freeway). Given this capability, the possible tolling policies can be grouped into two:

- Static Policies: Tolls are not adjusted in real-time.
  - Single Toll: A single toll is set and does not change over time.
  - Multiple Tolls: Pre-set tolls vary with time-of-day but do not change in response to current conditions.
- Adaptive Policies: Tolls are adjusted according to real-time traffic conditions.
  - Myopic: Tolls are set to maximize the expected revenue from every entering vehicle given the current congestion levels.

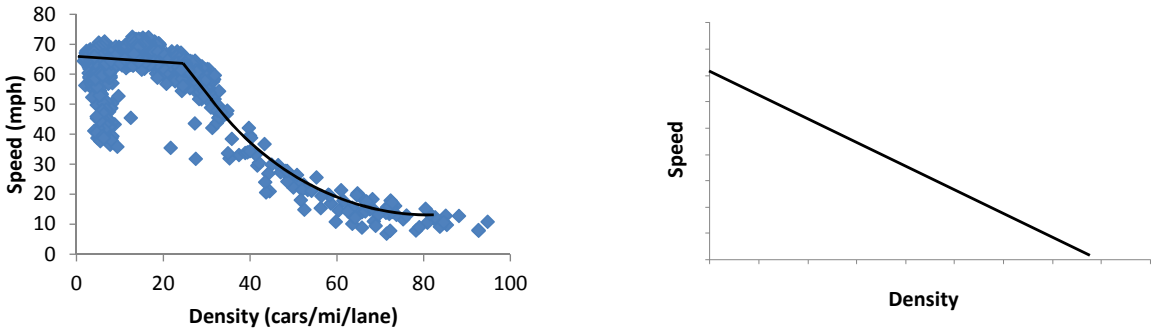

(a) Speed-density relationship obtained from California SR-91.

(b) Speed-density resulting from the $M/M/1$ assumption.

Figure 1.1: Speed-density relationships.

– Forward Looking: Tolls are set to maximize expected total revenue by taking into account the future congestion impact from cars currently entering the highway.

In chapters 2 and 3, we investigate various static and adaptive policies by employing different mathematical tools.

Traffic flows are typically expressed through speed-density relationships such as the one shown in Figure 1.1a. However, this relationship is quite complex to model so we take two different approaches.

In Chapter 2 we assume a much simpler linear form for the speed-density relationship as shown in Figure 1.1b by assuming that both managed and unmanaged lanes are governed by separate $M/M/1$ queues (Heidemann, 1996). Though this model is not entirely realistic, the tractable nature of these models enables us to show some important results. We show that the structure of the forward looking optimal policy is intuitive. The optimal tolls are an increasing function of the number of vehicles in the managed lanes and a decreasing function of the number of vehicles in the unmanaged lanes. One of our key findings is that the optimal toll is always higher than the myopic toll. Once a vehicle chooses either of the alternatives, it causes congestion for the following vehicle. The optimal policy accounts for this future congestion effect in the managed lanes, and thus adds a congestion premium.

Our numerical experiments show that both myopic and static policies fall well short of generating maximum revenue. This shows that the operator can achieve a significant amount of revenue improvement by adjusting the fees in real-time according to current conditions. Another important insight we get is regarding investments in managed lanes. In our experiments we saw that in heavily congested systems even a small level of capacity in the priced queue (managed lanes) is enough to reap most of the financial benefits.

Furthermore, in the case of a time-varying traffic load, the revenue-maximizing toll at any time strongly depends on anticipated future demand. In particular, for the same current state, the optimal forward looking tolls are generally higher when arrival intensity is forecast to increase than when arrival intensity is forecast to decrease. The intuition behind this result is that the optimal toll not only generates immediate revenue, it also channels users into the unmanaged lanes. When traffic is high and increasing (say entering a morning peak), it is profitable to use a higher fee to "steer" arriving vehicles to the unmanaged lanes. This increases congestion in the unmanaged lanes for some period, which allows higher tolls to be charged in the future. If, on the other hand, arrival intensity is decreasing (or is very low), steering additional vehicles to the unmanaged lanes will not result in much increased congestion in those lanes. In this case, the optimal policy comes closer to maximizing the expected revenue from each arriving vehicle (the myopic policy). A key managerial insight is that incorporating expectations of future arrivals into the determination of the current toll is critical if the goal is revenue maximization.

There is a close relationship between this chapter and the literature on pricing for queueing systems with time-sensitive customers. Hassin and Haviv (2003) provide an excellent survey of this literature. We analyze static policies as in Naor (1969) and also dynamic policies like Low (1974). Unlike Chapter 2, none of the existing work in this area consider dynamic pricing under the presence of multiple competing queueing systems and they do not consider non-homogeneous arrivals. Some work has also been done on the design of joint price and service-level menus for queueing systems. A notable example is Afeche (2010) who analyzes the design of a revenue-maximizing price/lead-time product menu for a multi-product $M/M/1$ queue. The congestion fee concept (difference between optimal forward looking and myopic tolls) described in the previous paragraphs is very similar in

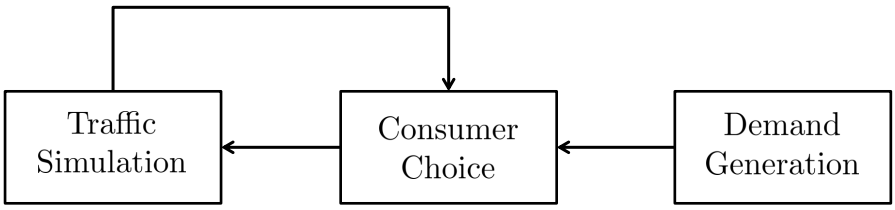

Figure 1.2: Constituent modules in the simulator.

flavor to his main finding where he shows that it can be optimal to induce "artificial" delay in one queue in order to increase the willingness-to-pay of arrivals to join the another queue. However, his setting is different from ours: we assume that introducing artificial delays are not permitted. How to cope with the time varying loads in queues has been well studied from a staffing perspective (Green *et al.*, 2009). However, in this study we keep the staffing fixed, i.e., there is only one server in each queue, and instead adjust the tolls dynamically over time.

Given the potential benefits surrounding adaptive tolling, we take a more practical viewpoint of the problem in Chapter 3 by building a simulation that models traffic propagation on a highway with a high degree of realism. This serves two purposes. First, we develop the methodology that can be easily used in practice to set revenue maximizing tolls for managed lanes. Second, using this methodology we analyze and compare the structure and performance of various tolling policies through a numerical study.

A high level overview of the simulation approach employed in this chapter is shown in Figure 1.2. The highway simulation is time based. In each time increment, the demand generation module determines how much new traffic arrives to the system. The consumer choice module takes the current traffic load as an input from the demand generation module. Based on the current toll and time differential between the managed and unmanaged lanes, it determines the proportions of the arriving traffic that choose the managed and unmanaged lanes. The highway simulation module uses that information to update the traffic on the managed and unmanaged lanes. This process keeps on repeating itself until the stopping time for the simulation is reached. In the numerical study, we start with an empty highway and simulate the system for a whole day.

This chapter provides a number of important insights into optimal managed lane tolling policies. First of all, managing tolls around peaks – especially entering into the peak – is the most important aspect of any revenue-maximizing policy. Secondly, optimal tolls have a "jam and harvest" character – by charging high tolls entering into a peak period, they divert cars into the unmanaged lanes increasing unmanaged lane congestion and enabling higher tolls later in the peak. These two observations are similar to the findings obtained in Chapter 2. Specifically, we see that accounting for the expectations of future arrivals in the current tolls provides substantial value. Finally, when the peak traffic is high relative to off-peak traffic, good heuristic policies can generate substantially more revenue than the myopic policy.

During our analysis we found that an adaptive tolling mechanism potentially provides substantial revenue improvements over a static time-of-use policy. We show that such a policy does not need to be very complex. What counts most is having the capability of sensing whether the traffic load is higher than usual or not.

In Chapter 4 we look at the revenue management of consumer options for sporting events. We study the potential revenue improvements of offering options, relative to only offering advance tickets. The World Cup final, the Super Bowl, and the final game of the NCAA Basketball Tournament in the United States (a.k.a. "March Madness") are among the most popular sporting events in the world. Typically, demand exceeds supply for the tickets for these events, even when the tickets cost hundreds of dollars. However, since these events are the final games of a tournament, the identities of the two teams who will be facing each other are typically not known until shortly before the event. For example, the identity of the two teams who faced each other in the 2010 World Cup final was determined only after the completion of the two semi-final games, five days prior to the final. Yet, tickets for the World Cup Final are offered for sale many months in advance. While there may be many fans who are eager to attend the final game no matter who plays, many fans would only be interested in attending if their favored team, say Germany, were playing in the final. These fans face a dilemma. If they purchase an advance ticket, and Germany does not advance to the final, then they have potentially wasted the price of the ticket, especially if there is no secondary market. On the other hand, tickets are likely to be sold out well before it is known who will be playing in

the finals, so if fans wait, they may be unable to attend at all. In response to this dilemma, some sporting events have begun to offer "ticket options" in which a fan can pay a nonrefundable deposit up front for the right to purchase a seat later once the identity of the teams playing is known. Essentially, this is a call option by which the fan can limit his cost should his team not make the final while guaranteeing a seat if his team does make the final. In this chapter, we address the revenue management problem faced by the event manager (or promoter) of a tournament final who has the opportunity to offer options for the final. We examine when it is most profitable to offer options to consumers and how the manager should set prices and availabilities for both the advance tickets and the options. We also address the social welfare implications of offering options.

Over the past five years, a number of events and third-parties have begun to offer call options for sporting event tickets. For example, the Rose Bowl is an annual post-season event in which two American college football teams are chosen to play against each other based on their records during the regular season. The identity of the teams playing is not known until a few weeks prior to the event, however, the Rose Bowl sells tickets many months in advance. In addition to general "advance tickets", the Rose Bowl also sells "Team Specific Reservations". As described on the Rose Bowl's web-site [2]:

> TeamTix are team specific reservations for the right and obligation to purchase a face value ticket, if and only if your team qualifies to play in the game. The price of the face value ticket(s) is an amount you pay that is over and above the amount you pay for the TeamTix, if your team qualifies for the game.

In addition to the Rose Bowl, at least one web site, www.OptionIT.com offers options for a variety of sporting events.

While options can be offered for any sporting event, in this chapter we consider only the case of *tournament options*, which are sold for a future event in which the two opponents who will face each other are *ex-ante* unknown. We assume that there are potential customers – "fans" – whose utility of attending the game is dependent upon whether or not their favored team is playing. In

[2] http://bcschampionship.teamtix.com/content/home

this case, the tournament option enables a fan to hedge against the possibility that his favored team is not selected to play in the game of interest – e.g. the World Cup final.

This chapter addresses a particular case of the classic revenue management problem of pricing and managing constrained capacity to maximize expected revenue in the face of uncertain demand. Overviews of revenue management can be found in Talluri and van Ryzin (2004) and Phillips (2005). While the revenue management literature is vast, there has been relatively little research on its applications to sporting events. Barlow (2000) discusses the application of revenue management to Birmingham FC, an English Premier League soccer team. Chapter 5 of Phillips (2005) discusses some pricing approaches used by baseball teams and Phillips *et al.* (2006) describe a software system for revenue management applicable to sporting events. Duran *et al.* (2011) and Drake *et al.* (2008) consider the optimal time to switch from offering bundles (e.g. season tickets) to individual tickets for sports and entertainment industries. None of these works address the use of options.

Research specifically on the use of options for sports events is very scarce. The first attempt to analyze such options was by Sainam *et al.* (2009). The authors devise a simple analytical model to evaluate the benefits of offering options to sports event organizers. They show that organizers can potentially increase their profits by offering options to consumers in addition to advance tickets. They also conduct a small numerical study to support their theoretical findings. However, they do not address the problem of pricing options or determining the number of tickets to sell.

In the absence of discounting, a consumer call option for a future service is equivalent to a partially refundable ticket. Gallego and Sahin (2010) show how such partially refundable tickets can increase revenue relative to either fully refundable or non-refundable tickets and that they can be used to allocate the surplus between consumers and capacity providers. They show that offering an option wherein an initial payment gives the option of purchasing a service for an additional payment at a later date can provide additional revenue for sellers. Gallego and Stefanescu (2012) discuss this as one of several "service engineering" approaches that sellers can use to increase profitability. The same result holds for a consumer call option in the case when the identity of the teams is known *ex-ante*. Our work extends their work by incorporating the correlation structure on *ex-post* customer utilities imposed by the structure of the tournament.

We propose a demand model where consumers are segmented by their preferred teams. We do not enforce any a priori segmentation across products. Instead, we postulate a neoclassical, risk-neutral, choice model where consumers maximize their expected surpluses. We allow fans to choose which product to purchase based on (i) prices, (ii) product availability, (iii) their intrinsic willingness-to-pay, and (iv) their rational expectations about the likelihood of the different outcomes. Thus, in our model, the demands for products are not independent, and a price-sensitive consumer choice model naturally arises.

In order to capture fans' sensitivity to the teams playing in the final game, we introduce a parameter termed *love-of-the-game* that measures the value to a fan of attending a game in which their favorite team does not play. The higher the value of this parameter, the more utility that fans derive from a game in which their favorite team is not playing. This parameter turns out to be critical in our model, and strongly influences the profitability of introducing options. Estimation of the fans' willingness-to-pay and their sensitivity to the teams playing in the final could be estimated, for example, with an empirical study similar to the one of Sainam *et al.* (2009) who estimated the willingness to pay of consumers for advance tickets and options under various probabilities of their favorite team playing in a final.

We address the joint problem of pricing and capacity allocation. We assume the event manager announces ticket prices at the beginning, and these remain fixed throughout the sales horizon. However, as demand realizes, the manager can control ticket sales by dynamically managing the availability of products. The sequential nature of these decisions suggests a two-stage optimization problem: set prices in the first stage, and allocate capacity given the fixed prices in the second stage. The capacity allocation problem in the second stage is a continuous time stochastic control problem under a discrete choice model, which in most real world applications can not be efficiently solved to optimality.

Different methods have been proposed in the literature to solve the capacity allocation problem. For example, Zhang and Adelman (2006) proposed an approximate dynamic programming approach in which the value function is approximated with an affine function of the state vector. Another popular approach, which we adopt here, considers a deterministic approximation of the capacity

allocation problem, in which random variables are replaced by their means and products are allowed to be sold in fractional amounts (Gallego *et al.*, 2004). The deterministic approximation results in a linear program. Unfortunately, the resulting LP grows exponentially with the number of teams. One of our contributions is an approximation that only grows quadratically with the number of teams. This allows us to efficiently solve instances of moderate size jointly on prices and capacity allocation. Additionally, we give precise bounds for the performance of that deterministic approximation and show that it is asymptotically optimal for the stochastic problem.

To provide some insight we analyze the symmetric problem, i.e., the case in which all teams have the same probability of reaching the final and the fans of all teams share the same valuations and love-of-the game. These simplifying assumptions allow us to characterize the conditions under which offering options is beneficial to the event manager. Though not entirely realistic, this analysis provides simple rules of thumb that can be applied to the general case. Specifically, we show that options are beneficial for the event manager only when the demand is high with respect to the stadium's capacity and fans strictly prefer their own team over any other. Additionally, we show that the value to the event manager of offering options decreases as the love-of-the-game parameter increases. That is, as fans become more averse to seeing other teams play, options become more attractive to them, and the event manager can take advantage of this by offering options. We also show that, under some mild assumptions, the introduction of options increases the consumer's surplus. This should not be surprising because options allow fans to hedge against the risk of watching a team that it is not of their preference. Lastly, we explore the idea of *full-information pricing* where the event manager prices the tickets after the finalists are determined, and show that offering options is a better strategy.

In the last chapter, we analyze infrastructure investments. In many industries, the historical trend is toward ever increasing unit size of technology. By *unit size* we mean the capacity of a single unit of technology, e.g., the number of people carried by a single aircraft, load capacity of a single mining truck, the watts of electric power produced by a single generator, etc. Food, once produced on small family plots, now comes overwhelmingly from industrial factory farms. Ships that in the early twentieth century carried 2,000 tons of cargo have been replaced by modern container ships

that routinely move 150,000 tons. Coal-fired power plants that averaged 50 MW of output in 1950 today approach 1 GW. The list goes on.

What underlies the trend of "bigger is better?" Before exploring this question further, we need to distinguish between the traditional notion of economies of scale, which encompasses all possible benefits associated with increasing total firm-wide output, and those benefits that are directly attributable to building and operating larger individual units of technology. Here we are interested in the latter, which we refer to as *economies of unit scale*.

While the development of ever larger unit size may have made sense historically, we submit that the incentives today for continuing the trend are less compelling - and indeed there may be tremendous benefit in reversing it. It is now realistic to consider a radically new approach to infrastructure design, one that replaces economies of unit scale with economies of numbers; that phases out custom-built, large-unit-scale installations and replaces them with large numbers of mass-produced, modular, small-unit-scale technology – operated in either centralized or distributed fashion – offering new possibilities for reducing cost and improving service. In the context of electricity generation, some of these concepts are reflected in the "Small Is Profitable" work of Lovins *et al.* (2002), but the idea applies much more broadly.

The total lifecycle cost of a unit can be divided into two parts: capital and operating costs. In this chapter we demonstrate that in many industries there is close to parity between small modular units and larger conventional units for both of these costs.

Specifically, we show that modern mass production of many small standardized units can achieve capital cost saving comparable to, or even larger than those achievable through large unit scale. For instance, a mass produced car engine costs \$10/kW, while a typical large-scale fossil fuel fired power plant costs about \$1000/kW (Larminie and Dick, 2003; EIA, 2010b). Since operating labor cost alone rendered small unit scale technology uneconomical in the past, there was little incentive to pursue the possibility of mass-produced capital; today, that situation is fundamentally altered.

Operating costs can be roughly divided into labor and fuel costs. We argue that technologies for automating processes exist today that were previously unavailable. In the past, a massively modular approach to infrastructure was simply infeasible because of excessive personnel cost. To-

day however, current computing, sensor and communication technologies make high degrees of automation possible at very low cost, radically undercutting the logic that significant labor savings can only be obtained through large unit scale. Through the use of several examples, we show that as the unit size gets larger and larger conversion efficiency of a unit does not necessarily increase significantly. As a result, for many industries, we demonstrate that the operating costs of large and small units are comparable to each other.

Lastly, there are many inherent flexibility benefits to small unit scale, which in the past have largely been ignored. Small-scale units can be used in multiples to better match the output requirements of a given project and can also be deployed gradually over time, both of which reduce investment cost and risk. They offer geographic flexibility; multiple small units can be aggregated at a single location to achieve economies of centralization (e.g. to reduce overhead or transport costs) or they can be distributed to be closer to either sources of supply or points of demand. Small unit scale also offers flexibility in output; having many units of small scale makes it possible to selectively operate varying numbers of units to better match short-run variations in demand. Also, one can achieve high reliability through enormous redundancy and statistical economies of numbers.

Since larger units no longer dominate smaller units from a capital and operating cost standpoint, the added flexibility benefits from smaller units suggest that not every industry requires large units to be cost-effective. We end the chapter by analyzing several industries where we believe a shift towards smaller unit sizes will introduce significant cost savings.

Chapter 2

Analysis of Pricing Managed Lanes Using Queueing Systems

This chapter deals with an important part of infrastructure systems, namely, transportation. We specifically focus on the pricing of managed lanes. Utilizing a simple queueing based model, we analyze the revenue maximizing tolling strategies for managed lanes. We pay particular attention to policies where the system operator has the flexibility to adjust the toll according to real time traffic conditions. Our analysis focuses on the characteristics of such policies and the potential revenue improvements that they can provide.

2.1 Model

We assume that both unmanaged and managed lanes are governed by different $M/M/1$ queues. The service rates of queues corresponding to both lanes are fixed and denoted by μ_i for $i = u, m$. Traffic arrives according to a Poisson process with rate λ. For stability, we assume that λ is strictly less than both μ_u and μ_m. The time-varying toll of the managed lane is denoted by $p(t)$, and the operator is subject to the nonnegative toll constraint $p(t) \geq 0$. The state of the system at time t is given by the vector $\mathbf{x}(t) = (x_u(t), x_m(t))$, where $x_m(t)$ and $x_u(t)$ denote the number of cars in the managed and unmanaged lanes, respectively. From this point on, bold characters will denote

two-dimensional vectors. Given the state of the system $\mathbf{x}(t)$, $\Delta T(\mathbf{x}(t))$ denotes the expected time savings an arriving vehicle can realize by choosing the managed lane,

$$\Delta T(\mathbf{x}(t)) = \frac{x_u(t)+1}{\mu_u} - \frac{x_m(t)+1}{\mu_m}.$$

When $\Delta T(\mathbf{x}(t)) > 0$, there are expected time savings from choosing the managed lanes.

We utilize a standard random utility model in which there is some distribution of "value-of-time" among drivers. We denote the value-of-time of a driver with V. Let F be the cumulative distribution function of this random valuation and $\bar{F}$ denote $1 - F$. We assume that the p.d.f. f is continuously differentiable, has support $[0, \bar{v}]$ for some $\bar{v} \in (0, \infty)$, and the valuations are i.i.d. across drivers. We will assume that the operator knows the distribution F but the individual value of each driver is private.

An arriving driver chooses the managed lanes if and only if $V\Delta T(\mathbf{x}(t)) \geq p(t)$. So, the corresponding probability that an arriving car chooses the managed lanes is $\bar{F}\left(\frac{p(t)}{\Delta T(\mathbf{x}(t))}\right)$. If the expected time it takes to traverse both lanes is equal and the toll is zero, then we assume that an motorist will choose one of the lanes with equal probability. In all other cases the managed lane arrival rate will be zero. With some abuse of notation, let $\lambda_m(\mathbf{x}(t), p(t))$ denote the arrival rate to the managed lane at time t which has the following structure

$$\lambda_m(\mathbf{x}(t), p(t)) = \begin{cases} \lambda \bar{F}\left(\frac{p(t)}{\Delta T(\mathbf{x}(t))}\right) & \text{if } \Delta T(\mathbf{x}(t)) > 0, \\ \lambda/2 & \text{if } \Delta T(\mathbf{x}(t)) = 0 \text{ and } p(t) = 0, \\ 0 & \text{o.w.} \end{cases}$$

Given a state $\mathbf{x}$, the toll operator is subject to the following control set

$$\mathcal{U}(\mathbf{x}) = \begin{cases} \{p | 0 \leq p \leq \bar{v}\Delta T(\mathbf{x})\} \text{ if } \Delta T(\mathbf{x}) > 0, \\ \{0, \underline{p}\} \text{ if } \Delta T(\mathbf{x}) = 0, \\ 0 \text{ o.w.} \end{cases}$$

When there are time savings, the operator can set his price as high as $\bar{v}\Delta T(\mathbf{x})$ which ensures that an arriving car chooses the unmanaged lanes. If there are no time savings, then the operator is faced with two choices. He can either set the toll to zero so that vehicles choose both lanes with equal probability, or he can set the toll to any positive scalar and an arriving vehicle will choose the unmanaged lanes. Lastly, if there are no time savings from taking the managed lanes, the operator sets the toll to either zero or some arbitrary positive toll $\underline{p}$.

In the next two sections, we explore the revenue maximization problem from two perspectives. First, we look at the expected discounted revenue, and then we analyze the average revenue maximization problem. In both cases we first formulate the problem using continuous time Markov chains. Afterwards, using a uniformization procedure we convert the problems into discrete time dynamic programs. Using the dynamic programs we obtain, we explore the structural properties of the optimal dynamic tolling policy. The last section extends the results to the case of non-stationary arrival rates.

2.1.1 Discounted Revenue Case

Let us start by writing down the discounted revenue case in the continuous time Markov chain (CTMC) framework. Our aim is to maximize the expected discounted revenue,

$$\lim_{T\to\infty} \mathbf{E}\left[\int_0^T e^{-\beta t}\lambda_m(\mathbf{x}(t), p(t))p(t)dt\right], \tag{2.1}$$

where $\beta > 0$ is the continuous discount rate.

Next, we show how we can obtain an optimal dynamic pricing policy for (2.1) using dynamic programming. The process $\mathbf{x}(t)$ is a continuous time Markov chain and the total transition rate out of any state is bounded by $\nu = \lambda + \mu_u + \mu_m$. Thus, we convert this problem into a discrete-time infinite horizon discounted dynamic programming problem by using uniformization. We also drop the time notation (Bertsekas 2007). The optimal discounted revenue when the initial state is $\mathbf{x}$,

denoted by $J(\mathbf{x})$ satisfies the Bellman equation

$$J(\mathbf{x}) = \left(\frac{\nu}{\beta+\nu}\right) \max_{p\in\mathcal{U}(\mathbf{x})} \left[\left(\frac{\lambda_m(\mathbf{x},p)}{\nu}\right)(p + J(\mathbf{x}+\mathbf{e}_2)) + \left(\frac{\lambda-\lambda_m(\mathbf{x},p)}{\nu}\right) J(\mathbf{x}+\mathbf{e}_1) \right. \tag{2.2}$$
$$\left. + \frac{\mu_u}{\nu} J(\mathbf{x}-\mathbf{e}_1)^+ + \frac{\mu_m}{\nu} J(\mathbf{x}-\mathbf{e}_2)^+ \right],$$

where $\mathbf{e}_i$ denotes the ith unit vector, and for $\mathbf{x} \in \mathcal{S}$, we have $\mathbf{x}^+ = (\max\{x_1, 0\}, \max\{x_2, 0\})$. The state space of this dynamic program is $\mathcal{S} = \{\mathbf{x} \in \mathbb{N}_0 \times \mathbb{N}_0\}$, and $\nu/(\beta+\nu) < 1$ is the discount factor. The expected revenue in a period is $r(\mathbf{x}, p) = \lambda_m(\mathbf{x}, p)p/(\beta+\nu)$. By cancelling out the common terms, we can express the DP in (2.2) as

$$J(\mathbf{x}) = \frac{1}{\beta+\nu} \max_{p\in\mathcal{U}(\mathbf{x})} [\lambda_m(\mathbf{x},p)(p + J(\mathbf{x}+\mathbf{e}_2)) + (\lambda-\lambda_m(\mathbf{x},p))J(\mathbf{x}+\mathbf{e}_1) \tag{2.3}$$
$$+ \mu_u J(\mathbf{x}-\mathbf{e}_1)^+ + \mu_m J(\mathbf{x}-\mathbf{e}_2)^+ \big].$$

In general, showing the existence of an optimal stationary policy for an infinite horizon discounted DP is straightforward when the per period reward is uniformly bounded on the state space. However, for the DP in (2.3) that is not the case. Furthermore, the existence of a value function J^* that satisfies the Bellman equation is not guaranteed. Using the next theorem we establish the existence of both an optimal stationary policy and a solution to the Bellman equation.

Theorem 1. *Assume that an arbitrary positive real-valued function w defined on $\mathcal{S}$, and positive scalars α and L exist that satisfy,*

1. $\inf_{\boldsymbol{x}\in\mathcal{S}} w(x) > 0$,
2. $\sup_{p\in\mathcal{U}(\boldsymbol{x})} |r(\boldsymbol{x}, p)| \leq \alpha w(\boldsymbol{x})$,
3. $\sum_{\boldsymbol{j}\in\mathcal{S}} q_\pi(\boldsymbol{j}|\boldsymbol{x}) w(\boldsymbol{j}) \leq w(\boldsymbol{x}) + L \ \forall p \in \mathcal{U}(\boldsymbol{x}), \forall \boldsymbol{x} \in \mathcal{S}$, *where $q_\pi(\boldsymbol{j}|\boldsymbol{x})$ denotes the probability of transitioning from state $\boldsymbol{x}$ to $\boldsymbol{j}$ under any arbitrary feasible policy π.*

Then, a unique solution J^* exists for the optimality equation given in (2.3) *that is obtainable through value iteration. Furthermore, an optimal stationary policy p_d exists for the DP.*

Proof: See Theorem 6.10.4 and Proposition 6.10.5 in Puterman (1994). □

Proposition 1. *For* $w(\boldsymbol{x}) = \max(\Delta T(\boldsymbol{x}), 1)$, $\alpha = \bar{v}$ *and* $L = \max\left(\frac{1}{\mu_u}, \frac{1}{\mu_m}\right)$, *all three conditions in Theorem 1 are satisfied.*

Proof: Condition 1 is satisfied by the definition of w. Now, we show that Condition 2 is also satisfied. We separate the state space into two disjoint sets: $\mathcal{S}_1 = \{\mathbf{x} \in \mathcal{S} | \Delta T(\mathbf{x}) \leq 0\}$ and $\mathcal{S}_2 = S \setminus S_1$. $\mathcal{S}_1$ is the set of states for which taking the managed lanes provides no time savings, and $\mathcal{S}_2$ contains the states for which taking the managed lanes provides time savings. For $\mathbf{x} \in \mathcal{S}_1$, we have $r(x, p) = 0$ and Condition 2 is satisfied. When $\mathbf{x} \in \mathcal{S}_2$, we have

$$r(\mathbf{x}, p) = \left(\frac{\lambda}{\beta + \nu}\right) \bar{F}\left(\frac{p}{\Delta T(\mathbf{x})}\right) p \leq \bar{v} \Delta T(\mathbf{x}) \leq \bar{v} w(\mathbf{x}). \tag{2.4}$$

The inequality comes from the fact that $\lambda/(\beta + \nu) < 1$, $\bar{F}$ is bounded by one, and $p \in [0, \bar{v}\Delta T(\mathbf{x})]$. So, Condition 2 is satisfied for this case as well.

Next, we show that Condition 3 is satisfied. First, note the following inequalities

$$\begin{aligned}
w(\mathbf{x} + \mathbf{e}_1) &\leq w(\mathbf{x}) + \frac{1}{\mu_u}, \\
w(\mathbf{x} - \mathbf{e}_1) &\leq w(\mathbf{x}), \\
w(\mathbf{x} + \mathbf{e}_2) &\leq w(\mathbf{x}), \\
w(\mathbf{x} - \mathbf{e}_2) &\leq w(\mathbf{x}) + \frac{1}{\mu_m}.
\end{aligned}$$

Using the above inequalities we get

$$\sum_{\mathbf{j} \in \mathcal{S}} q_\pi(\mathbf{j}|\mathbf{x}) w(\mathbf{j}) \leq w(\mathbf{x}) + \max\left(\frac{1}{\mu_u}, \frac{1}{\mu_m}\right),$$

for any arbitrary feasible policy π, and $\mathbf{x} \in \mathcal{S}$. Thus, we can see that the last condition is also satisfied. □

In addition to showing the existence of a unique solution to the Bellman equation in (2.3), Proposition 1 showed it can be obtained through a value iteration procedure. In the context of our problem, such a procedure iterates over

$$J_{k+1}(\mathbf{x}) = \left(\frac{1}{\beta+\nu}\right) \max_{p\in\mathcal{U}(\mathbf{x})} [\lambda_m(\mathbf{x},p)(p + J_k(\mathbf{x}+\mathbf{e}_2)) + (\lambda - \lambda_m(\mathbf{x},p))J_k(\mathbf{x}+\mathbf{e}_1) + \mu_u J_k(\mathbf{x}-\mathbf{e}_1)^+ + \mu_m J_k(\mathbf{x}-\mathbf{e}_2)^+],$$

where $J_0(\mathbf{x}) = 0$. J_k is also called the k-stage problem since it is a finite horizon dynamic program with k stages. The convergence of the value iteration procedure implies that $\lim_{k\to\infty} J_k(\mathbf{x}) = J^*(\mathbf{x})$.

Proposition 2. *For all* $\boldsymbol{x} \in \mathcal{S}$, $J^*(\boldsymbol{x}) \leq \frac{\bar{v}(\beta+\nu)}{\beta}\left(w(\boldsymbol{x}) + \frac{L\nu}{\beta}\right)$.

Proof: We start by proving that for any arbitrary feasible policy (possibly nonstationary) π and $\mathbf{x} \in \mathcal{S}$ we have,

$$E_\pi(r(\mathbf{x}^n, \pi^n)|\mathbf{x}^0 = \mathbf{x}) \leq \bar{v}(\Delta T(\mathbf{x}) + nL), \tag{2.5}$$

where $\mathbf{x}^n, \pi^n$ denote the state and action taken in period n, and E_π denotes the expectation operator under the policy π. We proceed by induction. It is easy to see that the case $n = 1$ holds. Now, assume the claim holds for $n = k - 1$. Then,

$$\begin{aligned}
E_\pi[r(\mathbf{x}^k, \pi^k)|\mathbf{x}^0 = \mathbf{x}] &= \sum_{\mathbf{y}\in\mathcal{S}} q_\pi^k(\mathbf{y}|\mathbf{x}) r(\mathbf{y}, \pi^k), \\
&= \sum_{\mathbf{y}\in\mathcal{S}}\sum_{\mathbf{z}\in\mathcal{S}} q_\pi^{k-1}(\mathbf{z}|\mathbf{x}) q_\pi(\mathbf{y}|\mathbf{z}) r(\mathbf{y}, \pi^k), \\
&= \sum_{\mathbf{z}\in\mathcal{S}} q_\pi^{k-1}(\mathbf{z}|\mathbf{x}) \sum_{\mathbf{y}\in\mathcal{S}} q_\pi(\mathbf{y}|\mathbf{z}) r(\mathbf{y}, \pi^k), \\
&\leq \sum_{\mathbf{z}\in\mathcal{S}} q_\pi^{k-1}(\mathbf{z}|\mathbf{x}) \sum_{\mathbf{y}\in\mathcal{S}} q_\pi(\mathbf{y}|\mathbf{z}) \bar{v} w(\mathbf{y}), \\
&\leq \bar{v} \sum_{\mathbf{z}\in\mathcal{S}} q_\pi^{k-1}(\mathbf{z}|\mathbf{x})(w(\mathbf{z}) + L), \\
&\leq \bar{v}(w(\mathbf{x}) + kL),
\end{aligned}$$

where the interchange of summations is justified since all terms are nonnegative. The first inequality above comes from (2.4), the second comes from the base case, and the last from the induction assumption.

We now use (2.5) to show that the value function is bounded for every $\mathbf{x} \in \mathcal{S}$.

$$\begin{aligned} J^*(\mathbf{x}) &= \sum_{n=0}^{\infty} \left(\frac{\nu}{\beta+\nu}\right)^n E_{p_d}[r(\mathbf{x}^n, p_d)|\mathbf{x}^0 = \mathbf{x}], \\ &\leq \bar{v} \sum_{n=0}^{\infty} \left(\frac{\nu}{\beta+\nu}\right)^n (w(\mathbf{x}) + nL), \\ &= \frac{\bar{v}(\beta+\nu)}{\beta} \left(w(\mathbf{x}) + \frac{L\nu}{\beta}\right). \end{aligned}$$

□

The bound established in Proposition 2 is linear with respect to the number of cars in the system. Specifically, the bound is increasing (decreasing) in the number of cars in the unmanaged (managed) lanes. This suggests that J^* might be a monotonic function and Proposition 3 establishes that is correct. It states that the value function actually moves in the same direction as its bound with respect to the number of cars in the system. This result is intuitive since as the unmanaged lanes get relatively more congested, the attractiveness of the managed lanes increases and the operator can charge a higher toll. On the other hand, as the managed lanes start to lose their attractiveness, the operator starts to charge a higher toll and the revenue potential decreases.

Proposition 3. *For all $\boldsymbol{x} \in \mathcal{S}$, we have $J^*(\boldsymbol{x} + \boldsymbol{e}_1) \geq J^*(\boldsymbol{x})$ and $J^*(\boldsymbol{x} + \boldsymbol{e}_2) \leq J^*(\boldsymbol{x})$.*

Proof: We use a coupling argument. Consider a k-stage problem with a terminal reward function $J_0(\mathbf{x}) = 0$ for all $\mathbf{x} \in \mathcal{S}$. We consider two different systems A and B starting from two different initial states $\mathbf{x}$ and $\mathbf{x} + \mathbf{e}_1$, respectively. By defining the systems on a common probability space, we can assume that for both A and B arrivals and departures happen at same points in time. We assume that System A follows the optimal policy p_d, and System B sets its toll such that at any time its probability of admitting a car into the managed lane is the same as System A. As a result, the toll that System B will be charging is always greater than or equal to the toll that System A

will be charging. So, the revenue stream generated by System B will be greater than or equal to the revenue stream generated by System A. Furthermore, the revenue generated by System B operated under this policy is less than or equal to the optimal. So, we get the following

$$J_k(\mathbf{x}+\mathbf{e}_1) - J_k(\mathbf{x}) \geq 0. \tag{2.6}$$

Since the convergence of the value iteration algorithm has already been established in Proposition 1, we take the limit as $k \to \infty$ in (2.6) to conclude

$$J^*(\mathbf{x}+\mathbf{e}_1) - J^*(\mathbf{x}) \geq 0.$$

This proves the first part of the proposition. The proof for the second part is similar and thus omitted. □

Next, we show the following simple corollary that will come in handy later.

Corollary 1. *For all* $\boldsymbol{x} \in \mathcal{S}$, $\Delta J^*(\boldsymbol{x}) = J^*(\boldsymbol{x}+\boldsymbol{e}_1) - J^*(\boldsymbol{x}+\boldsymbol{e}_2) \geq 0$.

Proof:

$$\begin{aligned}\Delta J^*(\mathbf{x}) &= J^*(\mathbf{x}+\mathbf{e}_1) - J^*(\mathbf{x}+\mathbf{e}_2),\\ &= J^*(\mathbf{x}+\mathbf{e}_1) - J^*(\mathbf{x}) + J^*(\mathbf{x}) - J^*(\mathbf{x}+\mathbf{e}_2),\\ &\geq 0,\end{aligned}$$

where the inequality comes from Proposition 3. □

We have showed the monotonicity of the value function in Proposition 3. However, it does not tell us anything about how fast the value function increases or decreases. In the next proposition we show that the speed is bounded.

Proposition 4. *For all* $\boldsymbol{x} \in \mathcal{S}$, $J^*(\boldsymbol{x}+k\boldsymbol{e}_1) - J^*(\boldsymbol{x}) \leq \frac{\bar{v}\nu(x_u+k)^2}{\mu_u(\mu_u-\lambda)}$, *and* $J^*(\boldsymbol{x}) - J^*(\boldsymbol{x}+k\boldsymbol{e}_2) \leq$

$\left(\frac{\bar{v}(x_m+k)}{\mu_m}\right)\left[\nu\left(\frac{x_u}{\mu_u}\right)+\lambda+\mu_u\right]$.

Proof: Similar to the proof of Proposition 3, we use a coupling argument. Let us start with the first part of the proposition. Consider two systems, A and A$'$, that are defined on a common probability space and start from the same state $\mathbf{x}+k\mathbf{e}_1$. System A$'$ is a modification to A defined as follows. Until some stopping time τ is reached, A$'$ earns $r'(\mathbf{x})=\bar{v}\Delta T(\mathbf{x})$ every period which is greater than the revenue rate of A for any policy. Once the stopping time τ is reached, then the revenue rate of A$'$ is replaced with the original $r(.)$. So, for any policy $\{p_1,p_2,\ldots\}$ and stopping time τ we have the following,

$$E\left(\sum_{t=0}^{\infty}\left(\frac{\nu}{\beta+\nu}\right)^t r(\mathbf{x}_t,p_t)\middle|\mathbf{x}_0=\mathbf{x}+k\mathbf{e}_1\right)\leq E\left(\sum_{t=0}^{\tau-1}\left(\frac{\nu}{\beta+\nu}\right)^t r'(\mathbf{x}_t)+\left(\frac{\nu}{\beta+\nu}\right)^{\tau}J(\mathbf{x}_\tau)\middle|\mathbf{x}_0=\mathbf{x}+k\mathbf{e}_1\right), \tag{2.7}$$

where $\mathbf{x}_t$ is a vector denoting the number of cars in the system at the beginning of each period. Now, let us define τ as the first time the number of cars in the unmanaged lanes hits zero. Note that $P(\tau<\infty)=1$ for any policy since $\lambda<\mu_u$. When A follows the optimal policy, the left hand side of (2.7) becomes equal to $J(\mathbf{x}+k\mathbf{e}_1)$. The policy that maximizes the right hand side of (2.7) is the one that directs all arrivals into the unmanaged lanes since it maximizes the period of time that passes before the revenue rate function is replaced with the original one. Furthermore, for any given sequence of events, it leaves the system in the best possible state, i.e. the state with the highest expected discounted revenue. Then we have,

$$J^*(\mathbf{x}+k\mathbf{e}_1)\leq E\left(\sum_{t=1}^{\tau-1}\left(\frac{\nu}{\beta+\nu}\right)^t r'(\mathbf{x}_t)+\left(\frac{\nu}{\beta+\nu}\right)^{\tau}J(\mathbf{x}_\tau)\middle|\mathbf{x}_1=\mathbf{x}+k\mathbf{e}_1\right). \tag{2.8}$$

Now, we define a second system B that is defined on the same probability space as A and A$'$. Assume that B directs all arrivals into the unmanaged lanes until the number of cars in the unmanaged lanes of A$'$ hits zero. Thus, the actual arrivals and departures from both systems are the same and they are found in the same state when the stopping time τ is reached. Clearly, this

is a suboptimal policy for B and we have,

$$J^*(\mathbf{x}) \geq E\left(\left(\frac{\nu}{\beta+\nu}\right)^{\tau} J(\mathbf{x}_\tau)\middle| \mathbf{x}_1 = \mathbf{x} + k\mathbf{e}_1\right). \tag{2.9}$$

Let y_t denote the change in the number of cars in the unmanaged lanes from period $t-1$ to t for the policy used in A$'$ and B. Then, y_t has the following distribution,

$$y_t = \begin{cases} 1 & \text{w.p. } \lambda/\nu, \\ 0 & \text{w.p. } \mu_m/\nu, \\ -1 & \text{w.p. } \mu_u/\nu. \end{cases}$$

We make a few observations before proceeding with the remainder of the proof. Note that $E\left(\sum_{t=1}^{\tau} y_t\right) = -(x_u + k)$ by the definition of stopping time τ, and from Wald's Equation $E(\tau) = E\left(\sum_{t=1}^{\tau} y_t\right)/E(y_t) = (x_u + k)\nu/(\mu_u - \lambda)$ (Ross, 1996). Combining this observation with (2.8) and (2.9) we get,

$$\begin{aligned} J^*(\mathbf{x} + k\mathbf{e}_1) - J^*(\mathbf{x}) &\leq E\left(\sum_{t=0}^{\tau-1}\left(\frac{\nu}{\beta+\nu}\right)^t r'(\mathbf{x}_t)\middle| \mathbf{x}_0 = \mathbf{x} + k\mathbf{e}_1\right), \\ &\leq E\left(\sum_{t=0}^{\tau} r'(\mathbf{x}_t)\middle| \mathbf{x}_0 = \mathbf{x} + k\mathbf{e}_1\right), \\ &\leq E\left(\sum_{t=0}^{\tau} \bar{v}\left(\frac{x_{u,t}}{\mu_u}\right)\middle| \mathbf{x}_0 = \mathbf{x} + k\mathbf{e}_1\right), \\ &= \bar{v}\left[E\left(\sum_{t=0}^{\tau}\frac{x_u + k}{\mu_u}\right) + E\left(\sum_{t=1}^{\tau}\frac{y_t}{\mu_u}\right)\right], \\ &= \bar{v}\left[(E(\tau)+1)\left(\frac{x_u+k}{\mu_u}\right) - \left(\frac{x_u+k}{\mu_u}\right)\right], \\ &= \frac{\bar{v}\nu(x_u+k)^2}{\mu_u(\mu_u-\lambda)}, \end{aligned}$$

where the second inequality comes from the nonnegativity of r' and $\nu/(\beta+\nu) < 1$, the third from $r'(\mathbf{x}_t) \leq x_{u,t}/\mu_u$ since $x_{u,t} \geq 0$ for $0 \leq t \leq \tau$, and the last inequality follows from Wald's Equation.

The second part of the proposition is proven similarly. Systems A and B now start from $\mathbf{x}$ and

$\mathbf{x} + k\mathbf{e}_2$, respectively. System B is operated under the suboptimal policy of directing all the cars into the unmanaged lanes. Now, the stopping time τ is defined as the first time the number of cars in the managed lanes of B is equal to zero, and $E(\tau) = x_m\nu/\mu_m$. Unlike the previous case, note that now τ is dependent on the state of System B. Again, A$'$ starts from $\mathbf{x}$ with r' as the revenue rate which is replaced with the original at τ. The optimal policy for A$'$ is still to direct all arriving cars into the unmanaged lanes. Note that the expected revenue from A$'$ is still an upper bound for the expected revenue from A that is operated optimally. Furthermore, systems A$'$ and B are found in the same state at time τ. Let z_t denote the absolute change in the number of cars in the unmanaged lanes from period $t-1$ to t for the policy used in A$'$ and B,

$$z_t = \begin{cases} 1 & \text{w.p. } (\lambda + \mu_u)/\nu, \\ 0 & \text{w.p. } \mu_m/\nu. \end{cases} \tag{2.10}$$

So, we have

$$\begin{aligned} J^*(\mathbf{x}) - J^*(\mathbf{x} + k\mathbf{e}_2) &\leq E\left(\sum_{t=1}^{\tau} r'(\mathbf{x}_t) \middle| \mathbf{x}_1 = \mathbf{x}\right), \\ &\leq \bar{v}\left[E\left(\sum_{t=1}^{\tau} \frac{x_u + k}{\mu_u}\right) + E\left(\sum_{t=1}^{\tau} \frac{z_t}{\mu_u}\right)\right], \\ &= \left(\frac{\bar{v}(x_m + k)}{\mu_m}\right)\left[\nu\left(\frac{x_u}{\mu_u}\right) + \lambda + \mu_u\right], \end{aligned}$$

where the first inequality comes from the first part of the proof, the second from $r'(\mathbf{x}_t) \leq (x_{u,t} + z_t/\mu_u)$, and the equality from Wald's Equation. □

Continuing with our results about the structure of the value function, we now show that it is convex nondecreasing (concave nonincreasing) with the number of cars in the unmanaged (managed) lanes. It worth pointing out that this result is independent of the distribution of V. Furthermore, this result will play an important role in establishing the structure of the optimal tolling policy.

Proposition 5. *For $\boldsymbol{x} \in \mathcal{S}$, $J^*(\boldsymbol{x})$ is convex in x_u and concave in x_m.*

Proof: We show the convexity of J^* in x_u by induction on the k-stage problem $J_k(\mathbf{x})$ with the boundary Condition $J_0(\mathbf{x}) = 0$. Note that given a state $\mathbf{x}$, such that $\Delta T(\mathbf{x}) > 0$, we have,

$$p(\mathbf{x}, \lambda_m) = \Delta T(\mathbf{x}) \bar{F}^{-1} \left(\frac{\lambda_m}{\lambda} \right).$$

With some abuse of notation, let $r(\mathbf{x}, \lambda_m)$ denote the expected revenue as a function of the managed lanes arrival rate rather than the toll, then

$$r(\mathbf{x}, \lambda_m) = \begin{cases} 0 & \text{if } \Delta T(\mathbf{x}) \leq 0, \\ \left(\frac{1}{\beta + \nu} \right) \Delta T(\mathbf{x}) \bar{F}^{-1} \left(\frac{\lambda_m}{\lambda} \right) & \text{if } \Delta T(\mathbf{x}) > 0. \end{cases}$$

Note that for any distribution F and $\lambda_m \in [0, \lambda]$, $r(\mathbf{x}, \lambda_m)$ is convex in x_u. Therefore, the base case $k = 1$ holds. Assume that $J_k(\mathbf{x})$ is convex for all $\mathbf{x} \in \mathcal{S}$. In writing $J_{k+1}(\mathbf{x})$ we treat λ_m as the decision variable, and we get

$$\begin{aligned} J_{k+1}(\mathbf{x}) = \frac{1}{\beta + v} \max_{\lambda_m \in \lambda(\mathbf{x})} & [\lambda_m p(\mathbf{x}, \lambda_m) + \lambda_m J_k(\mathbf{x} + \mathbf{e}_2)) + (\lambda - \lambda_m) J_k(\mathbf{x} + \mathbf{e}_1)) \\ & + \mu_u J_k(\mathbf{x} - \mathbf{e}_1)^+ + \mu_m J_k(\mathbf{x} - \mathbf{e}_2)^+], \end{aligned}$$

where $\lambda(\mathbf{x})$ denotes the set of feasible managed lanes arrival rates for state $\mathbf{x}$. For fixed λ_m, each of the elements in the expression being maximized above is convex in x_u by the induction assumption and the convexity of $r(\mathbf{x}, \lambda_m)$. Thus, the expression being maximized is convex since it is the nonnegative weighted sum of convex functions. We know that the maximum of convex functions is also convex (Boyd and Vandenberghe, 2004). Thus, $J_{k+1}(\mathbf{x})$ is convex in x_u and we have

$$J_{k+1}(\mathbf{x} + \mathbf{e}_1) - J_{k+1}(\mathbf{x}) \geq J_{k+1}(\mathbf{x}) - J_{k+1}(\mathbf{x} - \mathbf{e}_1)^+. \tag{2.11}$$

By taking the limit as $k \to \infty$ in (2.11) we get

$$J^*(\mathbf{x} + \mathbf{e}_1) - J^*(\mathbf{x}) \geq J^*(\mathbf{x}) - J^*(\mathbf{x} - \mathbf{e}_1)^+.$$

The proof of concavity in x_m is similar and thus omitted. □

Corollary 2. *$\Delta J^*(\boldsymbol{x})$ is nondecreasing in x_u and nonincreasing in x_m.*

Proof: We start by showing that $\Delta J(\mathbf{x})$ is nondecreasing in x_u. Let us start by noting the following

$$J^*(\mathbf{x}+2\mathbf{e}_1) - J^*(\mathbf{x}+\mathbf{e}_1) \geq J^*(\mathbf{x}+\mathbf{e}_1) - J^*(\mathbf{x}),$$
$$J^*(\mathbf{x}+\mathbf{e}_1+\mathbf{e}_2) - J^*(\mathbf{x}+\mathbf{e}_2) \leq J^*(\mathbf{x}+\mathbf{e}_1) - J^*(\mathbf{x}),$$

where the first inequality comes from the convexity of J^* in x_u and the latter from its concavity in x_m. By combining these two we get

$$J^*(\mathbf{x}+2\mathbf{e}_1) - J^*(\mathbf{x}+\mathbf{e}_1) \geq J^*(\mathbf{x}+\mathbf{e}_1+\mathbf{e}_2) - J^*(\mathbf{x}+\mathbf{e}_2),$$
$$J^*(\mathbf{x}+2\mathbf{e}_1) - J^*(\mathbf{x}+\mathbf{e}_1+\mathbf{e}_2) \geq J^*(\mathbf{x}+\mathbf{e}_1) - J^*(\mathbf{x}+\mathbf{e}_2).$$

The proof of the second part is similar and thus omitted. □

Given these properties of the value function, we can now start analyzing the structure of the optimal policy. An important aspect of our model is that the operator does not just try to maximize the expected revenue from an arriving vehicle. He also takes into account the future congestion that the vehicles joining the system might cause. For example, if an arriving vehicle joins the unamanaged lanes, then it increases the congestion for those lanes. This enables the operator to potentially charge a higher toll to the car that arrives next. An interesting question is how would the operator set the toll if he didn't take into account that congestion effect? That is, what if he set the tolls *myopically* to maximize revenue from each vehicle? What is the relationship between *myopic tolls* and *optimal tolls*? The *myopic toll* for state $\mathbf{x} \in \mathcal{S}$ is defined as

$$p_m(\mathbf{x}) := \text{argmax}_{\ p \in \mathcal{U}(\mathbf{x})} \lambda_m(\mathbf{x}, p) p.$$

Proposition 6. *Define* $\mathcal{S}^- = \{\boldsymbol{x} \in \mathcal{S} | \Delta T(\boldsymbol{x}) < 0\}$, $\mathcal{S}^0 = \{\boldsymbol{x} \in \mathcal{S} | \Delta T(\boldsymbol{x}) = 0\}$ *and* $\mathcal{S}^+ = \{\boldsymbol{x} \in \mathcal{S} | \Delta T(\boldsymbol{x}) > 0\}$. *The optimal and myopic policies have the following properties:*

1. *For* $\boldsymbol{x} \in \mathcal{S}^0$, $p_d(\boldsymbol{x}) = \underline{p}$.

For the remainder, assume V *satisfies IFR. Let* $h(.)$ *denote the hazard rate of* V *and* k *be the unique solution of* $k = 1/h(k)$.

2. *The optimal stationary policy is unique and strictly monotonic for* $\boldsymbol{x} \in \mathcal{S}^+$. *Specifically, the optimal toll increases as the number of cars in the unmanaged lanes increases and decreases if the number of cars in the managed lanes decreases.*

3. *For* $\boldsymbol{x} \in \mathcal{S}^+$, *the myopic toll is unique and satisfies* $p_m(\boldsymbol{x})/\Delta T(\boldsymbol{x}) = k$.

4. *For* $\boldsymbol{x} \in \mathcal{S}$, $p_d(\boldsymbol{x}) \geq p_m(\boldsymbol{x})$.

Proof: Let us start with proving the first claim. For $\mathbf{x} \in \mathcal{S}^0$, the revenue rate $\lambda_m(\mathbf{x}, p)p$ is zero regardless of the action that the operator takes. Thus, we can omit that term and rearrange the right hand side of (2.3) as follows,

$$J^*(\mathbf{x}) = \frac{1}{\beta + v} \max_{p \in \mathcal{U}(\mathbf{x})} [-\lambda_m(\mathbf{x}, p)\Delta J^*(\mathbf{x}) + \lambda J^*(\mathbf{x} + \mathbf{e}_1) + \mu_u J^*(\mathbf{x} - \mathbf{e}_1)^+ + \mu_m J^*(\mathbf{x} - \mathbf{e}_2)^+]$$

Since we have $\Delta J^*(\mathbf{x}) \geq 0$ from Corollary 1, the operator sets $p_d(\mathbf{x}) = \underline{p} > 0$ so that $\lambda_m(\mathbf{x}, p) = 0$.

We now proceed with the proof of the second claim. For $\mathcal{S}^-$ the optimal policy is unique by the definition of $\mathcal{U}(\mathbf{x})$, and for $\mathcal{S}^0$ the uniqueness of the optimal policy was shown above. What remains is to show uniqueness for $\mathcal{S}^+$. For an interior solution, the first order condition for the optimal toll is,

$$\begin{aligned} p_m(\mathbf{x}) &= \Delta T(\mathbf{x}) \frac{\bar{F}\left(\frac{p_m(\mathbf{x})}{\Delta T(\mathbf{x})}\right)}{f\left(\frac{p_m(\mathbf{x})}{\Delta T(\mathbf{x})}\right)} + \Delta J^*(\mathbf{x}), \\ \frac{p_m(\mathbf{x})}{\Delta T(\mathbf{x})} &= \frac{1}{h\left(\frac{p(\mathbf{x})}{\Delta T(\mathbf{x})}\right)} + \Delta J^*(\mathbf{x}). \end{aligned} \tag{2.12}$$

Since V is IFR, h is strictly decreasing in p and there exists a unique solution to (2.12). Now that we have shown the uniqueness of the optimal stationary policy, let us show that it is monotonic. First, let us define $g(\mathbf{x}, p)$ as

$$g(\mathbf{x}, p) = \Delta T(\mathbf{x}) \frac{1}{h\left(\frac{p}{\Delta T(\mathbf{x})}\right)} + \Delta J^*(\mathbf{x}).$$

So, (2.12) can be expressed as $p = g(\mathbf{x}, p)$. Proposition 5 we know that $\Delta J^*(\mathbf{x})$ is monotonic in $\mathbf{x}$. Combined with the IFR assumption, this implies that $g(\mathbf{x}, p)$ strictly increases (decreases) in x_u (x_m) and decreases in p. Thus, the fixed point for $g(\mathbf{x}, p)$ is strictly increasing (decreasing) in x_u (x_m), and we have shown that the optimal tolls are strictly monotonic in $\mathbf{x}$.

In order to show the third claim, we analyze the first order conditions for the optimal toll

$$\begin{aligned} p_m(\mathbf{x}) &= \Delta T(\mathbf{x}) \frac{\bar{F}\left(\frac{p_m(\mathbf{x})}{\Delta T(\mathbf{x})}\right)}{f\left(\frac{p_m(\mathbf{x})}{\Delta T(\mathbf{x})}\right)}, \\ \frac{p_m(\mathbf{x})}{\Delta T(\mathbf{x})} &= \frac{1}{h\left(\frac{p(\mathbf{x})}{\Delta T(\mathbf{x})}\right)}. \end{aligned} \tag{2.13}$$

Given that V is IFR and k is the unique fixed point of its inverse hazard rate, $p_m(\mathbf{x})$ is unique and satisfies $\frac{p_m(\mathbf{x})}{\Delta T(\mathbf{x})} = k$. The last claim follows immediately from comparing (2.12) and (2.13), and noticing the nonnegativity of $\Delta J^*(\mathbf{x}) \geq 0$. □

Now, let us analyze the implications of Proposition 6. When the managed lanes are more crowded than the unmanaged lanes, we already know that the operator cannot influence traffic with the toll so he just sets it to zero. But what about the case when both lanes have equal expected travel times? Should the operator set the toll to zero and try to congest the managed lanes even further hoping that he can charge more to cars coming later? Or is it time to set a positive toll and start clearing out the managed lanes? The second option is the optimal decision, that is, the operator should set a positive toll so that no arriving car chooses the managed lanes.

Given that V satisfies IFR, the optimal policy has a simple intuitive structure when there

are time savings from choosing the managed lanes. As the expected travel time savings from choosing the managed lanes increases, the operator should increase the tolls monotonically. Once the managed lanes become relatively more crowded, the operator should decrease the tolls. The structure of the myopic tolling policy is similar. We showed that there is a linear relationship between the expected time savings from choosing the managed lanes and the myopic tolls. This implies that the the myopic tolls are also strictly monotonic with respect to the number of cars in the managed and unmanaged lanes. Furthermore, it also implies that the fraction of cars choosing the managed lanes is not state-dependent and fixed.

We now analyze the relationship between myopic and optimal tolls. When the unmanaged lanes are faster, both policies set the tolls to zero by the definition of the control set. Unlike the optimal policy, the myopic policy is indifferent between setting the toll to zero and $\underline{p}$ when the expected travel times for both lanes are equal since the revenue rate is zero for both cases. However, the decision that the myopic policy takes is still important since it effects its future revenue stream. In the numerical examples we will assume that the myopic policy also sets the toll to $\underline{p}$ which provides the highest revenue. When the managed lanes are faster, the optimal toll balances the revenue that the operator can get from the current car versus the congestion it causes for the following car. Due to that congestion effect the optimal tolls are always greater than or equal to the myopic tolls. This implies that the probability of a car choosing the managed lanes will always be lower under the optimal policy.

2.1.2 Average Revenue Rate Case

In the previous section we analyzed the case of discounted revenues. Next, we look at the problem of maximizing the revenue rate of the system. The expected long-term average revenue is given by,

$$\lim_{T\to\infty} \frac{1}{T}\mathbf{E}\left[\int_0^T \lambda_m(\mathbf{x}(t), p(t))p(t)dt\right]. \tag{2.14}$$

Using the uniformization procedure as described in the previous section, we can express (2.14) as a discrete-time dynamic program with the Bellman equation

$$J^* + h(\mathbf{x}) = \max_{p \in \mathcal{U}(\mathbf{x})} \Big[\lambda_m(\mathbf{x}, p)p + \frac{\lambda_m(\mathbf{x}, p)}{v} h(\mathbf{x} + \mathbf{e}_2) + \frac{\lambda - \lambda_m(\mathbf{x}, p)}{v} h(\mathbf{x} + \mathbf{e}_1) + \frac{\mu_u}{v} h(\mathbf{x} - \mathbf{e}_1)^+ + \frac{\mu_m}{v} h(\mathbf{x} - \mathbf{e}_2)^+ \Big]. \tag{2.15}$$

In the above equation J^* is the optimal expected revenue per unit time and $h(\mathbf{x})$ is the relative revenue for state $\mathbf{x}$.

Average revenue dynamic programs suffer from serious pitfalls when the state and action spaces are not finite. Specifically, there is no guarantee that a unique J^* that is independent from the initial state will exist, and even if exists the value iteration algorithm used in the proofs of the previous section may not converge to it (Bertsekas 2007).

By taking advantage of its structure, we can show that our model does not suffer from these pitfalls. Specifically, we can show that regardless of the initial state, there exists a unique J^* and a bounded relative reward function that satisfies the Bellman equation in (2.15).

Theorem 2. *Let $J^*_\beta(\boldsymbol{x})$ denote the unique solution to the Bellman equation in (2.3) as a function of both the state $\boldsymbol{x} \in \mathcal{S}$ and the continuous discount factor β. Also, for a fixed state $\boldsymbol{z} \in \mathcal{S}$, let $h_\beta(\boldsymbol{x}) := J^*_\beta(\boldsymbol{x}) - J^*_\beta(\boldsymbol{z})$ for all $\boldsymbol{x} \in \mathcal{S}$. Assume that the following conditions are satisfied,*

1. *For some fixed state $\boldsymbol{z} \in \mathcal{S}$ the value function $J^*_\beta(\boldsymbol{z})$ is bounded for all $\beta > 0$,*
2. *There exists nonnegative finite functions L and N defined on $\mathcal{S}$ such that $-N(\boldsymbol{x}) \leq h_\beta(\boldsymbol{x}) \leq L(\boldsymbol{x})$ for all $\boldsymbol{x} \in \mathcal{S}$ and $\beta > 0$,*
3. *$\sum_{\boldsymbol{y} \in \mathcal{S}} q_\pi(\boldsymbol{y}|\boldsymbol{x}) L(\boldsymbol{y}) < \infty \ \forall \boldsymbol{x} \in \mathcal{S}$,*
4. *For any feasible stationary policy and initial state $\boldsymbol{x} \in \mathcal{S}$,*

$$E(L(\boldsymbol{x}_n)|\boldsymbol{x}_1 = \boldsymbol{x}) < \infty \quad \text{for } n \geq 2,$$

5. For any feasible stationary policy and initial state $\boldsymbol{x} \in \mathcal{S}$*,*

$$\lim_{n\to\infty} \frac{E(L(\boldsymbol{x}_n)|\boldsymbol{x}_1 = \boldsymbol{x})}{n} = 0,$$

where $\boldsymbol{x}_n$ *denotes the state of the system in the* n*th period. Then, there exists a unique constant* J^* *that is independent of the initial starting state, and a sequence of discount factors* $\beta_n \to 0$ *such that* $\lim_{n\to\infty} \left(\frac{\beta_n}{\beta_n+v}\right) J^*_{\beta_n}(\boldsymbol{x}) = J^*$ *for all* $\boldsymbol{x} \in \mathcal{S}$*. Furthermore, there exists a relative revenue function* h^* *that satisfies* $-N(\boldsymbol{x}) \leq h^*(\boldsymbol{x}) \leq L(\boldsymbol{x})$ *such that the pair* (h^*, J^*) *satisfies the Bellman equation in* (2.15)*, and any policy* p_a *that achieves the maximum in the Bellman equation is optimal.*

Proof: With the exception of one small technical detail, these assumptions correspond to (H1-H4) and (H*5) in Sennott (1999). The proof then follows from Theorem 7.4.3 and Proposition 7.7.2 therein[1].

Proposition 7.7.2 in Sennott (1999) assumes that the action space for each state is finite which is not the case here. However, the only reason she does so is to ensure the existence of a sequence of discount factors $\{\beta_n\}_{n=1}^{\infty}$ for which the resulting policies converge uniformly as $\beta_n \to 0$[2]. For our problem, we can find such a sequence of discount factors as follows. As in the proof of Proposition 5, consider the formulation of the Bellman equation (2.3) where λ_m is the decision variable. For all $\mathbf{x} \in \mathcal{S}$, let $\lambda_m^{\beta}(\mathbf{x})$ denote the optimal flow rate into the managed lanes for a discount factor of β. Take $\{\beta_n\}_{n=1}^{\infty}$ as any arbitrary sequence of discount factors such that $\beta_n \to 0$. Notice that $0 \leq \lambda_m^{\beta_n}(\mathbf{x}) \leq \lambda$, and via Theorem 3.6 of Rudin (1976) we can find a subsequence of $\{\beta_n\}_{n=1}^{\infty}$ such that $\lambda_m^{\beta_n}(\mathbf{x})$ converges uniformly as $n \to \infty$. Since there is one-to-one correspondence between tolls and managed lanes flow rates, the arguments in the proof of Proposition 7.7.2 apply for this subsequence of $\{\beta_n\}_{n=1}^{\infty}$. □

Proposition 7. *All the conditions in Theorem 2 are satisfied with* $L(\boldsymbol{x}) = \frac{\bar{v}\nu(x_u+k)^2}{\mu_u(\mu_u-\lambda)}$ *and* $N(\boldsymbol{x}) = \left(\frac{\bar{v}x_m}{\mu_m}\right)(\lambda+\mu_u)$ *for* $\boldsymbol{x} \in \mathcal{S}$*.*

[1] Condition (iv) in Theorem 7.4.3 coincides with our third assumption.

[2] See Remark 7.7.6 in Sennott (1999) for a detailed discussion of this assumption.

Proof: Let us show one by one that each assumption in Theorem 2 is satisfied. Proposition 2 implies that the first assumption is satisfied. To show that the second assumption holds, we set $\mathbf{z} = \mathbf{0}$, i.e., we choose the state of the system without any cars as the fixed state. Now, let us analyze the relative revenue function $h_\beta(\mathbf{x})$. We start by showing that it has a finite upper bound,

$$\begin{aligned} h_\beta(\mathbf{x}) &= J_\beta(\mathbf{x}) - J_\beta(\mathbf{0}), \\ &\leq J_\beta(x_u, 0) - J_\beta(\mathbf{0}), \\ &\leq \underbrace{\frac{\bar{v}\nu(x_u + k)^2}{\mu_u(\mu_u - \lambda)}}_{L(\mathbf{x})}, \end{aligned}$$

where the first inequality follows from Proposition 3, and the last one follows from Proposition 4. Next, we show the existence of a finite lower bound,

$$\begin{aligned} h_\beta(\mathbf{x}) &= J_\beta(\mathbf{x}) - J_\beta(\mathbf{0}), \\ &\geq J_\beta(0, x_m) - J_\beta(\mathbf{0}), \\ &\geq \underbrace{-\left(\frac{\bar{v}x_m}{\mu_m}\right)(\lambda + \mu_u)}_{N(\mathbf{x})}, \end{aligned}$$

where the first inequality follows Proposition 3, and the last one follows from Proposition 4. So, we have verified that the second assumption holds.

The third assumption,

$$\sum_{\mathbf{y}\mathcal{S}} q_\pi(\mathbf{y}|\mathbf{x}) L(\mathbf{y}) < \infty \ \forall \mathbf{x} \in \mathcal{S}, \tag{2.16}$$

holds since the number of states that one can transition to from any state $\mathbf{x} \in \mathcal{S}$ is finite.

Next, let us show that the fourth assumption holds. Note that $L(\mathbf{x})$ is increasing in only x_u. Thus, for any stationary policy, after n transitions the number of cars in the unmanaged lanes is at most $x_u + n$. So, $E(L(\mathbf{x}_n)|\mathbf{x}_1 = \mathbf{x}) \leq L(\mathbf{x} + n\mathbf{e}_1) < \infty$ for $n \geq 2$, and the fourth assumption holds.

We now argue that the last assumption also holds. Let E_π denote the expectation operator under

a stationary policy π and $\bar{\pi}$ denote the policy that directs all incoming traffic into the unmanaged lanes. Then, for all $\mathbf{x} \in \mathcal{S}$ and any feasible policy π we have,

$$E_{\pi}(L(\mathbf{x}_n)|\mathbf{x}_1 = \mathbf{x}) \leq E_{\bar{\pi}}(L(\mathbf{x}_n)|\mathbf{x}_1 = \mathbf{x}). \tag{2.17}$$

The Markov chain that policy $\bar{\pi}$ induces consists of transient states T and positive recurrent states R. All states that have a positive number of cars in the managed lanes are transient and the remaining states are positive recurrent. The states in R correspond to a birth-death process with a birth rate of λ and a death rate of μ_u, and the state variable is the number of cars in the unmanaged lanes[3]. For $\mathbf{x} \in R$, let $q_{\bar{\pi}}(\mathbf{x})$ denote the stationary distribution for policy $\bar{\pi}$. Then, we have

$$\begin{aligned}
\lim_{k\to\infty} L^k_{\mathbf{x}} &= \lim_{k\to\infty} \left(\frac{\sum_{n=1}^{k} E_{\bar{\pi}}(L(\mathbf{x}_n)|\mathbf{x}_1 = \mathbf{x})}{k} \right), \ \forall \mathbf{x} \in R, \\
&= \sum_{\mathbf{x}\in R} q_{\bar{\pi}}(\mathbf{x}) L(\mathbf{x}), \\
&= \sum_{n=1}^{\infty} \left(\frac{\lambda}{\mu_u}\right)^n q_{\bar{\pi}}(\mathbf{0}) \left(\frac{\bar{v}}{\mu_u}\right) \left[\frac{\nu(n)^2}{\mu_u - \lambda} + \frac{\mu_u - \lambda}{\nu}\right], \\
&= \underbrace{q_{\bar{\pi}}(\mathbf{0}) \left(\frac{\bar{v}}{\mu_u}\right) \sum_{n=1}^{\infty} \left(\frac{\lambda}{\mu_u}\right)^n \left[\frac{\nu(n)^2}{\mu_u - \lambda} + \frac{\mu_u - \lambda}{\nu}\right]}_{M} < \infty.
\end{aligned}$$

The second equality above comes from Proposition C.2.1(i) of Sennott (1999), the third from Ross (1996), and the summation in the last line is finite since it is the sum of two geometric series. Thus, we have shown that for any $\mathbf{x} \in R$, $\lim_{k\to\infty} L^k_{\mathbf{x}}$ converges to a finite quantity M. Next, let us show that $\lim_{k\to\infty} L^k_{\mathbf{x}} = M$ for any $\mathbf{x} \in T$. Let $\tau(\mathbf{x})$ denote the first time a system that starts from a transient state $\mathbf{x}$ enters into the class of recurrent states under the policy $\bar{\pi}$. Since there are no new arrivals into the managed lanes under the policy $\bar{\pi}$, we have $E_{\bar{\pi}}(\tau(\mathbf{x})) = x_m/\mu_m$. Then, for

[3]At every step of the birth-death process, the system stays in the same state with a rate of μ_m since there are no cars in the managed lanes. However, this does not effect the stationary probabilities.

any $\mathbf{x} \in T$ we have

$$E_{\bar{\pi}}\left(\sum_{n=1}^{\tau(\mathbf{x})-1} L(\mathbf{x}_n)\middle|\mathbf{x}_1=\mathbf{x}\right) \leq \left(\frac{\bar{v}}{\mu_u}\right)\left[\underbrace{E_{\bar{\pi}}\left(\sum_{n=1}^{\tau(\mathbf{x})}\frac{\nu(x_{u,t})^2}{\mu_u-\lambda}\middle|\mathbf{x}_1=\mathbf{x}\right)}_{(I)} + \underbrace{E_{\bar{\pi}}(\tau(\mathbf{x}))\left(\frac{\mu_u-\lambda}{\nu}\right)}_{(II)}\right], \tag{2.18}$$

where the inequality follows from the nonnegativity of the function L. Note that part (II) of (2.18) is finite since $E_{\bar{\pi}}(\tau(\mathbf{x})) < \infty$. We now show that (I) is also finite. Let z_t be defined as in (2.10), then

$$\begin{aligned}
E_{\bar{\pi}}\left(\sum_{n=1}^{\tau(\mathbf{x})}\frac{\nu(x_{u,t})^2}{\mu_u-\lambda}\middle|\mathbf{x}_1=\mathbf{x}\right) &\leq \left(\frac{\nu}{\mu_u-\lambda}\right)E_{\bar{\pi}}\left(\sum_{n=1}^{\tau(\mathbf{x})}(x_u+z_t)^2\right), \\
&= \left(\frac{\nu}{\mu_u-\lambda}\right)E_{\bar{\pi}}\left(\sum_{n=1}^{\tau(\mathbf{x})}x_u^2+2x_uz_t+z_t^2\right), \\
&= \left(\frac{\nu}{\mu_u-\lambda}\right)E_{\bar{\pi}}(\tau(\mathbf{x}))\left[x_u^2+\left(\frac{\lambda+\mu_u}{\nu}\right)(2x_u+1)\right],
\end{aligned}$$

where the first inequality comes $x_{u,t} \leq x_u + z_t$. Thus, given the finiteness of $E_{\bar{\pi}}(\tau(\mathbf{x}))$, we have shown that (I) is also finite. As a result, for all $\mathbf{x} \in \mathcal{S}$ we have $\lim_{k\to\infty} L^k_{\mathbf{x}} = M$ and this implies that $E_{\bar{\pi}}(L(\mathbf{x}_n)|\mathbf{x}_1=\mathbf{x})/n \to 0$ as $n \to \infty$. From (2.17) it follows that the last assumption also holds. □

The previous proposition established the existence of a solution pair (h^*, J^*) for the optimality equation (2.15). Note that it only guarantees the uniqueness of J^*. By definition, the relative revenue function h^* can only be unique up to a constant.

As discussed previously, since the state and action spaces are not finite, value iteration is not guaranteed to converge. The next proposition establishes that the value iteration algorithm indeed converges.

Theorem 3. *For all $\boldsymbol{x} \in \mathcal{S}$, define the following recursion*

$$J_{k+1}(\boldsymbol{x}) = \max_{p \in \mathcal{U}(\boldsymbol{x})} \Big[\lambda_m(\boldsymbol{x}, p)p + \frac{\lambda_m(\boldsymbol{x}, p)}{v} J_k(\boldsymbol{x} + \boldsymbol{e}_2) + \frac{\lambda - \lambda_m(\boldsymbol{x}, p)}{v} J_k(\boldsymbol{x} + \boldsymbol{e}_1) + \frac{\mu_u}{v} J_k(\boldsymbol{x} - \boldsymbol{e}_1)^+ + \frac{\mu_m}{v} J_k(\boldsymbol{x} - \boldsymbol{e}_2)^+ \Big], \tag{2.19}$$

with the boundary condition $J_0(\boldsymbol{x}) = 0$. Then, for all $\boldsymbol{x} \in \mathcal{S}$, $\lim_{k\to\infty} J_k(\boldsymbol{x}) - kJ^* = h^*(\boldsymbol{x})$, such that the pair (h^*, J^*) is a solution to the optimality equation (2.15) given that the following two assumptions hold,

1. *No stationary policy induces a Markov chain with a null recurrent class,*
2. *A function r on $\mathcal{S}$ exists such that $h^*(\boldsymbol{x}) \geq -Kr(\boldsymbol{x})$ for all $\boldsymbol{x} \in \mathcal{S}$, where K is some positive constant. Furthermore, any feasible policy π satisfies $E_\pi(r(\boldsymbol{x}_n)|\boldsymbol{x}_1 = \boldsymbol{x}) \leq cr(\boldsymbol{x})$ for all $n \geq 1$, where c is some positive constant.*

Proof: See Theorem 1 in Aviv and Federgruen (1999). The two statements given above correspond to assumptions (A) and (C) therein. □

Proposition 8. *All assumptions given in Theorem 3 are satisfied.*

Proof: To see that the first assumption holds, notice that the state $\mathbf{0}$ is positive recurrent under any policy since $\lambda < \mu_u, \mu_m$. Furthermore, the expected first entry time to $\mathbf{0}$ from any other state $\mathbf{x} \in \mathcal{S}$ is also finite. Thus, for any stationary policy, the states that communicate with $\mathbf{0}$ are positive recurrent, and the remaining states are transient since they lead to $\mathbf{0}$ in finite expected time.

We employ Theorem 2 in Aviv and Federgruen (1999) to show that the second assumption holds. We start by separating the state space into two parts, $G = \{\mathbf{x} \in \mathcal{S} | x_m = 0\}$, and $\bar{G} = \mathcal{S} \setminus G$. Note that

$$\bar{N}(\mathbf{x}) = \max_{p \in \mathcal{U}(\mathbf{x})} \sum_{\mathbf{y} \in \mathcal{S}} q_p(\mathbf{y}|\mathbf{x}) N(\mathbf{y}) < \infty, \forall \mathbf{x} \in G, \tag{2.20}$$

$$N(\mathbf{x}) \geq \sum_{\mathbf{y} \in \mathcal{S}} q_p(\mathbf{y}|\mathbf{x}) N(\mathbf{y}), \forall \mathbf{x} \in \bar{G} \text{ and } \forall p \in \mathcal{U}(\mathbf{x}), \tag{2.21}$$

where the function N is defined as in the proof of Proposition 7. Theorem 2 shows that when G is finite, (2.20) and (2.21) guarantee the existence of a function that satisfies assumption (C). However, the proof of Theorem 2 uses the finiteness of G to only ensure that $\max_{\mathbf{x}\in G} N(\mathbf{x})$ is finite. In our case, $N(\mathbf{x}) = 0$ for all $\mathbf{x} \in G$, thus the proof of Theorem 2 still holds and implies that a function satisfying assumption (C) exists. □

Next, let us show the analogue of Proposition 3 for the average revenue rate formulation. It states that the relative revenue function is nondecreasing (nonincreasing) as the number of cars in the unmanaged (managed) lanes increases.

Proposition 9. *For all $\boldsymbol{x} \in \mathcal{S}$, we have $h^*(\boldsymbol{x} + \boldsymbol{e}_1) \geq h^*(\boldsymbol{x})$ and $h^*(\boldsymbol{x} + \boldsymbol{e}_2) \leq h^*(\boldsymbol{x})$.*

Proof: Let J_k denote the undiscounted k-stage problem defined as in (2.19) with the starting state $\mathbf{x}$, and the boundary condition $J_0(\mathbf{x}) = 0$ for all $\mathbf{x} \in \mathcal{S}$. By employing a coupling argument identical to the one in the proof of Proposition 3, it is easy to see that

$$J_k(\mathbf{x} + \mathbf{e}_1) - J_k(\mathbf{x}) \geq 0. \tag{2.22}$$

Using Proposition 8, we take the limit as $k \to \infty$ in (2.22) and get

$$h^*(\mathbf{x} + \mathbf{e}_1) - h^*(\mathbf{x}) \geq 0. \tag{2.23}$$

The first part of the proposition is proven. The second part is similar to the first and is therefore omitted. □

Now, given that the relative revenue function is monotonic with respect to the number of cars in the system, it is easy to see that it has similar properties as the value function in the expected discounted revenue case.

Corollary 3. *For $\boldsymbol{x} \in \mathcal{S}$, we have*

1. $\Delta h^*(\boldsymbol{x}) = h^*(\boldsymbol{x} + \boldsymbol{e}_1) - h^*(\boldsymbol{x} + \boldsymbol{e}_2) \geq 0$,

2. $h^*(\boldsymbol{x})$ *is convex in* x_u *and concave in* x_m.

3. $\Delta h^*(\boldsymbol{x})$ *is nondecreasing in* x_u *and nonincreasing in* x_m.

Given Corollary 3, the structural results we obtained for the optimal policy in the discounted revenue case holds for the average revenue criterion as well.

Corollary 4. *The optimal and myopic policies have the following properties:*

1. *For* $\boldsymbol{x} \in \{\boldsymbol{x} \in \mathcal{S} | \Delta T(\boldsymbol{x}) = 0\}$, $p_a(\boldsymbol{x}) = \underline{p}$.

For the remainder, assume V *satisfies IFR. Let* $h(.)$ *denote the hazard rate of* V *and* k *be the unique solution of* $k = 1/h(k)$.

2. *The optimal stationary policy* $p_a(\boldsymbol{x})$ *is unique and strictly monotonic. Specifically, the optimal toll increases as the number of cars in the unmanaged lanes increases and decreases if the number of cars in the managed lanes decreases.*

3. *For* $\boldsymbol{x} \in \mathcal{S}$, $p_a(\boldsymbol{x}) \geq p_m(\boldsymbol{x})$.

Corollary 4 shows that the structure of the optimal policy does not change in the average revenue rate case. Note that we omitted the results for the myopic policy (which still hold) since it is independent of whether the objective is to maximize the expected discounted revenue or the average revenue rate.

2.1.3 Non-stationary Arrival Rates

In this section we allow the arrival rates to be time-varying. In order to handle this modification we assume that by a sufficiently fine discretization of time, at most one arrival or departure occurs in each period. Furthermore, we assume that the expected arrival rate pattern is known ahead of time and repeats itself periodically. Given the nature of traffic volumes this is a natural assumption (hcm, 2010).

Similar to highways, call centers also typically incur time-varying demand. An important part of the call center literature focuses on exploring different techniques to cope with time-varying

demand. Green *et al.* (2009) gives an overview of the work in this area. Unlike our problem, the call center literature's primary focus is on finding the minimum staffing quantities for which the call center provides an adequate level of service.

Let λ_t denote the probability of an arrival in period t and, μ_u and μ_m denote the probability of departure from unmanaged and managed lanes, respectively. Then, we must have,

$$\lambda_t + \mu_m + \mu_u \leq 1 \ \forall t \in \{1, 2, \ldots\},$$

due to the assumption of at most one arrival or departure per period. In addition, let T denote the periodicity of the arrival probabilities. Since the arrival pattern repeats itself every T periods, we have $\lambda_t = \lambda_{t+kT}$ for $k \in \mathbb{N}$. For $k \in \{0, 1, \ldots\}$, we will refer to the set of T periods $\{(k-1)T+1, (k-1)T+2, \ldots, kT\}$ as a *cycle*. This modeling approach designed to handle non-homogeneous arrival rates was first introduced for a finite horizon problem in the context of airline revenue management by Subramanian *et al.* (1999).

Given a toll p, the probability of a car arriving to the managed lanes in period t is analogous to the stationary arrival rate case and is given by,

$$\lambda_{m,t}(\mathbf{x}, p) = \begin{cases} \lambda_t \bar{F}\left(\frac{p}{\Delta T(\mathbf{x})}\right) & \text{if } \Delta T(\mathbf{x}) > 0, \\ \lambda_t/2 & \text{if } \Delta T(\mathbf{x}) = 0 \text{ and } p = 0, \\ 0 & \text{o.w.} \end{cases}$$

In order to make sure the system is stable we assume that the maximum arrival rate $\max_{1 \leq t \leq T} \lambda_t$ is less than both μ_u and μ_m. This guarantees that for any policy the system eventually returns to its empty state w.p.1.

Similar to the time-homogeneous case we analyze two different objectives: discounted and average revenue per cycle. For both models we keep the same assumptions regarding the state space. Before we start analyzing the problem formulations for both of these objectives let us note that the counterparts of the structural results obtained for the constant arrival rate case hold in this setting as well. Specifically, solutions exist for the dynamic programs corresponding to these

two different objectives and also the value iteration algorithms converge. The value functions, and similarly the relative value functions, are monotonic. Lastly, the time-varying counterparts of the structural results obtained for the optimal and myopic policies are still valid.

2.1.3.1 Discounted Revenue

In this section we assume that the managed lanes operator discounts the revenue earned in each cycle by a factor of $\gamma < 1$ which results in the following objective function

$$\lim_{k\to\infty} \mathbf{E}\left[\sum_{t=0}^{k(T-1)} \lambda_{m,t}(\mathbf{x}(t), p(t))p(t)\gamma^{\lfloor t/T \rfloor}\right]. \tag{2.24}$$

We can formulate this problem as a dynamic program with non-stationary parameters that results in the Bellman equation,

$$\begin{aligned} J_t(\mathbf{x}) = \max_{p\in\mathcal{U}(\mathbf{x})} [&\lambda_{m,t}(\mathbf{x}, p)(p + J_{t-1}(\mathbf{x}+\mathbf{e}_2) + (\lambda_t - \lambda_{m,t}(\mathbf{x}, p))J_{t-1}(\mathbf{x}+\mathbf{e}_1) \\ &+ \mu_u J_{t-1}(\mathbf{x}-\mathbf{e}_1)^+ + \mu_m J_{t-1}(\mathbf{x}-\mathbf{e}_2)^+ + (1-\lambda_t-\mu_u-\mu_m)J_{t-1}(\mathbf{x})], \end{aligned} \tag{2.25}$$

and $J_0(\mathbf{x}) = \gamma J_T(\mathbf{x})$. Here J_t denotes the expected discounted revenue earned when the system is started in period t.

2.1.3.2 Average Revenue Per Cycle

Unlike the previous section, there is no discounting here and the goal is to minimize the average revenue rate obtained in each cycle that is given by

$$\lim_{k\to\infty} \frac{1}{k}\mathbf{E}\left[\sum_{t=0}^{k(T-1)} \lambda_{m,t}(\mathbf{x}(t), p(t))p(t)\right].$$

We can formulate this problem as a dynamic program leading to the following Bellman equation

$$J^* + h(\mathbf{x}) = \max_{\pi\in\Pi}\left[\sum_{t=1}^{T} E[\lambda_m(\mathbf{x}_t, \pi_t(\mathbf{x}_t))\pi_t(\mathbf{x}_t)|\mathbf{x}_1 = \mathbf{x}] + \sum_{\mathbf{x}'\in\bar{S}} q^{\pi}_{\mathbf{x}\mathbf{x}'}h(\mathbf{x}')\right], \tag{2.26}$$

where Π denotes the set of feasible policies that are stationary across cycles, h is the relative value function, and J^* is the optimal expected revenue per cycle. Given that the system started a cycle in $\mathbf{x}$ and policy π is followed, $q^{\pi}_{\mathbf{x}\mathbf{x}'}$ denotes the probability of ending it in state $\mathbf{x}'$. In its current shape the right hand side of (2.26) is quite complex. We can simplify it by writing it as,

$$J_t(\mathbf{x}) = \max_{p \in \mathcal{U}(\mathbf{x})} [\lambda_{m,t}(\mathbf{x},p)(p + J_{t-1}(\mathbf{x}+\mathbf{e}_2)) + (\lambda_t - \lambda_{m,t}(\mathbf{x},p))J_{t-1}(\mathbf{x}+\mathbf{e}_1) \tag{2.27}$$
$$+ \mu_u J_{t-1}(\mathbf{x}-\mathbf{e}_1)^+ + \mu_m J_{t-1}(\mathbf{x}-\mathbf{e}_2)^+ + (1 - \lambda_t - \mu_u - \mu_m)J_{t-1}(\mathbf{x})],$$

and $J_0(\mathbf{x}) = h(\mathbf{x})$. This Bellman equation is identical to (2.25) with the exception of the boundary condition.

2.2 Computational Methods

In this section we describe the computational methods we employ to compute the optimal policy and various suboptimal policies. We also explore how to compute the steady state behavior of the system for these policies. For computational reasons, we limit the number of cars allowed in the unmanaged and managed lanes to a finite number. This assumption is realistic since in a real life setting there is a physical upper bound on the maximum number of cars that can use a highway at any given point in time. But how do we choose the truncation state? It is important to notice that as $\mathbf{x}$ increases, the probability of being in that state will start decreasing eventually due to our assumption $\lambda < \max\{\mu_u, \mu_m\}$. An upper bound for the limiting probability of being in any particular state can be found by employing birth-death models. One can find a truncation state such that the probability of being at that state or higher will be arbitrarily low. Properties of the states lying beyond the truncation point can be estimated by extrapolation or any other similar technique.

2.2.1 Constant Arrival Rate

For both the expected discounted revenue and the average revenue rate criterion, once the optimal value or the relative value function is computed numerically, we can use it to calculate an optimal stationary policy. For the discounted revenue formulation, the value iteration method is a simple and easy way to calculate the optimal value function. We have established that the value iteration method converges in the expected revenue rate case as well. However, in this case the value iteration process can only be used to compute the optimal revenue rate $\lim_{k\to\infty} J_k/k = J^*$ (where J_k is defined as in (2.19)). It only provides an estimate for h^* for some large k, and the process of computing J^* is not numerically stable since the iterates J_k do not converge.

In order to overcome these difficulties, we use a modified version of the value iteration algorithm known as *relative value iteration* (Bertsekas, 2007). Unlike the original value iteration algorithm, we now iterate over the following recursion

$$\begin{aligned} h_{k+1}(\mathbf{x}) &= J_{k+1}(\mathbf{x}) - J_{k+1}(\mathbf{x}') \\ &= \max_{p\in\mathcal{U}(\mathbf{x})} \left[\lambda_m(\mathbf{x},p)p + \frac{\lambda_m(\mathbf{x},p)}{v} h_k(\mathbf{x}+\mathbf{e}_2) + \frac{\lambda-\lambda_m(\mathbf{x},p)}{v} h_k(\mathbf{x}+\mathbf{e}_1)\right. \\ &\quad \left. + \frac{\mu_u}{v} h_k(\mathbf{x}-\mathbf{e}_1)^+ + \frac{\mu_m}{v} h_k(\mathbf{x}-\mathbf{e}_2)^+\right] \\ &\quad - \max_{p\in\mathcal{U}(\mathbf{x}')} \left[\lambda_m(\mathbf{x}',p)p + \frac{\lambda_m(\mathbf{x}',p)}{v} h_k(\mathbf{x}'+\mathbf{e}_2) + \frac{\lambda-\lambda_m(\mathbf{x}',p)}{v} h_k(\mathbf{x}'+\mathbf{e}_1)\right. \\ &\quad \left. + \frac{\mu_u}{v} h_k(\mathbf{x}'-\mathbf{e}_1)^+ + \frac{\mu_m}{v} h_k(\mathbf{x}'-\mathbf{e}_2)^+\right], \end{aligned} \tag{2.28}$$

for some fixed state $\mathbf{x}' \in \mathcal{S}$ instead of J_k. It is easy to see that the iterates h_k eventually converge to an optimal relative reward function h^*. As a result, this procedure does not have those computational issues of the conventional value iteration algorithm. Furthermore, this method also provides us with a way to compute an optimal relative reward function directly. Once we have such

a function h^*, the optimal average revenue rate J^* can be obtained as follows

$$J^* = \max_{p \in \mathcal{U}(\mathbf{x}')} \left[\lambda_m(\mathbf{x}', p)p + \frac{\lambda_m(\mathbf{x}', p)}{v} h^*(\mathbf{x}' + \mathbf{e}_2) + \frac{\lambda - \lambda_m(\mathbf{x}', p)}{v} h^*(\mathbf{x}' + \mathbf{e}_1) \right.$$
$$\left. + \frac{\mu_u}{v} h^*(\mathbf{x}' - \mathbf{e}_1)^+ + \frac{\mu_m}{v} h^*(\mathbf{x}' - \mathbf{e}_2)^+ \right],$$

where we take advantage of the fact that $h^*(\mathbf{x}') = 0$.

Before we explore how we can compute the steady state behavior of the system, we discuss the computation of two different benchmark policies. In the numerical study section, we will be comparing the performance of the optimal policy to the static and myopic pricing policies. Myopic tolls are straightforward to compute since the operator just needs to solve a univariate optimization problem for every state. In the case where V is IFR, we have shown that the process simplifies even further for states with positive expected time savings since the toll becomes the product of some constant k and the expected time savings for that state $\Delta T(\mathbf{x})$. Once we are done computing the myopic tolls, we can compute the resulting value function through the value iteration process for the discounted revenue criterion. For the average revenue rate formulation, we compute the resulting stationary probabilities for the system and use them to compute the myopic revenue rate. The procedure for computing the optimal static toll is slightly more complicated. The starting state is quite important in the discounted revenue criterion since the initial revenue stream that the operator collects from the system is more valuable. For different starting states, the toll that maximizes the initial revenue stream will be different. As a result, there is no single static toll that maximizes the expected discounted revenue over all starting states. However, it is possible to find such a toll for the average revenue rate case. Let p_s denote the static toll, then the problem that the operator needs to solve is the following,

$$\max_{p_s \geq 0} \sum_{\mathbf{x} \in \mathcal{S}} p_s \lambda_m(\mathbf{x}, p_s) q(\mathbf{x}, p_s),$$

where $q(\mathbf{x}, p_s)$ denotes the limiting probability of being in state $\mathbf{x}$ when the static toll is p_s. As will be discussed shortly, there is no closed form solution for the stationary probabilities q, we need

to solve a numerical optimization problem. In our work we used Brent's method (Brent, 1973), which is a well known derivative-free numerical optimization procedure for univariate functions, to compute the optimal static toll.

We now analyze how we compute the steady state behavior of the system. For any stationary policy, the resulting system is a quasi-birth-death (QBD) process. A QBD process is essentially a birth-death process where the state space is two-dimensional (see Latouche and Ramaswami (1987) for a review of QBD processes). In a birth-death process, the process can only transition into one of the neighbouring states. A QBD process has a similar restriction. It can only transition into one of the neighbouring states in one of the dimensions. For the other dimension there is no such restriction.

Unlike a birth-death process, there is no closed form solution for the steady state probabilities in a QBD process. However, formulating our problem within the framework of QBD processes brings us computational advantages. Given the structure of a QBD process, it is always possible to write its generator matrix in a block-diagonal form. By taking advantage of this block-diagonality, it is possible to compute the steady state probabilities of QBD processes faster and in a more robust way compared to the traditional approaches that are employed to compute the steady state probabilities of Markov chains. In this work, we apply the methodology proposed by Baumann and Sandmann (2010) to compute the steady state probabilities.

2.2.2 Variable Arrival Rates

Now, we analyze the non-homogeneous arrival rate case from a computational viewpoint. The value iteration and the relative value iteration techniques described in the preceding section can still be used for both types of objectives with a minor modification. In the constant arrival case the iterates are updated each time by solving a single-stage dynamic program. By analyzing (2.25) and (2.27) we can see that we now need to solve a T-stage finite horizon dynamic program in each iteration. Similar to the constant arrival rate case, we can use the output of this iteration process to compute the optimal stationary policy for both objective criterion. It is important to point out that the policy is now stationary across cycles.

Since the myopic tolls are independent of the arrival rate in each period, i.e., λ_t, they do not change over periods, and we compute them the same way we did in the preceding subsection. We have already discussed that employing a static tolling policy is only possible for the average revenue rate criterion. The counterpart of the static pricing policy in this case is to set a different static toll in every period of the cycle. We find the static tolls as follows. First, using Brent's method we compute a static toll that is constant throughout each cycle. Afterwards, treating this toll as a starting point we iteratively update the toll for each period again using Brent's method. This iterative process is stopped if tolls convergence or we reach a prespecified number of iterations. Clearly, this is a heuristic and may not give us the optimal static toll for each period.

Since the problem parameters vary periodically, there is no stationary distribution in the conventional sense. In order to find an analogue we employ the following strategy. We define the transition between the first periods of consecutive cycles as a single period transition in the Markov chain sense. So, given the system's state at the beginning of a cycle, the one-step transition probability matrix will give the probability distribution for the system's state at the beginning of the next cycle. Unfortunately, this is not a QBD process and we need to compute the limiting probability for this Markov chain using traditional approaches. Once we do that we compute the stationary probabilities for the remaining periods by using the within cycle transition probabilities.

2.3 Numerical Study

In this section we present results from a numerical study for both the constant and time-varying arrival rate models. We use the average revenue rate objective criterion. We believe that this criterion is more suitable for two reasons. First, managed lanes tolls are updated very frequently and the present value of the future revenue decays very slowly. Thus, discounting the future revenue is not very significant. In addition, this choice of objective allows us to evaluate the performance of the static policy.

2.3.1 Constant Arrival Rate

For the three different policies described in the previous section, Table 2.1 reports the average revenue rates for four different sets of capacities and two distinct arrival rates. We will assume that the value of time V is uniformly distributed in $[0, 100]$. We start by comparing the performance of the optimal policy to the myopic and optimal policies. The first observation is that even though the relative performance of the static policy compared to the dynamic policy stays constant, the relative performance of the myopic policy is highly dependent on the problem parameters. In all cases the gap between the optimal and the static policy is around 18%-22%, whereas the gap between the optimal and the myopic policy varies between 9%-44%. More specifically, for fixed capacity, the gap between optimal and myopic policies increases as the intensity of the arrival rates increases. For example, when $\mu_u = \mu_m = 3$, the gap shoots up from 18.08% to 32.60% when λ increases from 2 to 2.5. As a result, we can infer that the benefit of switching to the optimal policy from the myopic policy increases as capacity becomes more scarce. On the other hand, as the problem parameters change, the average revenue obtained through the optimal and the static policies changes in the same direction and roughly the same magnitude. The benefit of switching from the static to the optimal policy stays relatively independent of the problem parameters. Given that the performance of the static policy roughly stays the same, whether or not it performs better than the myopic policy depends on the problem parameters. In cases where the capacity is scarce, the static policy tends to perform better since the myopic policy's performance deteriorates. Lastly, the myopic policy seems to perform the best when the capacities of both lanes are the same.

The expected revenue rates are very sensitive to the changes in problem parameters. In all cases given in Table 2.1, when the arrival rates increase by 25% (λ increases from 2 to 2.5) the revenue rates increase by a factor of 1.5-2.5. The effect seems to be the most dramatic for optimal and static pricing policies when the managed lanes' capacity is less than the unmanaged lanes. Unsurprisingly, when the managed lanes' service rate increases, the revenue rates increase for all pricing policies. Even though the effect of additional capacity for the managed lanes is quite dramatic in the beginning, its influence decreases quickly. An interesting point is that the relative financial benefit of additional capacity for the managed lanes goes down as the arrival rates increase.

Case	λ	μ_u	μ_m	Optimal	Myopic	Static	Myopic Pol. Gap	Static Pol. Gap
1	2	3	2	10.19	7.36	7.99	27.77%	21.59%
2	2	3	3	13.83	11.33	10.98	18.08%	20.61%
3	2	3	4	15.96	11.74	12.49	26.44%	21.74%
4	2.5	3	2	23.65	13.23	18.68	44.06%	21.01%
5	2.5	3	3	28.07	18.92	21.99	32.60%	21.66%
6	2.5	3	4	30.79	18.92	24.29	38.55%	21.11%
7	2	4	2	2.95	2.59	2.35	12.20%	20.34%
8	2	4	3	5.13	4.37	3.99	14.81%	22.22%
9	2	4	4	6.75	6.12	5.51	9.33%	18.37%
10	2.5	4	2	6.21	4.92	4.91	20.77%	20.93%
11	2.5	4	3	9.32	7.13	7.44	23.50%	20.17%
12	2.5	4	4	11.63	9.84	9.15	15.39%	21.32%

Table 2.1: Average revenue rates for different policies.

A possible explanation is that when the arrival rate is low, there is more "competition" between managed and unmanaged lanes, so additional capacity is more beneficial. As the arrival rate increases, there will be more congestion in the system, so the managed lanes will have to compete less for the arriving traffic and, as a result, additional capacity will have a smaller effect on the revenue rate. Lastly, the revenue rates are also quite sensitive to the unmanaged lanes' service rate. We can see that for the same arrival and managed lanes' service rate, the revenue rates decrease by a factor of 2-3.5 when the unmanaged lanes' service rate increases from 3 to 4. Similar to how managed lanes' service rate affects the revenue rate, the effect of unmanaged lanes' service rate on the revenue rate is the most dramatic when the relative congestion in the system is low.

Now, we compare the myopic tolls to optimal tolls. Since V is IFR, we know that the results obtained in Corollary 4 must hold. Table 2.2 lists the ratio of dynamic to myopic tolls. This ratio decreases as the expected time savings from choosing the managed lanes increases, i.e., as the number of cars in the unmanaged (managed) lanes decreases (increases). So, we can see that the optimal strategy involves increasing the toll prices to a much higher level than the myopic when there are too many cars in the managed lanes or too few cars in the unmanaged lanes. The effect of this strategy is twofold. First, the cars in the managed lanes will start to clear out, since new cars arriving to the system will be more likely to choose the unmanaged lanes. This will in turn cause congestion in the unmanaged part of the system. As congestion starts building up in the

x_u \ x_m	**0**	**1**	**2**	**3**	**4**	**5**
0	0.00	0.00	0.00	0.00	0.00	0.00
1	1.75	0.00	0.00	0.00	0.00	0.00
2	1.59	2.00	0.00	0.00	0.00	0.00
3	1.54	1.81	2.00	0.00	0.00	0.00
4	1.52	1.70	2.00	2.00	0.00	0.00
5	1.50	1.64	1.84	2.00	2.00	0.00

Table 2.2: The ratio of optimal to myopic tolls for $\lambda = 2.5$, and $\mu_u = \mu_m = 3$.

unmanaged lanes and the managed lanes start clearing out, the operator brings the optimal toll closer to the myopic toll to *harvest* the congestion in the unmanaged lanes. We call this approach *jam and harvest* where the operator intentionally causes additional congestion in the free part of the system with the intention of harvesting it later by charging a high price. Another important observation about the toll ratios is the fact that it increases diagonally in Table 2.2. So, for two different states of the system where the time savings are equal, the optimal toll will be higher for the state that has more cars. A possible explanation for this is as follows. Take two systems that are in two different states, where choosing the managed lanes has the same expected time savings. Compared to the other system, the system with more cars has a higher probability of experiencing states in which the unmanaged lanes have relatively more congestion. So, in order to protect managed lanes capacity for such a situation, the state with more cars charges a higher toll.

Lastly, we analyze how the three policies effect the steady state behavior of the system. Figure 2.1 depicts the steady state probabilities for managed and unmanaged lanes. From the figure we can deduce that the myopic policy keeps the unmanaged lanes the least congested while the static policy keeps them the most congested. It is the other way around for the managed lanes. Since the myopic policy always underprices compared to the optimal policy, it utilizes the managed lanes the more than either of the other policies. In the static policy we do not have the capability of adjusting the toll as the state changes, so it is set to a relatively high level to exploit the situations where the unmanaged lanes are the most congested. As a result, the managed lane utilization rate is lower than the other two policies.

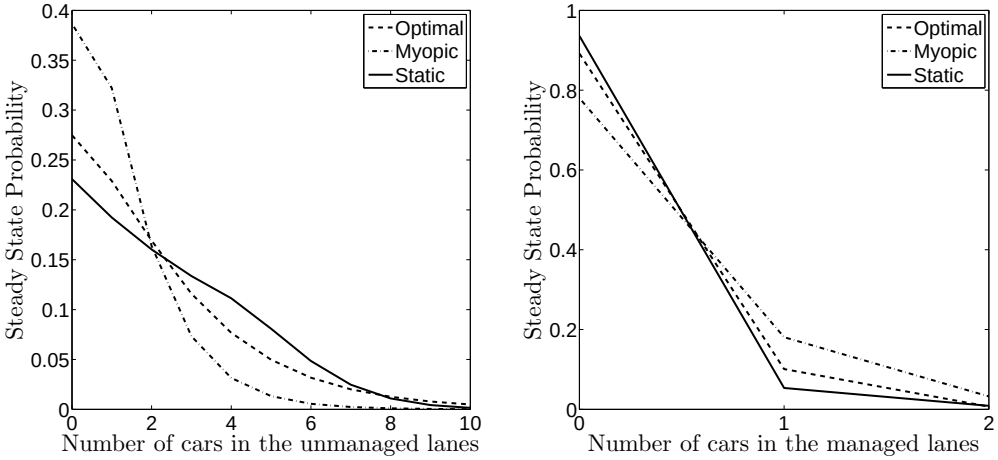

(a) Unmanaged lanes (b) Managed lanes

Figure 2.1: Steady state probabilities when $\lambda = 2.5$, and $\mu_u = \mu_m = 3$.

2.3.2 Variable Arrival Rate

Unlike the previous case, the arrival rates are no longer constant and follow the model described in §2.1.3. In this section we assume that $V \sim U[0, 10]$. The three different arrival patterns that are going to be analyzed are given in Figure 2.2. All of them have the same average arrival rate over a cycle but with different intensities for each period. One of the patterns provides a constant steady stream of arrivals and it will constitute the base case for our analysis.

Let us first start by analyzing how the variability in the arrival pattern effects the optimal toll structure. The left y-axis in Figure 2.3 is the arrival rate. The right y-axis in the figures are the average tolls charged in each period normalized by the first period's optimal tolls. Specifically, for each period, we normalize the toll for each state according to that state's toll in the first period, and calculate the expected normalized toll. We see that the expected normalized toll starts increasing before the arrivals rates go up. This is an important observation similar to the jam and harvest property of the optimal policy in the constant arrival rate case. It implies that anticipating the increase in arrival rates, the operator starts increasing the tolls beforehand. As a result, when the rush hour is reached the unmanaged lanes are already congested and the operator can exploit this to maximize his revenue. From Figure 2.4 we see that the static policy has a similar structure since

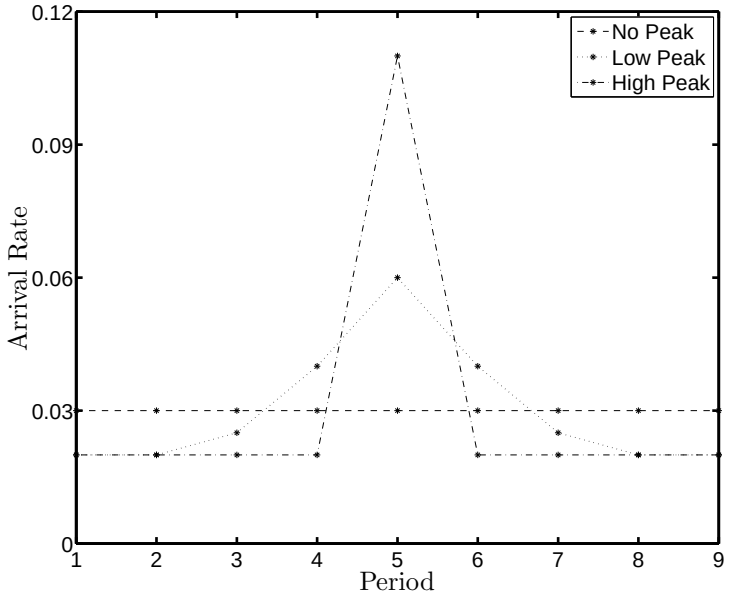

Figure 2.2: Nonhomogenous arrival rates.

operator starts increasing the tolls in anticipation of the peak arrival rate.

Now, let us compare what happens in each of the three arrival rate patterns. Table 2.3 reports the average revenue rates for optimal, myopic and static policies. An interesting question is how the variability in arrival rates affect revenues. Will the operator do better in the stability of constant arrival rates? Or will he be able to somehow take advantage of the peak arrival rates? We see that as the impact of the peak increases, in other words, as the variability in arrivals increase, the average revenue rate decreases for all three policies. In this example, everything else held equal, the operator will prefer the case of steady arrival arrival rates. We also see that there is no significant difference in the optimality gaps and they seem to be in line with the observations we made for the constant arrival rate case. Lastly, the myopic policy seems to be doing better than the static policy. However, we cannot generalize this result. As we demonstrated in the constant arrival rate case, which of these two policies outperforms the other one depends heavily on the problem parameters.

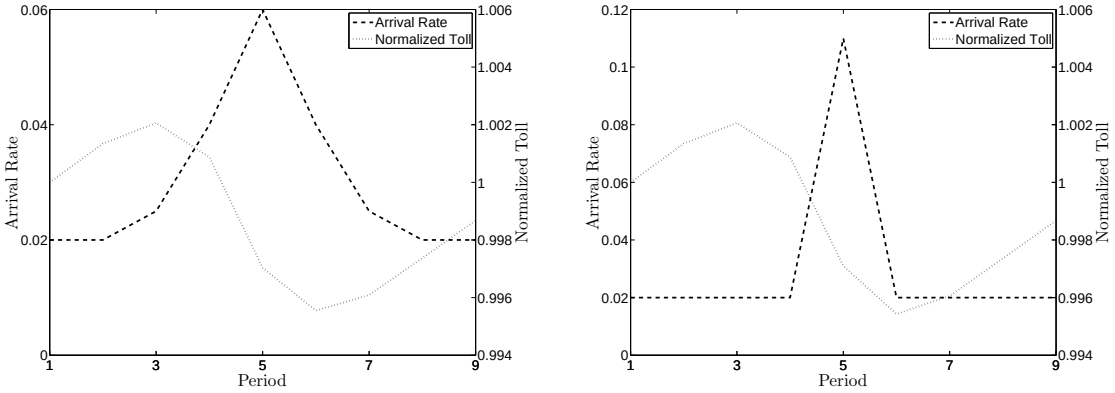

(a) Low peak case. (b) High peak case.

Figure 2.3: Normalized optimal tolls and arrival rates.

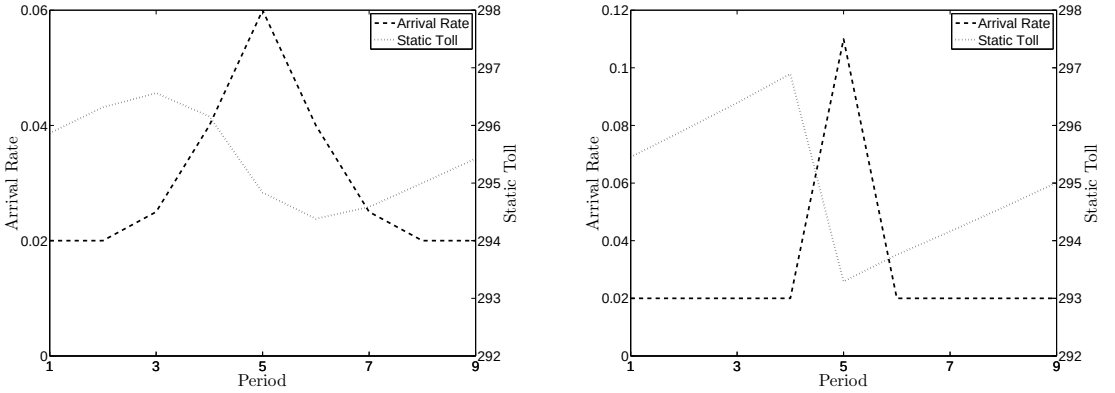

(a) Low peak case. (b) High peak case.

Figure 2.4: Static tolls and arrival rates.

2.4 Conclusion

In this chapter we analyzed the problem of setting revenue maximizing tolls for managed lanes. Our model was based on $M/M/1$ queueing models and allowed us to analyze the first order effects of congestion. We also introduced a variant of the stochastic model that takes into account the non-homogeneity of the traffic flows.

We found that dynamic pricing can provide significant revenue improvements over both static and myopic policies. We showed that the optimal policy has a very simple form. It is monotonic with respect to the number of cars in the system. Furthermore, we demonstrated that the myopic

policy always underprices compared to the dynamic policy. We observed that the relative difference between myopic and optimal tolls decreases as the unmanaged lanes are relatively more congested. For the time-varying arrival rate case we observed that the toll operator should increase the tolls before the peak arrival period. In the next chapter we will see that this aspect of the optimal tolling strategy turns out to be crucial.

We believe that the modeling approach we employ in the non-homogeneous arrival rate case can find applications in other areas where repetitive cyclic demand is observed, e.g. as call center staffing. An interesting open question is how the results in this chapter would change if the focus was on social welfare maximizing policies.

Case	Optimal	Myopic	Static	Myopic Pol. Gap	Static Pol. Gap
No Peak	9.43	8.11	7.34	14.03%	22.16%
Low Peak	9.39	8.08	7.31	13.97%	22.23%
High Peak	9.26	7.98	7.18	13.77%	22.44%

Table 2.3: Average revenue rates for different arrival patterns.

Chapter 3

Simulation Based Optimization for Pricing Managed Lanes

In this chapter we continue analyzing the pricing of managed lanes. Unlike the previous chapter, we take a more practical point of view of the problem. Through the use of a traffic simulator, we demonstrate how revenue maximizing tolls can be computed in practice. We also conduct an extensive numerical study to analyze the impact of such policies.

3.1 Traffic Simulation

We borrow our simulation methodology from the dynamic traffic assignment (DTA) literature that primarily deals with the problem of computing the user equilibrium and system optimal traffic flows on a transportation network. The solution approaches to these problems can be classified in two categories: analytical and simulation Peeta and Ziliaskopoulos (2001). Analytical approaches typically employ tools such as mathematical programming, optimal control and variational inequality to model traffic systems. Due to the ill-behaved nature of DTA problems, they are unsuitable for applications such as ours where real-time decisions influence drivers' behavior (Burghout, 2005).

Simulations can be categorized as macroscopic, microscopic and mesoscopic. In macroscopic simulations, aggregate traffic flows are calculated and individual vehicles are not modeled. Since

they do not model individual behavior, we cannot incorporate how drivers react to congestion and toll changes when they are making their routing decisions (Burghout, 2005). Two well known macroscopic simulation models are the LWR model that was devised by Lighthill and Whitham (1955) and Richards (1956), and the cell transmission model (CTM) that was introduced by Daganzo (1994).

Unlike macroscopic simulations, mesoscopic and microscopic simulations capture a greater level of detail by keeping track of individual vehicles with the latter being more detailed. Microscopic simulations model traffic dynamics in a detailed manner by building upon car following and lane changing models that are prevalent in the literature. This enables the microscopic approach to model the interactions between drivers themselves and how they change their behavior with changing road conditions. MITSIM, VISSIM and PARAMICS are some of the most well known microscopic simulation models (Olstam and Tapani, 2004).

However, the level of detail that microscopic simulations can capture comes at an additional cost. Compared to the other two approaches, there are many more parameters in this model that require calibration and the computational time required to run such a model is considerably much longer. Therefore, we will be employing the mesoscopic simulation approach in this study. In mesoscopic simulations the road is typically divided into several links and at each time step the vehicles are moved from one link to another by making use of speed, flow, and density relationships. The two most prominent mesoscopic simulation models are the DYNASMART (Jayakrishnan *et al.*, 1994) and the DynaMIT (Ben-Akiva *et al.*, 2002) upon which our simulation model is based. In our context, these two models are almost identical with the exception of a few details.

3.1.1 Model Description

In our traffic module, the highway is divided into various segments with equal length L. The number of lanes in each segment is denoted by w and the average space that a car occupies (including its headway at jam density) will be denoted by ℓ. As a result, the physical capacity of each segment is $w \times L/\ell$.

The segments will be split into two parts: moving and queueing. Cars that are queued up to

join the next segment will be in the queueing part and the remainder of the cars in the segment will be in the moving part. The lengths of both parts are dynamic and depend on the number of cars in the queueing part. Given that there are n_q cars queued, the length of the queueing part is $n_q\ell/w$. Accordingly, the length of the moving part is $L - n_q\ell/w$.

At each time step in our simulation, the vehicles in the moving part will traverse the segment according to the following two-regime speed-density relationship

$$v(k) = \begin{cases} v_{\max} + \beta_1 k, & \text{if } k \leq k_{bp}, \\ v_{\min} + \beta_2(1 - (k/k_j)^{\alpha_1})^{\alpha_2}, & \text{if } k > k_{bp}, \end{cases} \tag{3.1}$$

where k is the density of the moving part of the segment at the beginning of the time step, $v_{\max}$ is the free-flow speed, $v_{\min}$ is the minimum speed, k_j is the jam density, and α_1, α_2, β_1 and β_2 are user-specified parameters. All speeds are in mph and densities are in vehicles/mile/lane unless otherwise noted. After a car has traversed a segment it has two options. If there is space in the next segment, it will pass on to that segment directly and travel on that segment for the remainder of the time step. Otherwise, it will join a queue at the end of the segment.

In each time step the movement of cars is calculated in three stages. In the first stage, cars in the moving segment move according to the speed-density relationships in (3.1), and the ones that reach the end of the segment move into a queue to await transition into the next segment. We update the position of each car starting from the one that is closest to the highway's end and move towards the beginning of the highway. In the next step, cars move from the queues at the end of each segment to the next segment. Cars are allowed to pass on to the next segment until it reaches jam density. We allow partial cars to pass on to the next segment. The last step involves moving the cars that just changed segments. If a car waited in the queue for at least one iteration, then it is moved according to the prevailing moving part speed of its previous segment. Otherwise, that is if the car joined the queue in that iteration, it completes its movement by traveling the amount it was not allowed to complete before joining the queue.

Once the vehicles are moved, we calculate the expected travel times for each segment. The

expected travel time for each segment consists of the time it takes for a vehicle to traverse the moving part of a segment (T_m), and the waiting time in the queue (T_w). Let q_w denote the number of cars waiting in the queueing part of a segment, then the moving time is,

$$T_m = \frac{L - q_w \times \ell \times w}{v(k)},$$

and the waiting time is,

$$T_w = q_w/d,$$

where d is the moving average of the discharge rates observed in the previous periods. Those times are calculated for each segment and are turn used to calculate the expected travel time for both parts of the highway. The travel times are fed into the consumer choice model to calculate the demand for each part of the highway at the next time step.

Our traffic flow model is structurally identical to DYNASMART. It is also similar to DynaMIT, although we use a slightly different approach to calculate moving times and waiting times. These models have been used in many studies and have been extensively validated (Han *et al.*, 2006; Roelofsen, 2012; Ben-Akiva *et al.*, 2010).

3.1.2 Traffic Simulation Calibration

In our simulation, the speed in each segment is determined by the density in that segment according to equation (3.1). Figure 3.1 shows a scatterplot of the speed and density for the unmanaged lanes in the SR-91, for weekdays during the first four weeks of July 2011. We chose this period because there was no rain. The data is obtained through PeMS for VDS 1208147 with an aggregation level of 5 minutes. We deleted approximately 17% of the datapoints as outliers resulting from lane closures and accidents, resulting in 5,760 observations.

The black line in Figure 2 is the speed-density relationship that we fit to this data. We set the jam density to 100 vehicles/mile/lane since there were only three observations with densities greater than 100. We eliminated those three observations from our dataset. We set the minimum speed $v_{\min}$ to 15 mph in accordance with the average speed observed when density is around 100

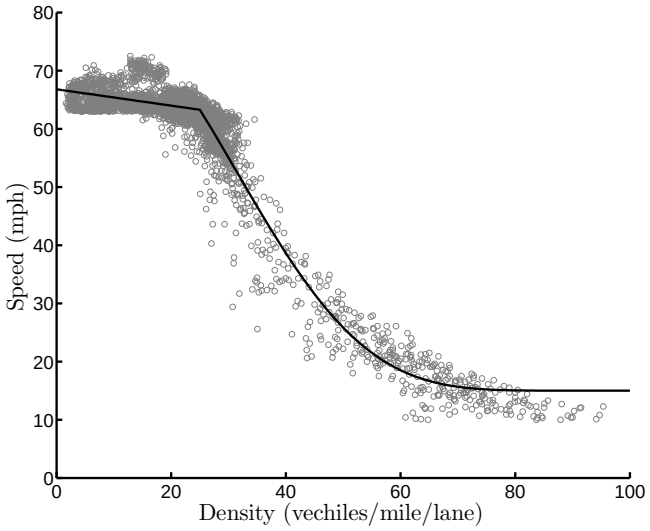

Figure 3.1: Speed-density relationship for SR-91.

vehicles/mile/lane. We set the simulation time-step to a minute. We found that the moving average of the last five periods gave a fairly accurate representation of the discharge rate from each segment when it is congested.

We set the breakpoint density to 25 vcl/m/ln because it minimizes the sum of squared residuals from both models. We used OLS regression to estimated the parameters for the first (linear) regime and NLS regression to estimate the parameters in the second (nonlinear) regime. After the estimation procedure we readjusted β_2 to avoid discontinuity at the breakpoint density. Table 3.1 gives the parameters we used in the simulation that were obtained through the abovementioned estimation procedure.

Since the current SR-91 policy sets tolls to encourage free-flow conditions in the managed lanes, there is no data for more congested conditions in the managed lanes. For this reason, we use the same speed-density relationship given by Figure 3.1 for both parts of the highway. Since the

Speed (mph)		Density (vcl/m/ln)		Slope		Shape	
$v_{\min}$	15.00	k_{bp}	25	β_1	-0.14	α_1	2.22
$v_{\max}$	66.80	k_j	100	β_2	69.33	α_2	7.69

Table 3.1: Parameters for the simulation model.

managed lanes run parallel to the unmanaged lanes, this is a reasonable assumption.

Similar to SR-91, the number of managed lanes is set to two. The number of unmanaged lanes on the SR-91 differs between four and five. In addition, different sections of the highway have different speed-density relationships. For the purposes of this study, we will assume that the highway we are analyzing is 10 miles long and consists uniformly of five unmanaged lanes with the speed density relationship given in Table 3.1. Since we are not accounting for the full geometric structure of SR-91, the travel times obtained by this simulation do not accurately represent the travel times observed on the SR-91.

3.2 Demand Generation

We generate traffic arriving to the system in two steps. In the first step we generate hourly demands, and in the second step we distribute the hourly traffic into five-minute intervals.

To calibrate the hourly demand generator we used the eastbound hourly flow information for the SR91 from January 2009 to August 2011. We combine the volume information from the managed and unmanaged lanes to calculate the total volume of traffic using the highway. Traffic data for managed lanes comes from VDS 1208156 and for unmanaged lanes we use the data from VDS 1208147. Figure 3.2 depicts the average hourly traffic volumes for each day of the week for Monday through Friday. From the figure we can see that the arrival pattern is very similar for all days. Thus, we will use the same hourly demands for each day of the week.

Starting from midnight, we generate hourly traffic loads according to

$$Y_t = \beta_t + \alpha_t^1 Y_{t-1} + \alpha_t^2 Y_{t-2} + \alpha_t^3 Y_{t-3} + \varepsilon_t, \tag{3.2}$$

where Y_t is the traffic volume for hour t; $\beta_t, \alpha_t^1, \alpha_t^2$ and α_t^3 are coefficients and ε_t is a normally distributed error term. We estimated the parameters of (3.2) using OLS regression. To start generating hourly loads from midnight and onwards, we need starting values for the hours 21, 22 and 23. For simplicity, we sampled the demand for these three hours from normal distributions whose means, standard deviations and pairwise correlations match their real-life values. These

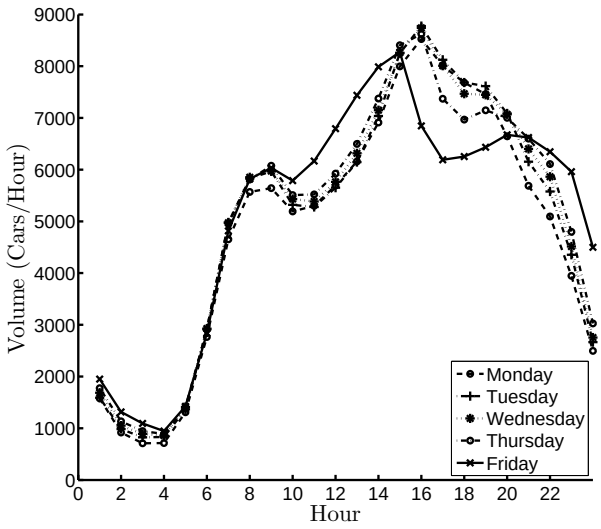

Figure 3.2: Average hourly volumes for SR-91 Eastbound between January 2009 - July 2011.

statistics can be found in Tables A.2 and A.3 in Appendix A.

In order to test the validity of this approach we generated 1000 sample paths and compared their statistics to the real-life traffic data. Figure 3.3 depicts the hourly means, standard deviations and autocorrelation (with a lag of one) for both the data and the sample paths. As can be seen from the figure, the statistics of the generated demand matched those of the real-life data quite well. Table A.1 in Appendix A gives the parameters for the fitted demand model.

In the next step we distribute the hourly traffic into five-minute intervals. For this purpose we used five-minute traffic volume data for July 2011. We omitted the first week of July due to the Independence Day holiday. For each hour, we calculated the fraction of hourly demand during in each 5-minute interval. By averaging those fractions across all days in our dataset, we calculated the average proportion of hourly demand each 5-minute interval for each hour. The results are shown in Table A.5 of Appendix A.

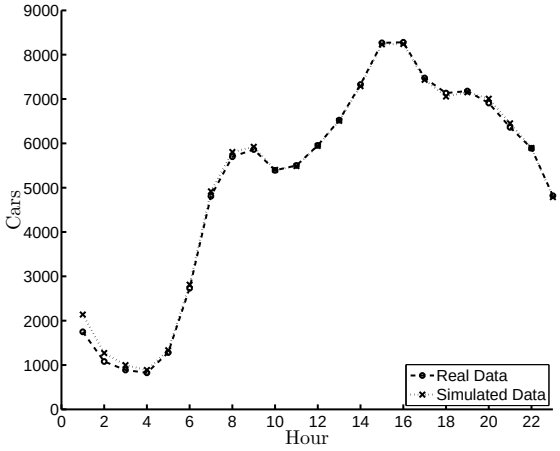

(a) Comparison of means

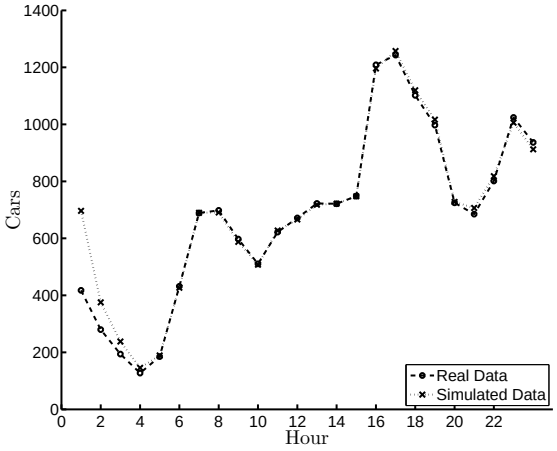

(b) Comparison of standard deviations

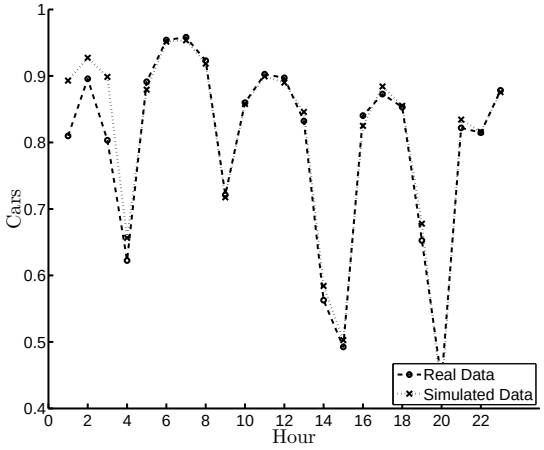

(c) Comparison of autocorrelations with a lag of one

Figure 3.3: Demand model validation

3.3 Consumer Choice Model

At the time a car enters the system, the driver chooses either the managed lanes or the unmanaged lanes. Each driver bases his decision on the expected travel time savings and the toll (Xu, 2009; Yin and Lou, 2009). We use historical data on lane choice for the SR91 to estimate the parameters of a consumer choice model as in Liu *et al.* (2004) and Liu *et al.* (2007). The expected travel time savings from choosing the managed lanes at time t is denoted by $\Delta T(t)$ and the toll by $p(t)$. Let $U_{in}^{(k)}(t) = g_{ik}(t) + \varepsilon_{in}$ denote the utility that driver n receives at time t by choosing alternative

$i = u, m$, where u and m denote the unmanaged and managed lanes, respectively. The index k denotes the structure we employed for the deterministic part of the utility function. The term ε_{in} accounts for driver n's unobserved utility from choosing alternative i. For the unmanaged lanes, the deterministic part of the utility function $g_{uk}(t)$ is set to zero. The different structures we estimated are,

$$
\begin{aligned}
g_{m1}(t) &= \beta_T(t)\Delta T(t) + \beta_p(t)p(t), \\
g_{m2}(t) &= \beta_T(t)\log(\Delta T(t)) + \beta_p(t)p(t), \\
g_{m3}(t) &= \beta_T(t)(\Delta T(t))^2 + \beta_p(t)p(t).
\end{aligned}
$$

The first model corresponds to the standard case in which a driver's utility increases linearly with the expected time savings. The second model corresponds to the case in which drivers get less sensitive to the expected travel time savings as it increases, and the latter model corresponds to the case where they become more sensitive. In all cases we allow β_T and β_p to vary over time.

For both lanes, we assume that the random term in the utility function is independently and identically distributed across drivers according to a Type I Extreme Value distribution. After evaluating the utility of both alternatives, each driver chooses the alternative for which he enjoys the highest utility. The probability that a driver chooses alternative i at time t is given by the logit function (Ben-Akiva and Lerman, 1985)

$$
P_i^{(k)}(t) = \frac{e^{g_{ik}(t)}}{1 + e^{g_{mk}(t)}}. \tag{3.3}
$$

We estimated β_T and β_p using maximum likelihood estimation (MLE). We use the same VDS sensors that we used in the previous section. We analyzed the lane choice decisions of eastbound commuters on SR-91 from Monday through Friday during the last two weeks of July 2011. Traffic in this direction has an afternoon peak as shown in Figure 3.2. Figure 3.4 shows the minimum, maximum and average hourly time savings observed in our dataset. Not surprisingly, the expected travel time savings is highest during the afternoon peak. There is also significant variation between

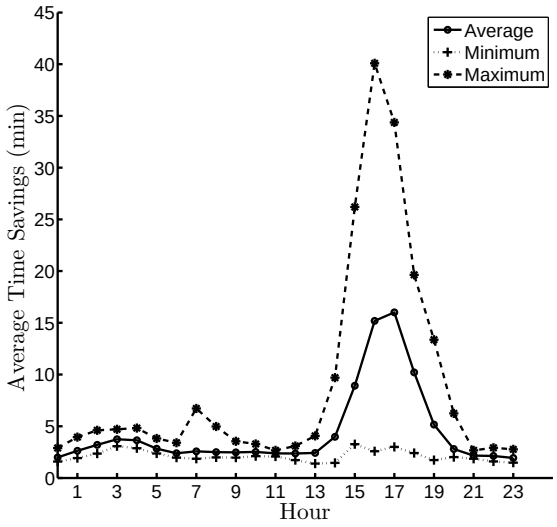

Figure 3.4: Average hourly time savings.

the time savings observed throughout this two week period.

From Figure 3.5 we can see that managed lanes traffic peaks in the afternoon when both the traffic load and the time savings are highest. During the off-peak hours, the managed lanes command a very low share of the traffic passing through this segment of the highway.

Currently, in SR-91 tolls are set ahead of time and vary hourly. Figure 3.6 shows how the tolls varied from Monday through Friday in the July-December 2011 period. The variation in tolls is quite dramatic: during the off-peak hours the toll goes as low as \$1.30, and during the peak hours it is as high as \$9.75. The aim of the SR-91 operator is to maintain free-flow conditions on the managed lanes. As a result, the structure of the tolls mirrors the expected travel time savings quite closely. The operator updates the tolls every few months to adjust for changing traffic patterns.

The SR-91's policy leads to high correlation between the tolls and time savings. Similar to Lam and Small (2001), to come up with estimates for β_T and β_p we exploit the variation in time savings during the peak hours when the tolls do not change very much. Figure 3.7 plots the average ratio of expected time savings to tolls in five minute intervals. There is significant variation in that ratio during both peak and early morning hours. For our analysis we choose the afternoon peak hours, specifically between the hours of 2pm and 8pm, since the traffic volume is significantly higher

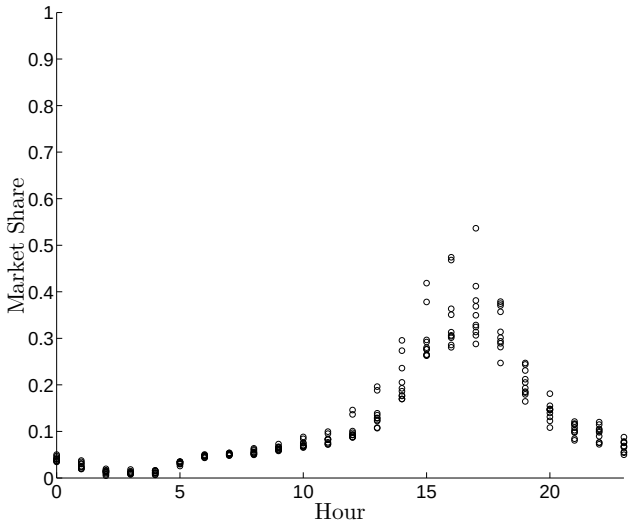

Figure 3.5: Hourly market share of the managed lanes.

compared to the early morning hours.

Now, we are in a position to use MLE to estimate β_T and β_p. The dataset we use contains the number of cars that chose the unmanaged and managed lanes between 2pm and 8pm in five minute granularity. It also contains the expected time savings the cars choosing the managed lanes enjoyed as well as the tolls they paid. There are 390,310 cars that chose the unmanaged and 140,931 that chose the managed lanes in the dataset.

In the estimation procedure we treat the aggregated five minute market share of the managed lanes as the dependent variable. The weight of each observation is equal to the total number of cars that pass through the unmanaged and managed lanes in that five minute timeframe.

We evaluated the performance of the three different structures introduced for g_{uk}. For each structure, we tested four models which correspond to cases where the coefficients are allowed to vary over time or kept fixed. In the former case, different values for coefficients are estimated on a hourly basis. The coefficients for a given point in time are determined by taking the weighted average of the estimates corresponding to the current and upcoming hour, where the weights are obtained proportionally. For example, the coefficients at 2:20pm would be the weighted averages of the coefficients for 2pm and 3pm with the weights 2/3 and 1/3, respectively. The summary of

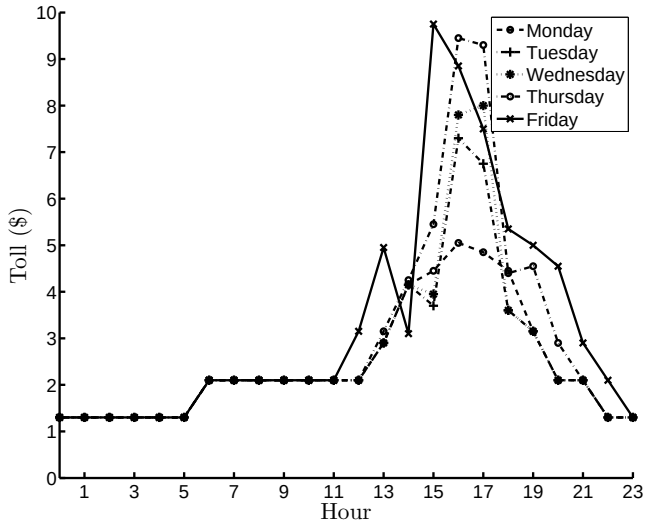

Figure 3.6: Hourly tolls for the managed lanes.

the models that were tested can be found in Appendix B. We use Model 3-2, which corresponds to the case of $k = 3$, as it has the best fit of the model with the correct signs on the coefficients. For the hours outside of the 2-8pm range, we use the coefficients corresponding to 8pm.

The goodness-of-fit plots for Model 3-2 are given in Figure 3.8. The color of each point in the scatterplots depicts its weight. The darker a point is, the more weight it has. From the plots we can see that the model fits reasonably well to the data and there is no evident bias.

We did not account for high occupancy vehicles in our choice model. Under SR-91s tolling policy, cars that have at least three occupants (HOV3+) can use the managed lanes for free except between 4pm-6pm when they have to pay 50% of the toll. According to traffic counts performed on the eastbound direction of SR-91 between 3.30pm-5.30pm, only 3.7% of the total cars that entered into the unmanaged and managed lanes were in the HOV3+ category (Sullivan, 2000). Because this percentage is so low, we do not feel that omitting the HOV3+ category significantly influenced our results.

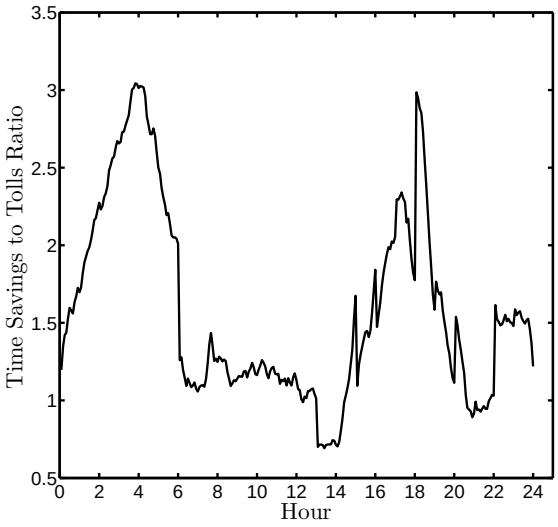

Figure 3.7: The average ratio of time savings to tolls.

3.4 Problem Formulation

3.4.1 Policy Description

Our goal is to compare policies for the managed lanes in terms of expected revenue generated. We consider both adaptive and non-adaptive policies. Adaptive policies adjust tolls dynamically depending on real-time traffic conditions, whereas non-adaptive ones keep tolls fixed regardless of the system's state.

We use a discrete time approach in which we divide the planning horizon into T intervals, and t denotes the interval index. The number of cars that arrive in an interval is random, and is denoted by the random variable $D(t)$. We assume that the toll stays constant over each interval. This is non-restrictive because all dynamic tolling schemes implemented to date enforce a minimum period between toll changes – for example, five minutes in the case of the LBJ Project. For the remainder of this section, the subscripts u and m denote unmanaged and managed lanes, respectively. The number of cars in the lanes and their locations are denoted by $x_i(t)$ for $i = u, m$.

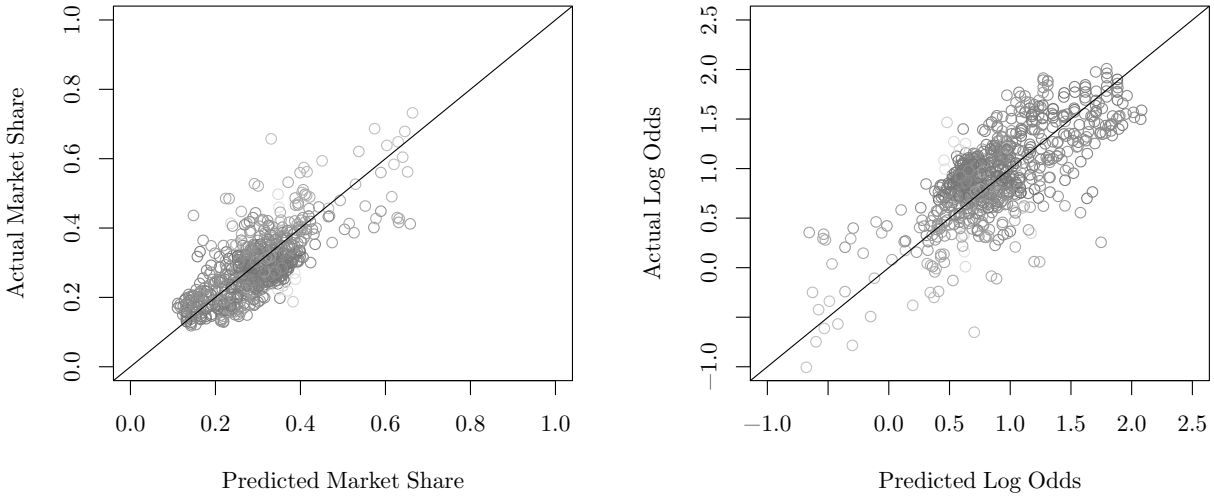

(a) Actual vs. predicted market shares

(b) Actual vs. predicted log of odds

Figure 3.8: Consumer choice model goodness-of-fit plots.

The revenue maximization problem for a non-adaptive policy is

$$\begin{aligned} \max \ & \sum_{t=1}^{T} \mathbb{E}\left[D(t)P_m^{(k)}(t)\right] p(t) \\ \text{s.t. } & x_i(t+1) = f_i(D(t), p(t), x_m(t), x_u(t)), \forall t \in \{1, \ldots, T-1\}, \ i = \{u, m\}, \\ & p(t) \geq 0, \forall t \in \{1, \ldots, T\}, \end{aligned}$$

where the mapping $f_i(.)$, for i in $\{u, m\}$, updates the list of cars and their locations in every period. The solution to this problem is a *time-of-use* policy since it tells the toll manager how much to charge at each point in time independent of the real-time state of the system.

The discrete-time counterpart of the adaptive policy is

$$\begin{aligned}
\max \ & \sum_{t=1}^{T} \mathbb{E}\left[D(t)P_m^{(k)}(t)\right] p(t, x_u(t), x_m(t)) \\
\text{s.t. } & x_i(t+1) = f_i(D(t), p(t, x_u(t), x_m(t)), x_m(t), x_u(t)), \forall t \in \{1, \ldots, T-1\},\ i = \{u, m\}, \\
& p(x_u(t), x_m(t)) \geq 0, \forall t \in [0, T].
\end{aligned}$$

Compared to the previous model, the toll is now dependent on the state of the system at each point in time as well as the time. The optimal adaptive policy is quite hard to compute due to the curse of dimensionality. We consider two simple heuristics.

The *myopic* tolling policy maximizes the *revenue rate* from the system according to the current travel time difference:

$$p(t) = \text{argmax}_{p \geq 0} P_m^{(k)}(t) p.$$

The major shortcoming of the myopic policy is its inability to take into account the future congestion effects due to the lane choice of arriving traffic. This also contributes to the simplicity of this policy since no calibration is necessary to implement it. Every time the toll is updated, the revenue rate maximizing toll can be computed numerically. We employ Brent's method which is a popular robust derivative-free approach for this purpose (Brent, 2002).

We also consider a more complex adaptive policy. This policy takes a set of base time-of-use tolls $\{\bar{p}(t)\}_{t=1}^{T}$ and travel time savings $\{\Delta\bar{T}(t)\}_{t=1}^{T}$ as inputs. Every time the toll is updated, it compares the current travel time savings to the base values. If the system is more congested than expected, the policy increases the toll relative to the base toll. If there is less congestion than expected, the policy decreases the toll. The form of this policy is given by

$$p(t, \Delta T(t)) = \bar{p}(t) + \alpha^{+}(t)(\Delta T(t) - \Delta\bar{T}(t))^{+} - \alpha^{-}(t)(\Delta\bar{T}(t) - \Delta T(t))^{+}, \tag{3.4}$$

where $\alpha^{+}(t)$ and $\alpha^{-}(t)$ are positive scalars. Since the tolling adjustments are based on linear travel time differences, we call this policy as the *linear travel time difference* (LinTD) policy.

3.4.2 Policy Calibration

In order to calibrate these two policies we used a combination of nonlinear optimization heuristics and stochastic approximation.

Our calibration strategy for both policies can be summarized as follows. First, we employed nonlinear optimization heuristics such as the Nelder-Mead and Brent's method to find initial starting points. Later, we fed these starting points into the stochastic approximation optimization routine.

Stochastic optimization problems are generally solved by iterative algorithms that start from some trial solution and update the trial solution using the stochastic gradient of the objective function. For maximization problems, this procedure is of the following iterative form

$$x_{k+1} = x_k + a_k g_k(x_k),$$

where k is the iteration index, $x_k \in \mathbb{R}^n$ denotes the current solution, $a_k \in \mathbb{R}^n_+$ is the updating step size that typically decreases in k, and $g_k(.)$ is the stochastic gradient estimate. If there are any constraints on the decision variables, the updated values are projected onto the set of feasible values to ensure that the constraints are satisfied.

Since no direct measurements of the gradient are available in our case, we employ the finite differences stochastic approximation (FDSA) method that estimates the gradient by calculating the difference quotient one-by-one for each decision variable using the Monte Carlo method. Kiefer and Wolfowitz (1952) introduced this method for univariate optimization problems and Blum (1954) extended it to the multivariate case. Let Ω denote the set of possible realizations of a random process, and $y(x, \omega)$ be a function whose value depends on some variable $x \in \mathbb{R}^n$ and the realization of the random outcome $\omega \in \Omega$. Using the FDSA method the gradient estimate of $y(.)$ for each iteration is obtained by

$$(\hat{g}_k(x_k))_i = \sum_{j=1}^{m} \frac{y(x_k + e_i c_k, \omega_{kj}) - y(x_k - e_i c_k, \omega_{ki})}{2c_k}, \ \forall i = 1, \ldots, n,$$

where c_{ki} is a small positive scalar that decreases in k, and $e_i \in \mathbb{R}^n$ is the unit vector in direction i.

Typically, smoothness and the differentiability of the objective function are required to establish convergence (Spall, 2003). In our problem the objective function is not tractable and we can assert neither smoothness nor differentiability. Thus, convergence is not guaranteed. Furthermore, due to the ill behaved nature of the problem, the final set of decision variables may depend on the initial starting points. So, the stochastic approximation methodology is purely a heuristic in our setting and is not guaranteed to terminate at a locally optimal solution. We stop the algorithm after a predetermined number of iterations denoted by $n_{\max}$.

The use of FDSA to calibrate the time-of-use policy is quite straightforward. Starting from a set of initial tolls, in each iteration the tolls are successively updated. The linear travel time difference policy needs three different sets of inputs: base tolls and time savings, and the adjustment factor α. For simplicity, rather than calibrating all three sets of parameters altogether, we use the output of the time-of-use policy for the base tolls and time savings. Specifically, we take the tolls calibrated for the time-of-use policy as the base tolls and the resulting expected travel time savings as the base travel time savings. Then, we calculate the adjustment factor using the FDSA method.

3.5 Numerical Study

In this section we conduct a numerical study to evaluate the performance of the tolling policies that were previously discussed. We start with two case studies where we analyze the Eastbound and Westbound directions on SR-91. We then perform a brief sensitivity analysis where we investigate the influence of various factors on our results. All the software components we use were coded in Java. We also made use of Nelder-Mead, a derivative-free nonlinear optimization heuristic for multivariate problems, and Brent's method implementations in Apache Commons Math (The Apache Software Foundation, 2013).

3.5.1 Case Studies

Example 1: Eastbound Direction. In this example we analyze the Eastbound traffic scenario. The calibration of the demand generation and consumer choice model components for this direction

were described earlier in §3.2 and §3.3. For variance reduction purposes, we generated 1000 sample paths for the traffic demand and, unless stated otherwise, we performed our analysis on the same set of sample paths in every case.

For the myopic policy, Table 3.2 reports the average revenues and the 90% confidence intervals for the revenue differences compared to the policy with the 1 minute tolling update. From the results we can see that there is a slightly consistent decrease in the expected revenues as the tolling frequency decreases. However, since all confidence intervals contain zero we cannot conclude that this decrease is statistically significant. Thus, the tolling frequency does not appear to have a significant effect on the performance of the myopic policy. Figure 3.9 shows the average myopic toll (60 min. tolling interval) and the average hourly traffic load. During the off-peak hours, the average toll is relatively stable. During the peak hours, the toll increases as the congestion build-ups in the unmanaged lanes, and later decreases to its off-peak value.

We continue our analysis with the time-of-use policy. We explored the performance of a hourly time-of-use tolling schedule to match the real-life implementations of such policies. Before starting the stochastic approximation procedure, we obtained two different starting points. For the first one we assumed that the demand is deterministic and equal to its certainty equivalent (CE) values. In the second case, we optimized over hundred randomly drawn sample paths (sample average approximation). We used the Nelder-Mead nonlinear optimization heuristic, and we tried one hundred different random starting points in each case. The resulting tolls are shown in Table C.1 of Appendix C.

In the stochastic approximation procedure we used the following sequences: $c_k = 0.5/k^{1/6}$, $a_k = a/(A+k)$ with $a = 1$ and $A = 100$ when $n_{\max} = 1000$, and $a = 5$ and $A = 500$ when $n_{\max} = 5000$. We also set the tolls' upper bound to \$100. Figure 3.10(a) depicts the tolls obtained

Tolling Interval	1 min.	5 min.	10 min.	15 min.	20 min.	30 min.	60 min.
Avg. Rev.	\$125,157	\$125,095	\$124,859	\$124,647	\$124,547	\$124,510	\$124,511
C.I. Lower Bound	-\$3500.61	-\$3254.63	-\$2219.23	-\$1184.97	-\$626.42	-\$473.75	-
C.I. Upper Bound	\$2207.17	\$2086.27	\$1522.01	\$912.19	\$554.71	\$475.85	-

Table 3.2: Average revenues and confidence intervals for the myopic policy.

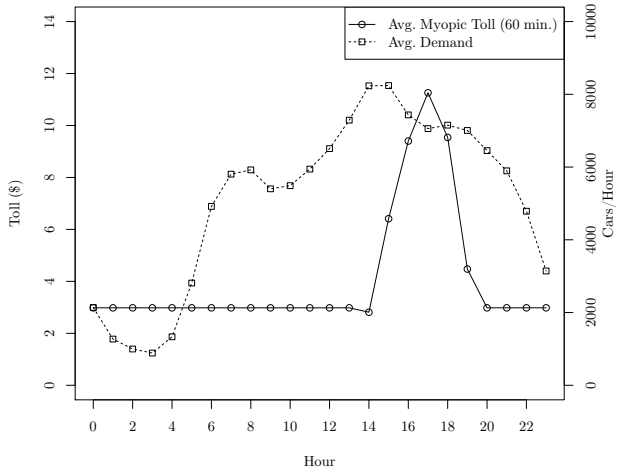

Figure 3.9: Myopic tolls and mean hourly demand.

through the stochastic approximation procedure, and also the average hourly traffic load. The 2-tuple in the legend indicates the starting point and the number of iterations performed, respectively. The second part of the figure reports the market shares of the managed lanes for the tolling schedules given in the first part of the figure. The structure of all three policies are very similar. When the traffic load is low, the tolls are also quite low and stable in the region of $3. A few hours before the peak arrival traffic is observed, the tolls go up to very high levels and effectively divert all arrivals into the managed lanes. This pattern, which was also observed in the numerical study of Chapter 2, is intuitive. By diverting almost all arriving cars into the unmanaged lanes, the toll operator achieves two goals: he reserves capacity in the managed lanes for the peak hours and increases congestions in the unmanaged lanes. These two effects combine to increase the attractiveness of the managed lanes during the peak hours – which enables the operator to extract more revenue from arriving traffic just when the volume of arrivals is highest. From Table 3.3 and Figure 3.11 we can see that this approach translates into substantial revenue improvements over the myopic policy. When the static policy sets its tolls high, no revenue is earned since all drivers choose the unmanaged lanes. By forgoing the revenue in this period of time, we can see that the operator earns substantially more revenues when the *jamming* period ends and the *harvest* period begins.

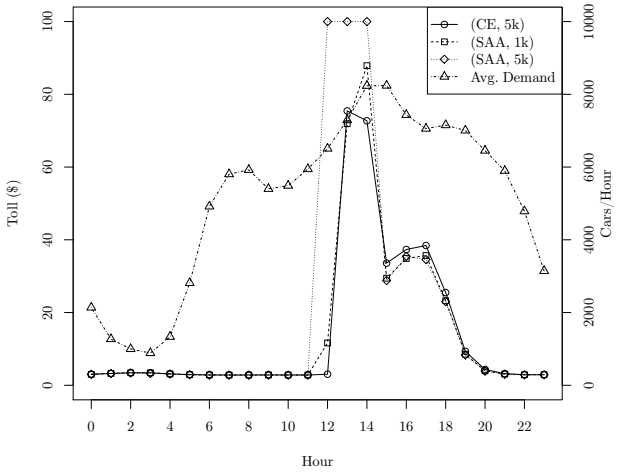

(a) Time-of-use tolls and average hourly traffic load.

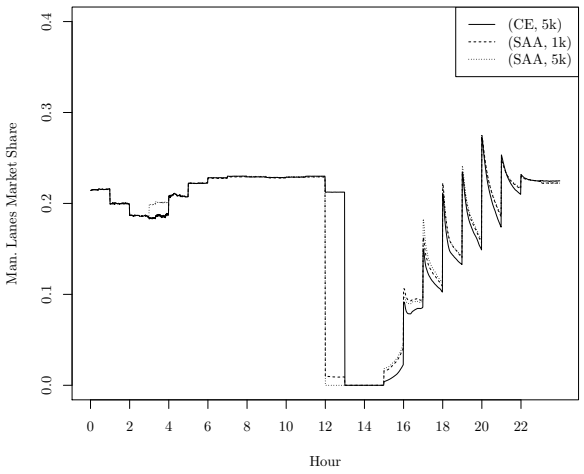

(b) Market share of managed lanes. (1 min. granularity)

Figure 3.10: Time-of-use tolls and the corresponding market share of managed lanes for the Eastbound case.

Almost 70% of the daily revenues come between the hours of 4-8pm. Thus, we calibrate the linear travel time difference policy for only those hours. We use the (CE, 5k) time-of-use tolling policy to form the base tolls and time savings since this policy resulted in the highest expected revenue. For simplicity, we allow α^- and α^+ to vary only hourly. In the stochastic approximation procedure we used the same c_k sequence as we did in the calibration of the time-of-use policy. Table C.2 in Appendix C reports the parameters used in the sequence a_k. We performed 1000 iterations for each parameter. We used the same updating intervals as in the myopic policy and calibrated a different set of parameters for each one. The starting points were obtained through the application of Brent's method over 100 randomly chosen sample paths. Table C.3 in Appendix C reports the

Static Policy	(CE, 5k)	(SAA, 1k)	(SAA, 5k)
Avg. Rev.	\$153,086.51	\$152,029.13	\$151,532.68
% Imp. over Myopic (1 min. tolling update)	22.38%	21.53%	21.13%

Table 3.3: Performance of the static time-of-use tolling policies.

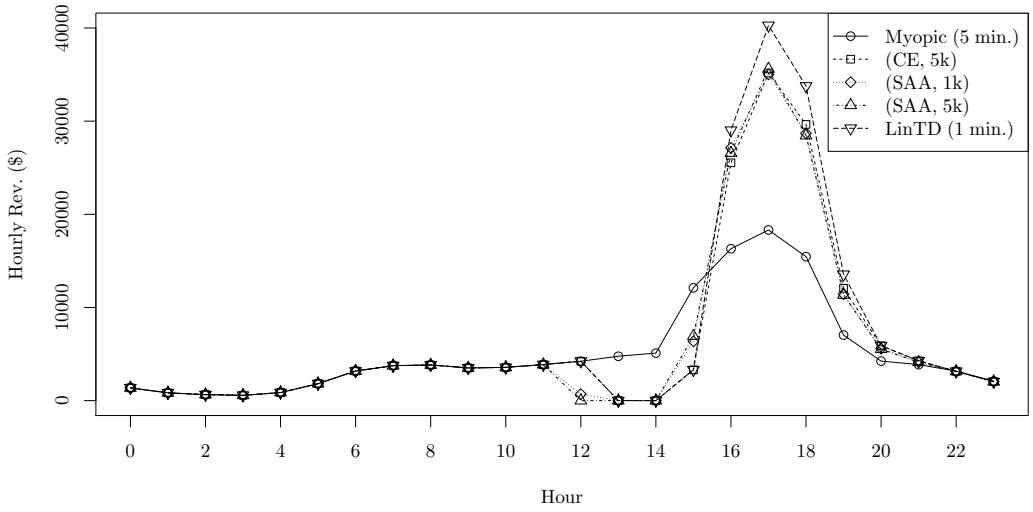

Figure 3.11: Average hourly revenues from different policies.

results of the calibration procedure. From the calibration results we can see that α^- is considerably higher than α^+. This is closely related to the high level of non-linearity attached to our system. Specifically, travel times get increasingly more sensitive to traffic load as it increases. Thus, the operator earns substantially more revenues in cases of high traffic loads. This is taken into account by setting the time-of-use tolls to high levels in order to be able to take advantage of high traffic load cases. If the travel time difference at any point is lower than expected, this is an indicator that the traffic load is lighter than usual since hourly traffic loads are highly correlated with each other. As a result, there is no reason to still keep the tolls high since it is very unlikely that high travel time differences will be observed that day.

Table 3.4 shows the average revenues for different tolling intervals for the linear travel time difference policy. It also shows the 90% confidence intervals for the revenue differences compared to the policy with the 60 minute tolling interval. Similar to the myopic policy, all the confidence intervals contain zero. Thus, we cannot conclude that increasing the tolling frequency provides a significant advantage. Furthermore, from Figure 3.11 we can see that the structure of the policy is similar to the time-of-use policy; it causes congestion in the unamanged lanes by diverting the

arrivals into the managed lanes for a period of time. Later on, this congestion gives it the ability to charge high tolls and recoup the revenue lost during the jamming phase.

So far we analyzed each policy separately. Now, we compare their performance to each other and also to a computational upper bound where the operator is assumed to know the whole traffic pattern for the day. The computational upper bound is obtained by computing the revenue-maximizing tolls for each sample path and then averaging them. To reduce computing times, we assumed that the tolls can only be changed hourly. We used the Nelder-Mead heuristic with twenty different randomly chosen starting points and the tolls obtained from the linear travel time difference procedure.

Table 3.5 shows the expected revenue from the computational upper bound. The difference between the computational bound and the expected revenue from any policy can be interpreted as the expected "cost of regret" for that policy. Table 3.5 also summarizes the three policies we explored so far as well as the gap between these policies and the computational upper bound. We can see that the myopic policy performs the worst. We can attribute this to the fact that the myopic policy does not take into account its future congestion effect. The time-of-use policy outperforms the myopic policy by more than 20%. Adding a real-time response capability, which results in the linear travel time difference policy, helps lift the expected revenues by around 10%. Furthermore, this policy achieves 93.66% of the upper bound. Given that we assume the demand is known ahead of time in the computational upper bound, the performance of the linear travel time difference policy is quite impressive.

Example 2: Westbound Direction. We now analyze the Westbound traffic scenario. We calibrate the demand generation component in the same manner as the Eastbound traffic scenario in §3.2. Specifically, we use the same models, and data from the same periods of time. Parameters

Tolling Interval	1 min.	5 min.	10 min.	15 min.	20 min.	30 min.	60 min.
Avg. Rev.	$167,338	$167,328	$167,456	$167,595	$168,058	$167,119	$167,709
C.I. Lower Bound	-$14473.18	-$8684.09	-$10190.90	-$7006.63	-$8920.62	-$9970.29	–
C.I. Upper Bound	$15213.38	$9444.61	$10695.74	$7233.73	$8221.04	$11149.70	–

Table 3.4: Average revenues and confidence intervals for the linear travel time difference policy.

Policy	Myopic (1 min.)	(CE, 5k)	LinTD (20 min.)	Comp. Bound
Avg. Rev.	\$125,157	\$153,087	\$168,058	\$179,444
Rel. Gap	30.25%	14.69%	6.34%	–

Table 3.5: Summary of policies and comparison to the computational upper bound.

for the demand model being utilized in this example can be found Appendix A. The data for this direction was obtained through PeMS for VDS 1208151 and VDS 1208159 for managed and unmanaged lanes, respectively. For simplicity, we used the consumer choice model 3-1 in Appendix B in which both coefficients in the model do not vary over time. Similar to the previous example, we generated 1000 sample paths for the traffic demand. In every case, unless stated otherwise, we perform our analysis on the same set of sample paths.

In this section we compare and contrast the same set of policies. The starting tolls for the stochastic approximation procedure are obtained by finding the revenue maximizing tolls for the certainty equivalent demand case using the Nelder-Mead heuristic. In the stochastic approximation procedure, we perform 1000 iterations and use the same set of sequences as we did in the Eastbound case. Figure 3.12 depicts the average hourly demand, the time-of-use tolls we obtained through stochastic approximation and the corresponding market share of managed lanes. Even though it is not as severe as it was in the previous example, we can see that the time-of-use policy again seeks to jam the unmanaged lanes by setting the toll very high between 6-7 am. As a result, the managed lanes' market share dips and most of the incoming cars choose the unmanaged lanes which in turn causes congestion in the unmanaged lanes.

Our calibration methodology for the linear travel time difference policy is identical to the Eastbound case with a few minor differences. In contrast to the Eastbound scenario, traffic is more evenly distributed throughout the day. So, we adjust the tolls for a wider range of hours, i.e. we apply the linear travel time difference policy between the hours of 5 am and 7 pm. We apply the same methodology as the previous example to obtain the starting points. We use the sequences $c_k = 1/k^{1/6}$ and $a_k = 0.5/(200 + k)$, and perform 1000 iterations in the stochastic approximation procedure. The resulting parameters can be found in Table C.4 of Appendix C.

The revenues obtained from different policies are given in Table 3.6. In line with the previous

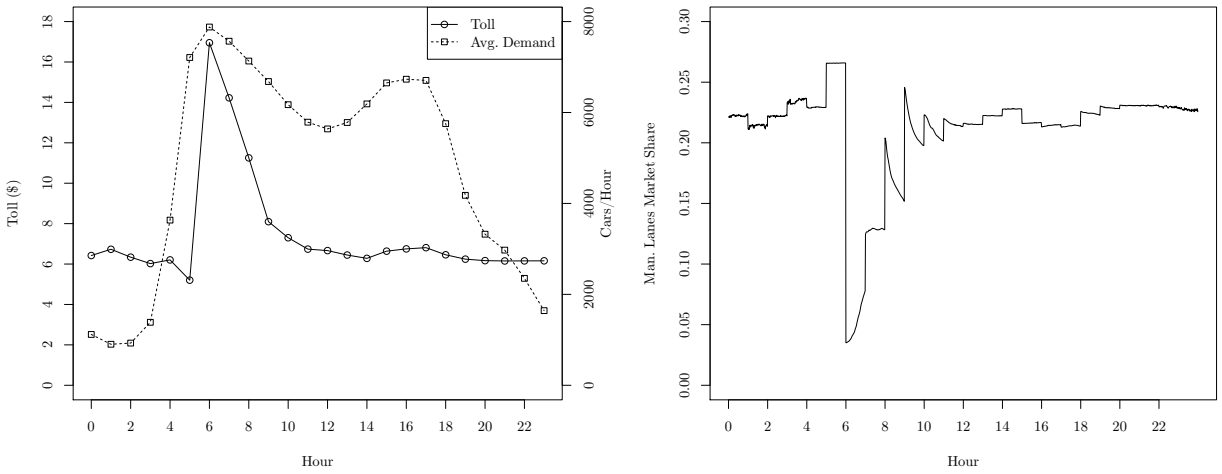

(a) Time-of-use tolls and average hourly traffic load.

(b) Market share of managed lanes. (1 min. granularity)

Figure 3.12: Time-of-use tolls and the market share of managed lanes for the Westbound case.

example, we can see that increasing the tolling frequency for adaptive policies does not result in any sizeable additional benefits. The time-of-use and linear travel time policies still provide a significant improvement over the myopic policy. Similarly, the linear travel time difference policy still provides a substantial improvement over the time-of-use policy (5-6%).

However, compared to the Eastbound example, the magnitude of these improvements are much lower. The gap between the time-of-use and linear travel time difference policies, and the computational upper bound is also much higher. A potential explanation for these two observations stems from the traffic load being spread out more evenly compared to the Eastbound case. As a result, the operator does not have the same scope for increasing unmanaged lane congestion by diverting traffic into the managed lanes. Since this jamming capability constitutes the main advantage of the time-of-use policy provides over the myopic policy, the revenue difference between these two policies is lower in this example. Since the peak is not as pronounced in this example, the best time to start diverting cars into the unmanaged lanes, how many cars to divert and for how long to do it for can change dramatically from sample path to sample path. The ability to anticipate the pattern of future demand for each sample path thus provides a greater relative advantage for

Policy	Myopic		Time-of-Use	LinTD		Comp. Bound
Tolling Interval	1 min.	60 min.	60 min.	1 min.	60 min.	60 min.
Revenue	$167,325	$167,031	$171,831	$181,454	$181,680	$210,698
Rel. Gap (vs. Comp. Bound)	20.59%	20.73%	18.45%	13.88%	13.77%	–
% Imp. over Myopic (1 min. tolling update)	–	–	2.69%	8.44%	8.58%	25.92%

Table 3.6: Revenues from different policies for the Westbound example.

the computational upper bound over the other policies than in the Eastbound Case.

3.5.2 Sensitivity Analysis

Our analysis of the SR91 traffic Eastbound and Westbound gave some insight and provided estimates of the relative benefits of particular policies. In particular, it showed that both time-of-day pricing and adjusted time-of-day pricing provided significant revenue gains over myopic pricing. The benefits were considerably greater on the Eastbound direction which had a very high afternoon peak than on the Westbound direction in which the peak was less pronounced. In both cases, the optimal policy had a "jam and harvest" character in which tolls are set high going into the peak in order to divert as much traffic as possible into the unmanaged lanes. This raises the question of how robust these patterns might be. To address this issue, we compared the myopic policy with the optimal dynamic policy on a number of artificial cases. In each case, we assumed deterministic arrival rates but used the same traffic model and choice model as described in Sections 3.1 and 3.3. The patterns we analyzed were of the form shown in Figure 3.13. We assumed a time horizon of one day. We varied the peak demand, the off-peak demand, the length of the peak, and also the length of the transition period.

Table 3.7 reports the gap between time-of-use and myopic tolling policies for different combinations of the settings. We used the Nelder-Mead heuristic with 20 different randomly chosen starting points to compute the revenue maximizing time-of-use tolls.

The most important factor in our analysis is the volume of peak demand. When peak arrivals are less than 9000 cars/hour, the optimality gap is relatively small. However, when the peak demand

Table 3.7: Gap between time-of-use and myopic tolling polices for different traffic patterns.

Transition Length	**0**			**1**			**2**		
Length of Peak	**1**	**2**	**3**	**1**	**2**	**3**	**1**	**2**	**3**
Peak Hourly Dem.									
7000	1.37%	1.24%	1.09%	1.41%	1.51%	1.61%	0.67%	1.23%	0.95%
8000	0.95%	1.22%	1.08%	1.09%	1.11%	0.98%	1.23%	1.01%	1.36%
9000	1.28%	4.70%	21.63%	1.64%	7.70%	17.53%	2.24%	9.14%	23.79%
10000	2.35%	22.28%	37.70%	2.93%	23.40%	38.39%	4.41%	34.74%	53.25%

(a) Off-peak demand is 4000 cars/hour.

Transition Length	**0**			**1**			**2**		
Length of Peak	**1**	**2**	**3**	**1**	**2**	**3**	**1**	**2**	**3**
Peak Hourly Dem.									
7000	2.53%	2.29%	2.69%	2.28%	2.21%	2.63%	2.45%	2.33%	2.45%
8000	2.75%	2.49%	2.65%	2.42%	1.81%	1.84%	2.29%	2.20%	1.97%
9000	2.80%	6.33%	12.94%	3.28%	9.09%	21.39%	3.75%	10.67%	31.85%
10000	3.84%	22.79%	40.63%	8.44%	25.96%	40.17%	13.13%	38.66%	54.97%

(b) Off-peak demand is 5000 cars/hour.

Transition Length	**0**			**1**			**2**		
Length of Peak	**1**	**2**	**3**	**1**	**2**	**3**	**1**	**2**	**3**
Peak Hourly Dem.									
7000	1.09%	1.16%	1.27%	0.85%	1.03%	0.97%	1.23%	1.20%	1.38%
8000	1.19%	0.99%	0.58%	1.04%	1.25%	0.96%	0.67%	0.48%	0.80%
9000	3.63%	5.40%	14.13%	3.92%	7.90%	17.83%	5.31%	11.60%	41.17%
10000	4.00%	17.50%	36.90%	4.67%	34.65%	54.69%	24.66%	50.81%	66.29%

(c) Off-peak demand is 6000 cars/hour.

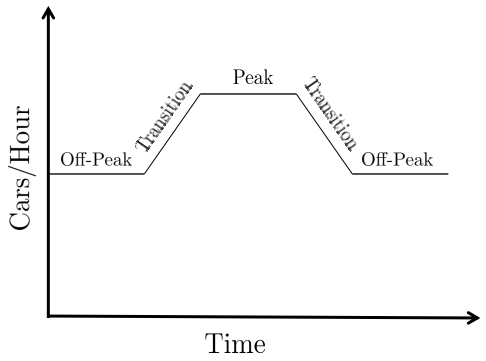

Figure 3.13: Demand pattern used in the sensitivity analysis.

passes that threshold, the gap increases substantially. As discussed in the traffic simulation section, highway speeds are are quite insensitive to traffic loads up to a certain point. Once that threshold is passed, however, speed is highly dependent on volume. When the peak demand stays below 9000 cars/hour, the unmanaged lanes have enough capacity to handle all the traffic flow without slowing substantially. However, that is not the case when the peak demand rises to 9000 cars/hour. This enables the controller to diver the traffic into the unmanaged lanes and reap the benefits from the increased congestion as discussed in the previous section.

The influence of the number of transition periods, and the number of periods where the peak demand is observed is clear once the peak demand is high. Similarly, the gap is also the most sensitive to the peak demand when it is high. As all of these parameters increase, the static policy has the capability of causing increasing levels of congestion in the unmanaged lanes. This increases the attractiveness of the managed lanes further down the road, and gives the operator the ability to charge tolls – much higher than the ones prescribed by the myopic policy.

3.5.3 Discussion

Our work provides a number of important insights into optimal managed lane tolling policies. First of all, managing tolls around peaks – especially entering into the peak – is the most important aspect of any revenue-maximizing policy. Secondly, optimal tolls have a "jam and harvest" character – by charging high tolls entering into a peak period, they divert cars into the unmanaged lanes, thereby increasing unmanaged lane congestion and enabling higher tolls later in the peak. Finally, when the

peak traffic is high relative to off-peak traffic, good heuristic policies can generate substantially more revenue than the myopic policy. These observations are consistent with the results in Chapter 2. In both of the dynamic policies we studied, increasing tolling frequency did not result in substantial additional benefits. Thus, having the capability of updating the tolls frequently does not seem to add a lot of value. A smart dynamic tolling mechanism potentially provides substantial revenue improvements over a static time-of-use policy. However, we saw that such a policy does not need to be very complex. What counts most is having the capability of sensing whether the traffic load is higher than usual or not. A simple adaptive policy appears to be quite effective. Once it has been calibrated, the linear travel time difference policy is quite simple to implement.

Our analysis assumed that all customers were tactical, that is that their arrival times are exogenous and not dependent on either the tolls or the travel times. In actuality, some drivers may have the flexibility to change their travel plans in order to avoid high tolls and/or high congestion. Incorporation of such strategic behavior into the model might change the optimal tolls. However, this would effectively require incorporating an equilibrium constraint into the model, which would significantly increase its complexity. Furthermore, the persistence of highly predictable traffic jams during certain periods shows that a very high number of travelers do not have great flexibility to adjust their departure times.

Chapter 4

Revenue Management of Consumer Options for Tournaments

This chapter is based on the paper "Revenue Management of Consumer Options for Tournaments" which is a joint work with Santiago Balseiro, Prof. Robert Phillips and Prof. Guillermo Gallego.

This chapter diverts from the traffic theme of the previous two chapters. Instead, we focus on the pricing of tournaments that utilize a different type of infrastructure (e.g., stadiums, tennis courts, basketball courts). Unlike the previous chapters that focused on the pricing of a new infrastructure (the *managed lanes*), we analyze how an organizer can extract more revenue through the introduction of a new product (*consumer options*) while utilizing the same existing infrastructure.

4.1 Model

We consider a tournament with $N \geq 3$ teams, where there is uncertainty about the finalists. The final is held in a venue with a capacity of C seats, which we assume of uniform quality. In the case where the seats have heterogeneous quality, the stadium can be partitioned in sections, and then each section can be considered independently. Alternatively, one could consider all sections simultaneously using a nested revenue management model with upgrades (Gallego and Stefanescu,

2009).[1]

We address the problem of pricing and management of tickets and options for the final game. The event manager offers $N+1$ different products for the event: *advance tickets*, denoted by A and *options* for each team i, denoted by O^i. Advance tickets require a payment of p_a in advance and guarantee a seat at the final game. An option O^i for team i is purchased at a price p_o^i, and confers the buyer a right to exercise and purchase the underlying ticket at a strike price p_e^i only in the event that team i advances to the final game. If the team fails to advance to the final game, the option expires worthless and the premium paid is lost.

The event manager is a monopolist who can influence demand by varying the price. Hence, he faces the problem of pricing the products and determining the number of products of each type to offer so as to maximize his expected revenue. A common practice in sporting events is that prices are announced in advance, and the organizer commits to those prices throughout the sales horizon. We adhere to that static pricing practice in our model. However, the event manager does not commit in advance to allocate a fixed number of seats for each product, and he can dynamically react to demand by changing the set of products offered at each point in time.

For ease of exposition, the event manager is assumed to be risk-neutral, and performs no discounting. Additionally, all costs incurred by the event manager are assumed to be sunk, so that there is no marginal cost for additional tickets sold. From the event manager's point of view seats are perishable, that is, unsold seats have no value after the tournament starts since they cannot be sold anymore. Finally, in agreement with current practice no overbooking is allowed in our model.

The timing of the events is as follows. First, the event manager announces the advance ticket's price p_a, and the options' premium and strike price (p_o^i, p_e^i) for each team i. Then, the box office opens, and advance tickets and options are sold at those prices. Sales are allowed during a finite horizon T that ends when the tournament starts. Afterwards, the tournament is played out, and the two teams playing in the final are revealed. At this point the holders of options for the two finalists decide whether to exercise their rights and redeem a seat at the corresponding strike price.

[1] In the model of Gallego and Stefanescu (2009) the event manager may upgrade customers to higher quality seats. Even though we do not pursue this direction in here, we note that upgrades help balance demand and supply by shifting excess capacity of high grade products to low grade products with excess demand.

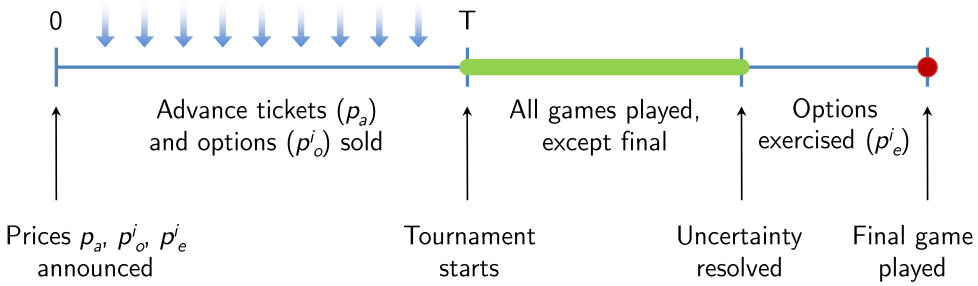

Figure 4.1: Sales horizon and actions involved in each period.

Finally, the championship game is played and the fans attend the event. Figure 4.1 illustrates the timing of the events.

The set of possible combinations of teams that might advance to the finals is denoted by $\mathcal{T}$. For example, in the case where any combination of teams may play in the final game, we have $\mathcal{T} = \{\{i, j\} : 1 \leq i < j \leq N\}$. In the case of a dyadic tournament such as a single-elimination tournament, teams can be divided into two groups, denoted by $\mathcal{T}_1 = \{1, \ldots, \lfloor N/2 \rfloor\}$ and $\mathcal{T}_2 = \{\lfloor N/2 \rfloor + 1, \ldots, N\}$, in such a way that exactly one team from each group advances to the final game. In this case the space of future outcomes is $\mathcal{T} = \mathcal{T}_1 \times \mathcal{T}_2$.

As agents form rational expectations about the outcome of the tournament, we assume that there is an objective probability of team i advancing to the final game, denoted by q^i, that is common knowledge. In practice, one can obtain estimates of these probabilities from bookmakers' betting odds, and tournaments participants' characteristics such as past performance and injury status; both of which are publicly available. Additionally, we impose that these probabilities are invariant throughout the sales horizon. The latter assumption is reasonable since the box office closes before the tournament starts. Finally, note that the probabilities will satisfy $\sum_{i=1}^{N} q^i = 2$.

A critical assumption of our model is that tickets and options are not transferrable. This can be enforced, for instance, by demanding some proof of identification at the entry gate. Non-transferability precludes the existence of a secondary market for tickets, that is, tickets cannot be resold and they can only be purchased from the event manager. This assumption, although somewhat restrictive, simplifies the analysis.

Consumer Choice Model. Consumers are assumed to be risk-neutral and utility-maximizing.

The demand is naturally segmented with respect to team preference, with N disjoint segments corresponding to each team: we refer to consumers within segment i as *fans* of team i. In our model, demand is stochastic and price sensitive, with customers arriving according to independent Poisson processes with homogeneous intensity Λ^i for segment i. Time-dependent arrival intensities can be handled by partitioning the sales horizon into intervals where the arrival rate is constant (Liu and van Ryzin, 2008).

A fan of team i has two sources of utility, (i) attending a final game with his favorite team playing, and (ii) attending the event when his team is not playing. The fan's willingness-to-pay for attending his favorite team's final game, denoted by V, is drawn independently and at random from a team-specific cumulative distribution function $F_v^i(\cdot)$. Fans do not update their valuations over time, and as a result, expected utilities of the possible alternatives remain constant, which means that the fans will not switch decisions, and there will be no cancellations or no-shows. Furthermore, every option bought will be exercised. When his preferred team is not playing, the fan is not sensitive to the finalists and will obtain only a fraction $\ell^i \in [0, 1]$ of his original valuation if he watches the final. We refer to ℓ^i as the "love-of-the-game"; and it captures the fact that a fan's utility for attending a game without his preferred team is mostly influenced by his "love" for the sport rather than by the identities of the actual finalists. In the extreme case when $\ell^i = 1$, a fan's utility of attending the game is independent of whichever teams are playing. Conversely, when ℓ^i is close to zero, fans have a strong preference towards their team, and are willing to attend the game only if their team is playing. We shall see that the parameter ℓ^i turns out to be critical in our model, and determines to a great extent the profitability of introducing options. The parameters ℓ^i, $F_v^i(\cdot)$, and Λ^i are common knowledge.

At the moment of purchase, a fan of team i has three choices, (i) buy an advance ticket, (ii) buy an option for his preferred team, or (iii) buy nothing. The first choice requires the payment of the advance ticket price p_a. Then, with probability q^i, the fan expects to get a value of V from seeing his team in the final and with probability $1 - q^i$ he expects to get a value of $\ell^i V$. Hence, the fan's expected utility for product A given a valuation of V, denoted by $U_a^i(V)$, is $U_a^i(V) = (q^i + (1 - q^i)\ell^i)V - p_a$. The second choice, buying the option O^i, requires the payment of

Decision	Pays	Value	Ex. Utility
n: don't buy	0	0	0
a: buy A	p_a	V w.p. q^i $\ell^i V$ w.p. $1-q^i$	$(q^i + (1-q^i)\ell^i)V - p_a$
o: buy O^i	$p_o^i + p_e^i$ w.p. q^i p_o^i w.p. $1-q^i$	V w.p. q^i 0 w.p. $1-q^i$	$q^i V - (p_o^i + q^i p_e^i)$

Table 4.1: Expenditures, values and expected utilities related to each decision.

the premium price p_o^i at the moment of purchase. Since valuations are not updated over time, once a fan buys an option, he will always exercise if his team makes the final. Hence, with probability q^i his preferred team advances to the final, and he exercises by paying the strike price p_e^i and extracts a value V in return. The expected utility for product O^i given a valuation of V, denoted by $U_o^i(V)$, is $U_o^i(V) = q^i V - (p_o^i + q^i p_e^i)$. Finally, the utility of no purchase is $U_n = 0$. Table 4.1 summarizes the expenditures, values and expected utilities related to each decision.

A fan makes the choice that maximizes his expected utility. The actual decision, however, depends on the availability of advance tickets and options at the moment of arrival to the box office. For instance, when the first-best choice is not available, the consumer pursues his second-best choice, and if this is also not available, he buys nothing.

We now address the problem of characterizing the demand rate of every product subject to a given set of offered products. We partition the space of valuations for each market segment into five disjoint sets as shown in Table 4.2. Decision priority xyz denotes the case where x is the first-best choice, y is the second-best choice, and z is the least preferred choice. For example, *aon* corresponds to the case where an advance ticket is the most highly preferred product, an option is the second most highly preferred product and buying nothing is the least preferred choice. The linearity of expected utilities implies the valuation sets corresponding to these priorities are intervals of $\mathbb{R}_+$. Figure 4.2 illustrates the expected utility for the three choices versus the realized value of V for the particular market segment i, and the corresponding valuation intervals. Observe that depending on prices and problem parameters, this graph can take on two forms. Using the distribution of valuations in the population, the event manager can compute the probability that the private valuation of an arriving customer of team i belongs to a particular interval which is

Decision Priorities	Valuation Sets	Probability (π_{xyz})
n	$\{V : U_a(V) \le 0, U_o(V) \le 0\}$	$F_v(\min(c, b))$
on	$\{V : U_o(V) \ge 0 \ge U_a(V)\}$	$(F_v(c) - F_v(b))^+$
an	$\{V : U_a(V) \ge 0 \ge U_o(V)\}$	$(F_v(b) - F_v(c))^+$
oan	$\{V : U_a(V) \ge U_o(V) \ge 0\}$	$(F_v(a) - F_v(c))^+$
aon	$\{V : U_o(V) \ge U_a(V) \ge 0\}$	$1 - F_v(\max(a, b))$

Table 4.2: Decision priorities and corresponding valuation sets. For simplicity we drop the superscript indicating the team. The intersection points are given by $a = \frac{p_a - (p_o + qp_e)}{(1-q)\ell}$, $b = \frac{1}{q}(p_o + qp_e)$, and $c = \frac{p_a}{q+(1-q)\ell}$. Additionally, $(x)^+ = \max\{x, 0\}$.

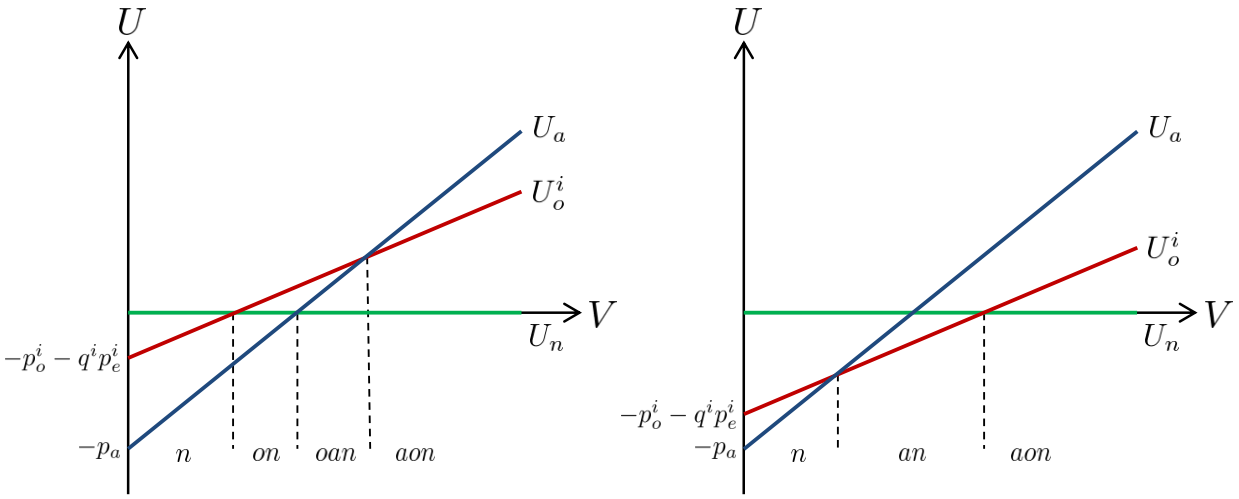

Figure 4.2: Graphs showing expected surplus for the three choices. The horizontal axis is divided in segments matching each decision. For instance, if V falls in the segment oan the fan would buy an option, and else he would buy an advance ticket.

denoted by π^i_{xyz}. The last column of Table 4.2 shows corresponding probabilities for each possible choice ordering.

Now we turn to the problem of determining the demand rate for each product when the event manager offers only a subset $S \subseteq \mathcal{S} \equiv \{A, O^1, \ldots, O^N\}$ of the available products. Under our model the instantaneous arrival rate of fans of team i purchasing advance tickets when offering $S \subseteq \mathcal{S}$, denoted by $\lambda^i_a(S)$, is

$$\lambda^i_a(S) = \Lambda^i \mathbf{1}_{\{A \in S\}}(\pi^i_{an} + \pi^i_{aon} + \mathbf{1}_{\{O^i \notin S\}}\pi^i_{oan}). \tag{4.1}$$

The arrival rate for advance ticket purchases is composed of three terms. The first term accounts for fans that are only willing to buy those tickets. The second term accounts for fans that are willing to buy the advance tickets, but when they are no longer available will buy the options as a second choice. Finally, the third term considers fans that prefer options as their first choice, but may end up buying advance tickets when options are not available. The aggregate arrival rate for advance ticket purchases when offering subset S is $\lambda_a(S) = \sum_{i=1}^{N} \lambda_a^i(S)$. Similarly, the arrival rate of fans of team i buying options when offering S, denoted by $\lambda_o^i(S)$, is

$$\lambda_o^i(S) = \Lambda^i \mathbf{1}_{\{O^i \in S\}}(\pi_{on}^i + \pi_{oan}^i + \mathbf{1}_{\{A \notin S\}}\pi_{aon}^i). \tag{4.2}$$

4.2 Pricing and Capacity Allocation Problem

In this section we look at the combined problem of pricing and managing advance tickets and options faced by the organizer. Recall that prices are determined in advance, disclosed at the beginning of the sales horizon, and remain constant thereon. However, the number of seats allocated to each product are not disclosed in advance. The organizer can control the number of tickets and options sold to dynamically react to the demand by playing with the availability of the products. Since the resulting pricing and capacity allocation problem is intractable, we develop a novel approximation, which we show to be asymptotically optimal when capacity and time are simultaneously scaled up. Then, we conclude this section by addressing some of the practical issues that one might face in the application of this approximation.

4.2.1 Problem Formulation

The sequential nature of the decisions involved suggests a partition of the problem into a two-stage optimization problem. The decision variables are prices in the first stage and product availabilities in the second stage. In the first stage, the organizer looks for the set of prices $p = (p_a, p_o, p_e)$ that maximizes the optimal value of the second-stage problem, which is the maximum expected revenue that can be extracted under fixed prices p. This partition is well-defined because prices

are determined before the demand is realized, and are independent of the actual realization of the demand. The optimal value of the first-stage problem, denoted by R^*, is

$$R^* \equiv \max_{p \geq 0} R^*(p)$$

where $R^*(p)$ denotes the optimal value of the second-stage problem.

The second-stage problem takes prices as given, and optimizes the expected revenue by controlling the subset of products that is offered at each point in time. Notice that the second-stage decision variable is a control policy over the offer sets, which is determined as the demand realizes. We refer to this second-stage problem as the *Capacity Allocation Problem*. Next, we turn to the problem of determining the optimal value of the second-stage problem under fixed prices p.

Once prices are fixed, the organizer attempts to maximize his revenue by implementing adaptive non-anticipating policies that offer some subset $S \subseteq \mathcal{S} \equiv \{A, O^1, \ldots, O^N\}$ of the available products at each point in time. A control policy μ maps states of the system to control actions, i.e. the set of offered products. We denote by $S_\mu(t)$ the subset of products offered under policy μ at time t. The organizer can affect the arrival intensity of purchase requests by controlling the offer set $S_\mu(t)$. As such, the total number of advance tickets sold up to time t is a non-homogeneous Poisson process with arrival intensity $\lambda_a(S_\mu(t))$ as defined in (4.1). We denote the event of an advance ticket being sold at time t by $\mathrm{d}X_a(S_\mu(t)) = 1$. Similarly, the number of options sold follow a non-homogenous Poisson process with arrival intensity $\lambda_o^i(S_\mu(t))$ as defined in (4.2), and we let $\mathrm{d}X_o^i(S_\mu(t)) = 1$ when an option is sold at time t. With some abuse of notation, we define $X_a = \int_0^T \mathrm{d}X_a(S_\mu(t))$ and $X_o^i = \int_0^T \mathrm{d}X_o^i(S_\mu(t))$ to be the total number of advance tickets and options sold, respectively.

The second-stage or Capacity Allocation Problem can be formalized as the following stochastic

control problem which is similar to the one given in Liu and van Ryzin (2008):

$$
\begin{aligned}
R^*(p) = \max_{\mu \in \mathcal{M}} \mathbb{E}\left[p_a X_a + \sum_{i=1}^{N} (p_o^i + q^i p_e^i) X_o^i \right] \\
\text{s.t. } X_a = \int_0^T \mathrm{d}X_a(S_\mu(t)), \\
X_o^i = \int_0^T \mathrm{d}X_o^i(S_\mu(t)), \qquad \forall i = 1, \ldots, N, \\
X_a + X_o^i + X_o^j \le C, \qquad \text{(a.s.) } \forall \{i,j\} \in \mathcal{T},
\end{aligned}
\tag{4.3}
$$

where $\mathcal{M}$ is the set of all adaptive non-anticipating policies, and $R^*(p)$ is the expected revenue under the optimal policy μ^*. The first term in the objective accounts for the revenue from advance ticket sales and the second term accounts for the revenue from options under the assumption that *all options are exercised*, which was previously discussed in §4.1. Notice that because prices remain constant during the time horizon, the expected revenue depends only on the expected number of tickets sold. Unfortunately, this problem is very difficult to solve in most cases. The next section gives a tractable and provably good deterministic approximation of (4.3).

4.2.2 Deterministic Approximation for the Second Stage Problem

In this section we follow Gallego *et al.* (2004), and solve a deterministic approximation of (4.3) in which random variables are replaced by their means and quantities are assumed to be continuous. We denote by $r_a = p_a$ the expected revenue from selling an advance ticket, and by $r_o^i = p_o^i + q^i p_e^i$ the expected revenue from selling an option of team i. Under this approximation, when a subset of products S is offered, advance tickets (resp. options for team i) are purchased at a rate of $\lambda_a(S)$ (resp. $\lambda_o^i(S)$). Since r_a (resp. r_o^i) is the expected revenue from the sale of an advance ticket (resp. option for team i), the rate of revenue generated from the sales of advance tickets is $r_a \lambda_a(S)$ (resp. $r_o^i \lambda_o^i(S)$ for options of team i). Additionally, because demand is deterministic and the choice probabilities are time homogeneous, we only care about the total amount of time each subset of products is offered and not the order in which they are offered. Thus, we only need to consider the amount of time each subset S is offered, denoted by $t(S)$, as the decision variables. Under this

notation, the number of advance tickets sold is $\sum_{S\subseteq\mathcal{S}} t(S)\lambda_a(S)$, while the number of options sold for team i is $\sum_{S\subseteq\mathcal{S}} t(S)\lambda_o^i(S)$. Finally, the total revenue of the organizer is $\sum_{S\subseteq\mathcal{S}} r(S)t(S)$, where $r(S) = r^T\lambda(S)$ is the revenue rate when subset S is offered, and $r = \left(r_a, r_o^1, \ldots, r_o^N\right)$ is the vector of expected revenues.

Thus, we obtain the following choice-based deterministic LP model (CDLP):

$$R^{CDLP}(p) \equiv \max_{t(S)} \sum_{S\subseteq\mathcal{S}} r(S)t(S) \tag{4.4}$$

$$\text{s.t.} \sum_{S\subseteq\mathcal{S}} t(S) = T,$$

$$\sum_{S\subseteq\mathcal{S}} t(S)\left(\lambda_a(S) + \lambda_o^i(S) + \lambda_o^j(S)\right) \leq C, \qquad \forall\{i,j\} \in \mathcal{T} \tag{4.5}$$

$$t(S) \geq 0 \qquad \forall S \subseteq \mathcal{S}$$

where $R^{CDLP}(p)$ denotes the maximum revenue of the CDLP under prices p.

Since the linear program in (4.4) has one variable for each offer subset, it has 2^{N+1} variables in total. For instance, if the tournament has 32 teams the program would have more than 8 billion variables! Fortunately, by exploiting the structure of our choice model it is possible to derive an alternative formulation with a linear number of variables and constraints.

Recall that consumers are partitioned into N different market segments, each associated with a different team. Two different products are potentially offered to each segment $i = 1, \ldots, N$: (i) advance tickets (A) and (ii) options for the associated team (O^i). We denote by $\mathcal{S}^i = \{A, O^i\}$ the set of products available for market segment i. Demands across segments are independent, and different segments are only linked through the capacity constraints. Since each segment has two products, only four offer sets need to be considered. Thus, for each market segment we only need the following decision variables: (i) the time both advance tickets and options are offered, denoted by $t^i\left(\{A, O^i\}\right)$, (ii) the time only advance tickets are offered, denoted by $t^i\left(\{A\}\right)$, (iii) the time only options are offered, denoted by $t^i\left(\{O^i\}\right)$, and (iv) the time no product is offered, denoted by $t^i\left(\emptyset\right)$. Given a solution $\{t(S)\}_{S\subseteq\mathcal{S}}$ for the CDLP, the value of the new decision variables can be

computed as follows

$$t^i(S) = \sum_{S' \subseteq \mathcal{S}: S' \cap \mathcal{S}^i = S} t(S'). \tag{4.6}$$

Observe that for each segment offer times should sum up to length of the horizon, that is $\sum_{S \subseteq \mathcal{S}^i} t^i(S) = T$. An important observation is that by requiring $\sum_{S \subseteq \mathcal{S}^i \setminus \emptyset} t^i(S) \leq T$ we do not need to keep track of the time in which no product is offered for each segment. Additionally, in order for the offer sets to be consistent across market segments, the total time that advance tickets are offered should be equal for all segments, i.e., for some $T_a \geq 0$ it should be the case that $t^i\left(\{A, O^i\}\right) + t^i\left(\{A\}\right) = T_a$ for all $i = 1, \ldots, N$ where T_a denotes the total time advance tickets are offered throughout the sales horizon.

After applying the aforementioned changes, we obtain the following market-based deterministic LP (MBLP)

$$R^{MBLP}(p) \equiv \max_{t^i(S), T_a} \sum_{i=1}^{N} \sum_{S \subseteq \mathcal{S}^i} r^i(S) t^i(S) \tag{4.7}$$

$$\text{s.t.} \sum_{S \subseteq \mathcal{S}^i} t^i(S) \leq T \qquad \forall i = 1, \ldots, N \tag{4.8}$$

$$t^i\left(\{A, O^i\}\right) + t^i\left(\{A\}\right) = T_a \qquad \forall i = 1, \ldots, N \tag{4.9}$$

$$\sum_{k=1}^{N} \sum_{S \subseteq \mathcal{S}^k} t^k(S) \lambda_a^k(S) + \sum_{S \subseteq \mathcal{S}^i} t^i(S) \lambda_o^i(S) + \sum_{S \subseteq \mathcal{S}^j} t^j(S) \lambda_o^j(S) \leq C \qquad \forall \{i, j\} \in \mathcal{T} \tag{4.10}$$

$$T_a \geq 0, t^i(S) \geq 0 \qquad \forall S \subseteq \mathcal{S}^i, i = 1, \ldots, N,$$

where $r^i(S) = p_a \lambda_a^i(S) + r_o^i \lambda_o^i(S)$ is the revenue rate from market segment i when subset $S \subseteq \mathcal{S}^i$ is offered. Notice that the new optimization problem has $3N + 1$ variables, which is much less than CDLP, and $O(N^2)$ constraints.

Proposition 1. *The MBLP is equivalent to the CDLP, i.e.* $R^{MBLP}(p) = R^{CDLP}(p)$ *for all prices*

$p \geq 0$.

Proof: We first show that $R^{CDLP}(p) \leq R^{MBLP}(p)$ by showing that any solution of the CDLP can be used to construct a feasible solution to the MBLP with the same objective value. Let $\{t(S)\}_{S\subseteq\mathcal{S}}$ be a feasible solution to the CDLP. First, using the decision variables given by (4.6), the total number of advance tickets sold can be written as

$$\begin{aligned} X_a &= \sum_{S\subseteq\mathcal{S}} t(S)\lambda_a(S) = \sum_{S\subseteq\mathcal{S}} t(S) \sum_{i=1}^{N} \Lambda^i \mathbf{1}_{\{A\in S\}}(\pi^i_{an} + \pi^i_{aon} + \mathbf{1}_{\{O^i\notin S\}}\pi^i_{oan}) \\ &= \sum_{i=1}^{N} \Big(\sum_{S\subseteq\mathcal{S}: A\in S, O^i\in S} t(S)\Big)\Lambda^i(\pi^i_{an} + \pi^i_{aon}) + \Big(\sum_{S\subseteq\mathcal{S}: A\in S, O^i\notin S} t(S)\Big)\Lambda^i(\pi^i_{an} + \pi^i_{aon} + \pi^i_{oan}) \\ &= \sum_{i=1}^{N} t^i\left(\{A, O^i\}\right)\lambda^i_a\left(\{A, O^i\}\right) + t^i\left(\{A\}\right)\lambda^i_a\left(\{A\}\right) = \sum_{i=1}^{N}\sum_{S\subseteq\mathcal{S}^i} t^i(S)\lambda^i_a(S), \end{aligned} \tag{4.11}$$

where the second equality follows from (4.1), the third from exchanging summations, and the fourth from (4.1) again. Similarly, the number of options sold in market segment i can be written as

$$\begin{aligned} X^i_o &= \sum_{S\subseteq\mathcal{S}} t(S)\lambda^i_o(S) = \sum_{S\subseteq\mathcal{S}} t(S)\Lambda^i \mathbf{1}_{\{O^i\in S\}}\left(\pi^i_{on} + \pi^i_{oan} + \mathbf{1}_{\{A\notin S\}}\pi^i_{aon}\right) \\ &= \Big(\sum_{S\subseteq\mathcal{S}: A\in S, O^i\in S} t(S)\Big)\Lambda^i(\pi^i_{on} + \pi^i_{oan}) + \Big(\sum_{S\subseteq\mathcal{S}: A\in S, O^i\notin S} t(S)\Big)\Lambda^i(\pi^i_{on} + \pi^i_{oan} + \pi^i_{aon}) \\ &= t^i\left(\{A, O^i\}\right)\lambda^i_o\left(\{A, O^i\}\right) + t^i\left(\{A\}\right)\lambda^i_o\left(\{A\}\right) = \sum_{S\subseteq\mathcal{S}^i} t^i(S)\lambda^i_o(S), \end{aligned} \tag{4.12}$$

where the second equality follows from (4.2), the third from exchanging summations, and the fourth from (4.2) again. Thus, the capacity constraint (4.10) is verified.

The non-negativity constrains and the time-horizon length constraints (4.8) follow trivially. Next, for the advance selling market consistency constraints (4.9) notice that for all $i = 1, \ldots, N$ we have that

$$t^i\left(\{A, O^i\}\right) + t^i\left(\{A\}\right) = \sum_{S\subseteq\mathcal{S}: A\in S, O^i\in S} t(S) + \sum_{S\subseteq\mathcal{S}: A\in S, O^i\notin S} t(S) = \sum_{S\subseteq\mathcal{S}: A\in S} t(S) = T_a.$$

Thus, advance tickets are offered the same amount of time in all markets.

Finally, the next string of equalities show that both solutions attain the same objective value

$$\begin{aligned}\sum_{S\subseteq\mathcal{S}} r(S)t(S) &= \sum_{S\subseteq\mathcal{S}} r^T\lambda(S)t(S) = \sum_{S\subseteq\mathcal{S}}\sum_{i=1}^{N}\left(r_a\lambda_a^i(S)+r_o^i\lambda_o^i(S)\right)t(S)\\ &= \sum_{i=1}^{N}\sum_{S\subseteq\mathcal{S}^i} r_a\lambda_a^i(S)t^i(S)+r_o^i\lambda_o^i(S)t^i(S) = \sum_{i=1}^{N}\sum_{S\subseteq\mathcal{S}^i} r^i(S)t^i(S),\end{aligned}$$

where the third equality follows from (4.11) and (4.12).

Next, we show that $R^{CDLP}(p) \geq R^{MBLP}(p)$ by showing that any solution of the MBLP can be used to construct a feasible solution to the CDLP with the same objective value. Let $\left\{t^i(S)\right\}_{S\subseteq\mathcal{S}^i,i=1,\ldots,N}$ be a feasible solution to the MBLP. In the following, we give a simple algorithm to compute a feasible solution $\{t(S)\}_{S\subseteq\mathcal{S}}$ for the CDLP.

First, we deal with offer sets containing advance tickets, and compute $t(S)$ for all $S\in\mathcal{S}$ such that $A\in S$. Let $[i]_{i=1,\ldots,N}$ be the permutation in which teams are sorted in increasing order with respect to $t^i\left(\{A,O^i\}\right)$, i.e. $t^{[i]}\left(\{A,O^{[i]}\}\right)\leq t^{[i+1]}\left(\{A,O^{[i+1]}\}\right)$. Consider the following offer sets

$$\begin{aligned}S^{[i]} &= \left\{A,O^{[i]},O^{[i+1]},\ldots,O^{[N]}\right\} \quad \forall i=1,\ldots,N\\ S^{[N+1]} &= \{A\}\end{aligned}$$

and associated times $t\left(S^{[i]}\right) = t^{[i]}\left(\{A,O^{[i]}\}\right) - t^{[i-1]}\left(\{A,O^{[i-1]}\}\right)$ for all $i=1,\ldots,N+1$, with $t^{[0]}\left(\{A,O^{[0]}\}\right)=0$, and $t^{[N+1]}\left(\{A,O^{[N+1]}\}\right)=T_a$. Since teams are sorted with respect to $t^i\left(\{A,O^i\}\right)$, we have $t\left(S^{[i]}\right)\geq 0$. Notice that this construction is valid because the market consistency constraints (4.9) guarantee that advance tickets are offered the same amount of time in all markets. Figure 4.3 sketches a graphical representation of the algorithm.

Next, we look at the intuition behind this construction. Although the order is not important, consider a solution for the CDLP that offers the sets $S^{[i]}$ in sequential order; it starts with $S^{[1]}$, then $S^{[2]}$, and so forth until $S^{[N+1]}$. Hence, at first it offers all products, then team 1's options are removed, then team 2's options are removed, and so forth until the end when only advance tickets

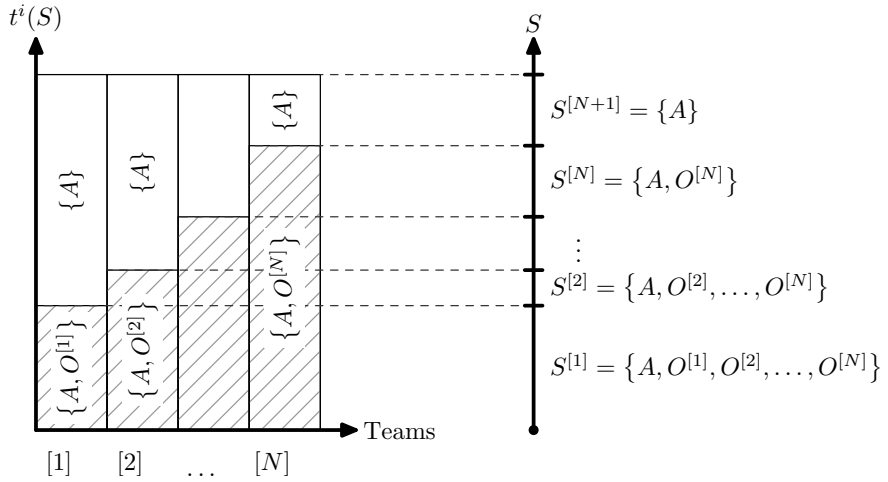

Figure 4.3: Computing a feasible solution for the CDLP (showed on the right) from a feasible solution from the MBLP (on the left) in the case of offer sets containing advance tickets.

are offered. Hence, the optimal policy has a nested structure. A similar argument holds for offer sets not containing advance tickets. □

An interesting consequence of the proof is that the optimal policy has a nested structure. Because demands across segments are independent, one can sequentially order the offer sets containing advance tickets such that each set is a subset of the previous one. The same holds for offer sets that do not include advance tickets. Additionally, the number of active sets in the optimal solution is at most $2N + 1$.

As with most deterministic approximations, it is the case that the optimal value of the MBLP (also the CDLP) provides an upper bound to the optimal value of the stochastic program (4.3) (see, e.g., Liu and van Ryzin (2008)). In the next result, we show that for every fixed price the revenue difference between the deterministic approximations and the stochastic problem is of order $O(\sqrt{T})$. In order to show this bound we use an argument similar, yet slightly simpler, to that of Gallego *et al.* (2004). We show this result for the CDLP formulation. First, we construct a theoretical *offer time* (OT) policy from the optimal solution of the CDLP. In such a policy (i) each set is offered for the time prescribed by the deterministic solution in an arbitrary order, and (ii) the number of products sold in each set is limited to the expected demand. We then show that the expected time

each set is offered in the OT policy is close to the the deterministic solution, and then conclude that the performance of such a policy is close to the deterministic upper bound.

Theorem 1. *Fix prices $p \geq 0$. Let $\{t^*(S)\}_{S\in\mathcal{S}}$ be an optimal solution for the CDLP for the given prices, and $\mathcal{S}^* = \{S \in \mathcal{S} : t^*(S) > 0\}$ be the subsets of products with positive offer times in the optimal solution. Then, then the revenue loss of the stochastic control problem with respect to the CDLP is bounded by*

$$0 \leq R^{CDLP}(p) - R^*(p) \leq r_{\max}|\mathcal{S}^*| \left(\lambda_{\min}^{-1} + \sqrt{(N+1)\lambda_{\min}^{-1}T}\right),$$

where $r_{\max}$ is the maximum revenue rate among all products available in the offer sets in $\mathcal{S}^*$. Similarly, $\lambda_{\min}$ be the minimum arrival rate among all products available in the offer sets in $\mathcal{S}^*$. [2]

Proof: Fix prices p. The first bound follows from Proposition 1 in Liu and van Ryzin (2008), which they proved by using the optimal policy μ^* of the stochastic control problem to construct a candidate solution for the CDLP. In the candidate solution each set is offered for an amount of time $t_{\mu^*}(S) = \mathbb{E}\left[\int_0^T \mathbf{1}\{S_{\mu^*}(t) = S\}\, dt\right]$. Such a solution is easily shown to be feasible for the CDLP and attains the same objective value as the original stochastic problem. Thus, one concludes that $R^*(p) \leq R^{CDLP}(p)$ since every solution of the CDLP is upper bounded by its optimal value.

In order to show the second bound we use an argument similar to that of Gallego *et al.* (2004). First, we construct a theoretical *offer time* (OT) policy from the optimal solution of the CDLP. In such a policy one offers each set for the time prescribed by the deterministic solution in an arbitrary order. Additionally, the number of products sold in each set is limited to the expected demand, and each set is offered until either the time or any of the products run out. We denote by $R^{OT}(p)$ to be the expected revenue of the offer time control. Clearly, it is the case that $R^{OT}(p) \leq R^*(p)$. We shall bound the difference between $R^{OT}(p)$ and the upper bound $R^{CDLP}(p)$.

We construct the OT policy as follows. Let $t^*(S)$ be the optimal solution of the CDLP. With some abuse of notation we refer to advance tickets as the zero option, i.e., $A \equiv O^0$, $X_a \equiv X_o^0$,

[2] Let $A \equiv O^0$ and $p_a \equiv r_o^0$. Then, $r_{\max} = \max_{S\subseteq\mathcal{S}^*, O^i\in S}\{r_o^i(S)\}$ be the maximum revenue rate and $\lambda_{\min} = \min_{S\subseteq\mathcal{S}^*, O^i\in S}\{\lambda_o^i(S)\}$ be the minimum arrival rate.

$p_a \equiv r_o^0$, and $\lambda_a(S) \equiv \lambda_o^0(S)$. Under the OT policy, set S is offered for a time $\tau^{OT}(S) \stackrel{d}{=} \min\{t^*(S), \min_{O^i \in S} \tau_o^i(S)\}$, where $\tau_o^i(S)$ is the first time we run out of options for team i^{th} in an alternate system in which products are sold independently of each other. More formally, we have that

$$\tau_o^i(S) = \inf\{t : X_o^i(S,t) \geq \lfloor \lambda_o^i(S) t^*(S) \rfloor\},$$

options sold by time t when offering set S in the alternate system, and $\lfloor x \rfloor$ is largest integer not greater than x. For the sake of simplicity we assume that the limits on the number of tickets sold are stricly positive, else they can be excluded from the offer set. Notice that $\tau_o^i(S)$ is an Erlang random variable with rate $\lambda_o^i(S)$ and shape parameter $\lfloor \lambda_o^i(S) t^*(S) \rfloor$.

Before proceeding we state some definitions. Let $r_{\max} = \max_{S \subseteq \mathcal{S}^*, O^i \in S}\{r_o^i(S)\}$ be the maximum revenue rate and $\lambda_{\min} = \min_{S \subseteq \mathcal{S}^*, O^i \in S}\{\lambda_o^i(S)\}$ be the minimum arrival rate.

We can lower bound the expected value of the random time $\tau^{OT}(S)$ using the bound for the minimum of random variables from Aven (1985) by

$$\begin{aligned}
\mathbb{E}\left[\tau^{OT}(S)\right] &\geq \min\{t^*(S), \min_{O^i \in S} \mathbb{E}[\tau_o^i(S)]\} - \sqrt{\frac{|S|}{|S|+1} \sum_{O^i \in S} \text{Var}\left[\tau_o^i(S)\right]} \\
&\geq t^*(S) - \max_{O^i \in S} \lambda_o^i(S)^{-1} - \sqrt{t^*(S) \sum_{O^i \in S} \lambda_o^i(S)^{-1}} \\
&\geq t^*(S) - \lambda_{\min}^{-1} - \sqrt{t^*(S)(N+1)\lambda_{\min}^{-1}},
\end{aligned}$$

where the second inequality follows from the fact that $\mathbb{E}\left[\tau_o^i(S)\right] = \lfloor \lambda_o^i(S) t^*(S) \rfloor / \lambda_o^i(S) \geq t^*(S) - 1/\lambda_o^i(S)$, and $\text{Var}\left[\tau_o^i(S)\right] = \lfloor \lambda_o^i(S) t^*(S) \rfloor / \lambda_o^i(S)^2 \leq t^*(S)/\lambda_o^i(S)$.

Next, we bound the expected revenue of the offer time policy. Using the fact that $\tau^{OT}(S)$ is a

bounded stopping time together with the previous bound we obtain that

$$\begin{aligned} R^{OT}(p) &= \mathbb{E}\left[\sum_{S\subseteq\mathcal{S}}\sum_{O^i\in S} r_o^i X_o^i(S,\tau^{OT}(S))\right] = \sum_{S\subseteq\mathcal{S}}\sum_{O^i\in S} r_o^i \lambda_o^i(S)\mathbb{E}\left[\tau^{OT}(S)\right] \\ &\geq \sum_{S\subseteq\mathcal{S}} r(S)t^*(S) - \sum_{S\subseteq\mathcal{S}} r(S)(\lambda_{\min}^{-1} + \sqrt{t^*(S)(N+1)\lambda_{\min}^{-1}}) \\ &\geq R^{CDLP}(p) - r_{\max}\lambda_{\min}^{-1}|\mathcal{S}^*| - r_{\max}\sqrt{(N+1)\lambda_{\min}^{-1}}\sum_{S\subseteq\mathcal{S}}\sqrt{t^*(S)} \\ &\geq R^{CDLP}(p) - r_{\max}|\mathcal{S}^*|\left(\lambda_{\min}^{-1} + \sqrt{(N+1)\lambda_{\min}^{-1}}\sqrt{T}\right), \end{aligned}$$

where the last inequality follows from the fact that $\sum_{S\subseteq\mathcal{S}}\sqrt{t^*(S)} \leq |\mathcal{S}^*|\sqrt{\sum_{S\subseteq\mathcal{S}} t^*(S)}$. Note that the OT policy, in spite of its simplicity, is asymptotically optimal for the stochastic control problem.

□

As a corollary, we get that the CDLP becomes asymptotically optimal as the stadium capacity and length of the time horizon are simultaneously scaled up. To see this, let $R_\theta^*(p)$ be the optimal objective of a scaled stochastic problem in which capacity is set to θC and time horizon to θT for some $\theta \geq 1$. Similarly, let $R_\theta^{CDLP}(p)$ be the optimal objective of a scaled CDLP. Notice that the CDLP is insensitive to the scaling, that is, $\frac{1}{\theta}R_\theta^{CDLP}(p) = R^{CDLP}(p)$. Then from Theorem 1 one gets that the CDLP is asymptotically optimal for the second-stage problem, or equivalently $\frac{1}{\theta}R_\theta^*(p)$ converges to $R^{CDLP}(p)$ as $\theta \to \infty$ for all $p \geq 0$. Moreover, it is not hard to see that the asymptotic optimality of the CDLP carries over to the first-stage problem. Solving the CDLP instead of the stochastic control in the second-stage is asymptotically optimal for the first-stage problem.

4.2.3 Implementation and Practical Considerations

As we previously discussed, the optimal value of the capacity allocation problem $R^*(p)$ is hard to compute. Hence, in order to tackle our problem, we replace the objective of the first-stage problem with the upper-bound provided by the deterministic approximation $R^{MBLP}(p)$. This new problem provides an upper bound to the truly optimal objective value R^*. However, in view of

the asymptotic optimality of the deterministic approximation, and the large scale of the problem in terms of stadium's capacity, our policy is expected to perform reasonably well.

Using our approximation for the second-state problem, the first-stage problem amounts to optimizing the non-linear function $R^{MBLP}(p)$ over the polyhedron of prices. Because the objective is not necessarily convex as a function of price, multiple different starting points need to be taken. Given our efficient method to evaluate the approximate objective value of the capacity allocation problem, we are able to find good solutions for real problems of moderate size despite the non-convexity of the objective.

After the optimal solution is computed, a remaining issue is how tickets should be sold. Clearly, the event manager should announce the optimal prices p^* at the beginning, and commit to that price throughout the sales horizon. However, one important issue is the capacity allocation of the tickets, and constructing a good dynamic control policy from the output of the approximation. The optimal solution of the deterministic approximation prescribes only how long each subset should be offered, but does not specify how to implement the actual policy. One straightforward approach is to offer each subset S for the amount of time given by $t(S)$. As pointed out by Liu and van Ryzin (2008), this approach has a few problems. First, the order in which the sets are offered is not specified, and the resulting policy is static and does not react to changes in demand.

Various heuristics have been proposed to address the first problem. Liu and van Ryzin (2008) proposed a decomposition approach in which the dual optimal solutions of the deterministic problem are used to decompose the network dynamic program into a collection of leg-level DPs which can be solved exactly. These are then used to construct a control policy. Kunnumkal and Topaloglu (2010) improved upon this idea by considering an alternative dynamic programming decomposition method that performs the allocations by solving an auxiliary optimization problem. Alternatively, Zhang and Adelman (2006) employ an approximate dynamic programming scheme in which the value function is approximated with affine functions of the state vector. This allows them to obtain dynamic bid-prices that are later used to construct control policies.

Inspired by our efficient formulation, we propose a simple *sales limit* policy. The policy offers all tickets from the beginning, and limits the number of each product sold to the expected value given

by the deterministic approximation. That is, tickets are sold either until the end of horizon or the limit is reached, whichever happens first. The limits are given by X_a for the advance tickets, and X_o^i for the i^{th} team options. This policy is not guaranteed to be optimal, but performs surprisingly well. Two attractive features of this policy are its ease of implementation, and the fact that it concurs with the current sales practice.

To address the static nature of the control policy, one could periodically resolve the deterministic approximation. Recently, Jasin and Kumar (2010) showed that carefully chosen periodic resolving schemes together with probabilistic allocation controls can achieve a bounded revenue loss w.r.t. the optimal online policy (static control policies are guaranteed to achieve a revenue loss that grows as the squared root of the size of the problem). We do not pursue this direction in here, but note that one could attempt to periodically resolve the MBLP to improve the performance.

4.3 The Symmetric Case

In this section we consider a *symmetric* version of the problem that has the following characteristics, (i) all teams have the same probability of advancing to the final, (ii) arrival rates are the same for all teams, (iii) valuations are i.i.d. across teams, and (iv) the love-of-the-game is constant throughout the population. These assumptions, albeit not entirely realistic, allows us to theoretically characterize the benefits of introducing options. As we shall later see in the numerical analysis part, the conditions under which options are beneficial frequently carry over to the most general case.

The following analysis will be based on the deterministic approximation of the problem and not the actual stochastic performance. Due to the asymptotic optimality of the deterministic approximation and the large scale of the problem, it should be expected that these results carry over to the fully stochastic setting.

We start this section by first formulating the ticket pricing problem for the symmetric case. Then, we show that offering options increases the revenue of the organizer, and also provide bounds on the revenue improvement. Lastly, we analyze the social efficiency of offering options.

4.3.1 Advance Ticket and Options Pricing Problem

In a symmetric problem with N teams, each team has the same probability $q = \frac{2}{N}$ of advancing to the final game. The arrival rate of fans of each team is $\lambda = \frac{\Lambda}{N}$, where Λ denotes the aggregate arrival rate. Due to the symmetry of the teams, we look for solutions in which the organizer charges the same expected price $r_o = p_o + qp_e$ for options for all teams. Hence, we will sell the same number of options to all teams.

The aggregate arrival intensity of advance tickets and options under prices p_a and r_o can be computed as

$$\lambda_a(p_a, r_o) = \Lambda \bar{F}_v\left(\frac{p_a - r_o}{(1-q)\ell}\right),$$
$$\lambda_o(p_a, r_o) = \Lambda\left[\bar{F}_v\left(\frac{r_o}{q}\right) - \bar{F}_v\left(\frac{p_a - r_o}{(1-q)\ell}\right)\right],$$

where we denote by λ_o the aggregate arrival intensity of all consumers buying options. We assume that the c.d.f. of the values $F_v(\cdot)$ is continuous and strictly increasing. Thus, there is a one-to-one correspondence between prices and arrival rates, and the inverse functions are given by

$$r_o(\lambda_a, \lambda_o) = q\bar{F}_v{}^{-1}\left(\frac{\lambda_a + \lambda_o}{\Lambda}\right),$$
$$p_a(\lambda_a, \lambda_o) = q\bar{F}_v{}^{-1}\left(\frac{\lambda_a + \lambda_o}{\Lambda}\right) + (1-q)\ell\bar{F}_v{}^{-1}\left(\frac{\lambda_a}{\Lambda}\right).$$

The one-to-one correspondence between prices and arrival intensity allows us to recast the problem with the arrival intensities as the decision variables; the promoter determines target sales intensities λ_a and λ_o and the market determines the prices based on this quantity. Under this change of variables, the deterministic approximation of the advance ticket and options pricing

problem becomes

$$R_o^D = \max_{\lambda_a \geq 0, \lambda_o \geq 0} T(1-q)\ell v(\lambda_a) + Tqv(\lambda_a + \lambda_o) \tag{4.13a}$$

$$\text{s.t. } T\lambda_a + T\frac{2}{N}\lambda_o \leq C, \tag{4.13b}$$

$$\lambda_a + \lambda_o \leq \Lambda,$$

where we have written the objective in terms of the *value rate* $v(\lambda_a) = \lambda_a \bar{F_v}^{-1}\left(\frac{\lambda_a}{\Lambda}\right)$.

In the following, we assume that the value rate is *regular* and differentiable. Regularity implies that $v(\cdot)$ is continuous, bounded, concave, satisfies $\lim_{\lambda_a \to 0} v(\lambda_a) = 0$, and has a least maximizer λ_a^*. These assumptions are common in the RM literature (see, e.g., Gallego and van Ryzin (1994)). A sufficient condition for the concavity of the value rate is that valuations have *increasing failure rate* (IFR), or equivalently that the failure rate of values as given by $h(x) = f_v(x)/\bar{F}_v(x)$ is non-decreasing. A consequence of regularity is that the objective of program (4.13) is concave. Hence, (4.13) is a concave maximization problem with linear inequality constraints. Additionally, because the objective is continuous and the feasible set is compact, by Weierstrass' Theorem, there exists an optimal solution (Luenberger, 1969).

We are now in a position to characterize some conditions under which options are beneficial to the organizer. In the following we denote by R_a^D the optimal revenue of the deterministic approximation for the organizer when only advance tickets are sold, which amounts to setting $\lambda_o = 0$ in program (4.13).

Theorem 2. *In the symmetric case, when the seats are scarce ($C < \lambda_a^* T$) and fans strictly prefer their own team ($\ell < 1$), introducing options increases the revenue of the organizer ($R_o^D > R_a^D$). However, when the capacity of the stadium is large ($C \geq \lambda_a^* T$) or fans are indifferent among teams ($\ell = 1$) options do not increase the revenue.*

Proof: Recall that the deterministic approximation of the advance ticket pricing problem is equal to the option pricing problem (4.13) under the condition that $\lambda_o = 0$. This can be equivalently

written as

$$R_a^D = \max_{\lambda_a \geq 0} \quad T\left(q + (1-q)\ell\right) v(\lambda_a) \tag{4.14}$$
$$\text{s.t. } T\lambda_a \leq C, \lambda_a \leq \Lambda.$$

We write the gradient of the option pricing problem objective

$$\frac{\partial R_o^D}{\partial \lambda_o} = Tqv'(\lambda_a + \lambda_o),$$
$$\frac{\partial R_o^D}{\partial \lambda_a} = T(1-q)\ell v'(\lambda_a) + Tqv'(\lambda_a + \lambda_o).$$

First, we look at the case where the seats are scarce ($C < \lambda_a^* T$). In the advance ticket pricing problem (4.14) the organizer can afford to price higher, and prices at the run-out rate $\lambda_a^0 = C/T$, i.e., the intensity at which all seats are sold over the time horizon. Note that λ_a^0 is a constrained global optimum of the advance selling problem, and $v'(\lambda_a^0) > 0$. Starting from $(\lambda_a^0, 0)$ in the options pricing problem, we will study the impact of increasing the options' intensity on the revenue. Clearly, $(\lambda_a^0, 0)$ is a feasible solution of (4.13). Since capacity is binding, to compensate for an increase in λ_o the organizer needs to decrease the intensity of advance tickets. Thus, from (4.13b) we obtain that $\frac{d\lambda_a}{d\lambda_o} = -\frac{2}{N} = -q$. Evaluating the total derivative of the objective at $(\lambda_a^0, 0)$ we obtain

$$\begin{aligned}\frac{dR_o^D}{d\lambda_o} &= \frac{\partial R_o^D}{\partial \lambda_o} + \frac{\partial R_o^D}{\partial \lambda_a}\frac{d\lambda_a}{d\lambda_o} \\ &= Tqv'(\lambda_a^0) - Tq\left((1-q)\ell + q\right)v'(\lambda_a^0) \\ &= Tq(1-q)(1-\ell)v'(\lambda_a^0) > 0.\end{aligned}$$

This implies that the current solution can be improved by introducing except when $\ell = 1$, in which case there is no benefit from selling options.

Second, we consider the case where the capacity of the stadium is large ($C \geq \lambda_a^* T$). In the advance ticket pricing problem (4.14) the organizer ignores the problem of running out of seats

and prices according to the revenue maximizing rate λ_a^*. Note that λ_a^* is an unconstrained global optimum, and thus $v'(\lambda_a^*) = 0$. Clearly, $(\lambda_a^*, 0)$ is a feasible solution of (4.13), and the gradient of the objective is zero at $(\lambda_a^*, 0)$ since $v'(\lambda_a^*) = 0$. Hence, this solution is an unconstrained local optimum and the concavity of the program implies this is also a global optimum. Thus, the current solution cannot be improved by introducing options and this result is independent of ℓ. □

The previous result shows that options are beneficial for the event manager only when the demand is high with respect to the stadium's capacity and fans strictly prefer their own team over any other. In the case that fans are indifferent among teams ($\ell = 1$), the result is trivial since consumers strictly prefer advance tickets over options. The most interesting case is when fans strictly prefer their own team over any other ($\ell < 1$). From the point of view of a consumer, the main difference between the products is that an advance ticket allows him to attend the final game even when his favorite team is not playing, providing an extra source of utility. Therefore, if both products have the same expected cost, a risk-neutral consumer would choose an advance ticket over an option. When capacity is abundant, the organizer can ignore the problem of running out of seats, and for the same expected revenue per product sold he can elicit a stronger demand for advance tickets. Thus, in this case the introduction of options is not beneficial for the organizer.

However, when capacity is scarce the organizer should balance the expected revenue and the expected capacity consumed for each unit of product sold. While each advance ticket consumes exactly one seat, options from different teams can be assigned to the same seat, which allows the organizer to effectively sell more than one option per unit of capacity. Even though at most one fan will exercise the option assigned to that seat, the organizer gets to keep the premiums paid by the other consumers. Thus, when capacity is scarce, there are two conflicting effects associated to the introduction of options. On one hand, consumers buy options only when the expected cost of an option is less than that of an advance ticket. Thus, the expected revenue per option sold is dominated by the revenue per advanced ticket sold. On the other hand, each option sold consumes less capacity in expectation than an advance ticket, allowing the organizer to sell more tickets. In the proof of Theorem 2 we show that the second effect dominates: the organizer can compensate for

the reduced revenue per option by selling more tickets, and the introduction of options is beneficial when capacity is scarce. Note that as the scarcity increases (as T increases), the benefit from offering options will also increase.

Theorem 2, however, does not show how the benefit from options chaanges as a function of ℓ. Next, we perform some comparative statics w.r.t. the love-of-the-game. As the love-of-the-game parameter is increased, fans become less sensitive to the teams playing at the final. As a result, options start to lose their attractiveness, and demand for advance tickets increases. Hence, as shown in the next Proposition, one should expect the benefit from introducing options to decrease as ℓ is increased.

Proposition 2. *In the symmetric case, when seats are scarce ($C < \lambda_a^* T$) and fans strictly prefer their own team over any other ($\ell < 1$), both the absolute and relative benefit of introducing options decreases as ℓ increases.*

Proof: Let $R_a^D(\ell)$ and $R_o^D(\ell)$ be the optimal values of (4.14) and (4.13) as a function of ℓ, respectively. First, we show that the absolute benefit of introducing options decreases as ℓ increases. We proceed by showing that the difference $R_o^D(\ell) - R_a^D(\ell)$ is decreasing in ℓ. Notice that the objective function of both problems is convex as a function of ℓ. By the Maximum Theorem the functions $R_a^D(\ell)$ and $R_o^D(\ell)$ are convex, and differentiable almost everywhere. We proceed by calculating the total derivatives of $R_a^D(\ell)$ and $R_o^D(\ell)$ with respect to ℓ.

For the advance ticket pricing problem, we have that the optimal solution of (4.14) is λ_a^0 because $C < \lambda_a^* T$. Then, any change in ℓ does not affect the optimal solution and the derivative of $R_a^D(\ell)$ with respect to ℓ is given by

$$\frac{dR_a^D(\ell)}{d\ell} = T(1-q)v(\lambda_a^0). \tag{4.15}$$

For the options pricing problem, we have from the Envelope Theorem that the derivative of $R_o^D(\ell)$ with respect to ℓ is

$$\frac{dR_o^D(\ell)}{d\ell} = T(1-q)v(\lambda_a(\ell)), \tag{4.16}$$

where $\lambda_a(\ell)$ denotes the optimal arrival intensity for advance tickets in 4.13 for fixed ℓ.

A trivial consequence of the capacity constraint (4.13b) is that $\lambda_a(\ell) \leq \lambda_a^0$. Additionally, because seats are scarce we have $\lambda_a^0 < \lambda_a^*$. Finally, since the value rate is increasing in $[0, \lambda_a^*)$, we conclude that $\frac{dR_a^D(\ell)}{d\ell} \geq \frac{dR_o^D(\ell)}{d\ell}$, and the difference is decreasing in ℓ.

For the relative benefit, we first write the ratio of revenues as $\frac{R_o^D(\ell)}{R_a^D(\ell)} = 1 + \frac{R_o^D(\ell) - R_a^D(\ell)}{R_a^D(\ell)}$. From (4.15) it is clear that $R_a^D(\ell)$ is increasing in ℓ, and the result follows. □

Next, we establish bounds on the revenue improvement that offering options provides when the seats are scarce (if seats are not scarce, Theorem 2 shows that offering options does not increase revenue).

Proposition 3. *In the symmetric case, when the seats are scarce ($C < \lambda_a^* T$) we have the following bounds on the revenue improvements that offering options provide.*

1. *If fans obtain a positive surplus from attending a game without their own team ($\ell > 0$), the revenue under options pricing converges to the revenue under advance selling as N grows to infinity. Moreover, the convergence rate is given by*

$$1 \leq \frac{R_o^D}{R_a^D} \leq 1 + \frac{2}{N\ell} \frac{v(\lambda_a^*)}{v(\lambda_a^0)}.$$

2. *If fans obtain zero surplus from attending a game without their own team ($\ell = 0$), the revenue obtained when both advance tickets and options are offered strictly dominates the case when only advance tickets are offered. Moreover, their ratio is given by*

$$\begin{aligned} \frac{R_o^D}{R_a^D} &= \frac{v\left(\min\left\{\lambda_a^*, \lambda_a^0 \frac{N}{2}\right\}\right)}{v(\lambda_a^0)} \\ &= \frac{v(\lambda_a^*)}{v(\lambda_a^0)} > 1 \quad \textit{when } N \geq 2\left\lceil \frac{\lambda_a^*}{\lambda_a^0} \right\rceil. \end{aligned}$$

Proof: First, let us prove the first part of the proposition when $\ell > 0$. Observe that since capacity is scarce, the optimal solution of the advance ticket pricing problem (4.14) is the run-out rate

$\lambda_a^0 = C/T$, and it is independent of the number of teams. Let $\left\{\left(\lambda_a^{(N)}, \lambda_o^{(N)}\right)\right\}_N$ be a sequence of optimal solutions to the advance ticket and options pricing problem (4.13) indexed by the number of teams. Scarcity of seats together with concavity guarantee that the capacity constraint (4.13b) is binding at the optimal solution. Since intensities are bounded from above by Λ, this guarantees that $\lim_{N\to\infty} \lambda_a^{(N)} = \lambda_a^0$. As a side note, it is not necessarily the case that $\lambda_o^{(N)}$ converges to zero as N goes to infinity.

Second, we show that the following inequality holds

$$\lambda_a^{(N)} \leq \lambda_a^0 \leq \lambda_a^{(N)} + \lambda_o^{(N)} \leq \lambda_a^*. \tag{4.17}$$

The first inequality is a trivial consequence of the capacity constraint (4.13b). For the second inequality observe that the capacity constraint (4.13b) is binding, and thus $\lambda_a^0 = \lambda_a^{(N)} + \frac{2}{N}\lambda_o^{(N)} \leq \lambda_a^{(N)} + \lambda_o^{(N)}$. For the third inequality suppose that $\lambda_a^{(N)} + \lambda_o^{(N)} > \lambda_a^*$ for some N, and consider an alternate solution in which the options' intensity is decreased to $\tilde{\lambda}_o^{(N)} = \lambda_a^* - \lambda_a^{(N)}$. Clearly, $\tilde{\lambda}_o^{(N)} \geq 0$, and the new solution satisfies the capacity constraint and the third inequality. Moreover,

$$\begin{aligned} R_o^D\left(\lambda_a^{(N)}, \lambda_o^{(N)}\right) &= T(1-\frac{2}{N})\ell v(\lambda_a^{(N)}) + T\frac{2}{N}v(\lambda_a^{(N)} + \lambda_o^{(N)}) \\ &\leq T(1-\frac{2}{N})\ell v(\lambda_a^{(N)}) + T\frac{2}{N}v(\lambda_a^*) = R_o^D\left(\lambda_a^{(N)}, \tilde{\lambda}_o^{(N)}\right), \end{aligned}$$

where the first inequality follows since λ_a^* is the least maximizer of v. Thus, the new solution is also optimal. This shows that if the third inequality does not hold for any N, we can construct a solution $\left(\lambda_a^{(N)}, \tilde{\lambda}_o^{(N)}\right)$ for which it holds. So, without loss of generality, we can conclude that the third inequality holds.

So, the ratio of optimal revenues can be written as

$$\begin{aligned}\frac{R_o^D\left(\lambda_a^{(N)},\lambda_o^{(N)}\right)}{R_a^D(\lambda_a^0)} &= \frac{T(1-\frac{2}{N})\ell v(\lambda_a^{(N)})+T\frac{2}{N}v(\lambda_a^{(N)}+\lambda_o^{(N)})}{T\left[(1-\frac{2}{N})\ell+\frac{2}{N}\right]v(\lambda_a^0)}\\ &= \frac{N\ell-2\ell}{N\ell+2(1-\ell)}\frac{v(\lambda_a^{(N)})}{v(\lambda_a^0)}+\frac{2}{N\ell+2(1-\ell)}\frac{v(\lambda_a^{(N)}+\lambda_o^{(N)})}{v(\lambda_a^0)}\\ &\leq \frac{v(\lambda_a^{(N)})}{v(\lambda_a^0)}+\frac{2}{N\ell}\frac{v(\lambda_a^{(N)}+\lambda_o^{(N)})}{v(\lambda_a^0)} \leq 1+\frac{2}{N\ell}\frac{v(\lambda_a^*)}{v(\lambda_a^0)},\end{aligned}$$

where the second equation is obtained by algebraic manipulation, the first inequality follows from bounding the leading factor of the first term by 1 and the leading factor of the second term by $\frac{2}{N\ell}$, and the second inequality follows from (4.17) together with the fact that $v(.)$ is non-decreasing in $[0,\lambda_a^*]$.

Now, if $\ell=0$ options and advance tickets are equivalent to customers, and customers choose the product with the lowest expected price. Thus, we only need to consider the case where the organizer sells only options the whole time horizon. The options pricing problem is now

$$\begin{aligned}R_o^D = \max_{\lambda_o^\Sigma\geq 0}\quad & T\frac{2}{N}v(\lambda_o^\Sigma)\\ \text{s.t. } & T\lambda_o^\Sigma \leq \frac{N}{2}C,\quad \lambda_o^\Sigma\leq\Lambda.\end{aligned}$$

This problem is similar to the advance selling problem (4.14) except that capacity is scaled by $\frac{N}{2}$. Scarcity implies that $C<\lambda_a^* T$, and thus the optimal solution is $\lambda_o^{(N)}=\min\left\{\lambda_a^*,\lambda_a^0\frac{N}{2}\right\}$. Then, the optimal value is $R_o^D=T\frac{2}{N}v(\min\left\{\lambda_a^*,\lambda_a^0\frac{N}{2}\right\})$. Finally, observe that for $N\geq 2\left\lceil\frac{\lambda_a^*}{\lambda_a^0}\right\rceil$ the organizer may price according to the revenue maximizing rate λ_a^* and $R_o^D=T\frac{2}{N}v(\lambda_a^*)$. □

The previous result shows that when $\ell>0$ the revenue under options pricing converges to the revenue under advance selling as N grows to infinity. Furthermore, the convergence rate is $O\left(\frac{1}{N}\right)$. The intuition behind this result is that, as the number of teams grows, fans are aware that the probability of their own team reaching the final event decreases. So, in order to keep options attractive for consumers, the organizer needs to set lower prices, and thus revenues generated by

options subside. Because fans also obtain a positive surplus from attending a game without their own team, more consumers choose to buy advance tickets as the number of teams grows. However, when $\ell = 0$ options and advance tickets are equivalent to customers, and they are only interested in one outcome: their own team advancing to the final game. Because the probability of that outcome converges to zero, the number of tickets sold converges to zero as well. This observation, combined with the existence of the *null price* (or $\lim_{\lambda_a \to 0} v(\lambda_a) = 0$), causes the organizer's revenue to diminish to zero in all pricing schemes as the number of teams increases. Surprisingly, even though the revenues when only advance tickets are offered and, when both advance ticket and options are offered converge to zero, they do so at different rates. The rationale is that when the organizer offers only options each team has up to $C/2$ tickets available. Hence, the capacity of the stadium is extended, and for a suitable large N the organizer may price according to the revenue maximizer rate λ_a^*.

4.3.2 Social Efficiency

How do the introduction of options affect customers' surplus? Options allow fans to hedge against the risk of watching a team that it is not of their preference. As a consequence, a larger number of seats will be taken by fans of the teams that are playing in the final. So, intuitively we expect the introduction of options to increase the total surplus of the fans.

Recall that, from Theorem 2, options are beneficial to the organizer only if the capacity is scarce and fans strictly prefer their own team over any other. Hence, we only need to consider the consumer surplus under those assumptions, else the organizer has no incentive to sell options. The following proposition shows that under these assumptions if the valuation random variable is IFR, then options do increase consumer surplus. This result shows that offering options can benefit both the promoter and the consumers. Furthermore, the result also shows that benefit increases for both parties as ℓ decreases.

Proposition 4. *Assume that the valuation random variable is strictly IFR. Then, in the symmetric case, when the seats are scarce ($C < \lambda_a^* T$) and the fans strictly prefer their own team over any other ($\ell < 1$), introducing options increases consumer surplus. Furthermore, both the absolute and*

relative benefit of introducing options decreases as ℓ increases.

Proof: Let us begin by defining the total surplus of consumers that will buy an advance ticket when the arrival intensity is λ_a,

$$\begin{aligned} S_a^D(\lambda_a) &= T\Lambda(q+(1-q)\ell)\bar{G_v}\left(\frac{p_a(\lambda_a)}{q+(1-q)\ell}\right) \\ &= T(q+(1-q)\ell)s(\lambda_a) \end{aligned}$$

where the surplus rate is defined as $s(\lambda_a) = \Lambda\bar{G_v}\left(\bar{F_v}^{-1}\left(\frac{\lambda_a}{\Lambda}\right)\right)$, and $\bar{G_v^i}(x) = \mathbb{E}\left[(V-x)^+\right] = \int_x^\infty \bar{F_v^i}(v)\mathrm{d}v$ the integrated tail of the valuations. Notice that the surplus rate is defined on $[0,\Lambda]$. Additionally, it is increasing, continuous, differentiable, non-negative, and bounded. The monotonicity stems from the fact that $\bar{F_v}^{-1}$ is decreasing and $\bar{G_v}$ is non-increasing. Moreover, it satisfies $\lim_{\lambda_a\to 0} s(\lambda_a) = 0$, and $\lim_{\lambda_a\to\Lambda} = \Lambda\mathbb{E}V$. In contrast to the revenue rate, the maximum is reached when the intensity is set to Λ, or equivalently the price set to zero. Not surprisingly, total consumer surplus is maximized when the tickets are given away for free.

In the advance ticket and options pricing problem, two sources contribute to the total consumer surplus. The first source is consumers who choose advance tickets over options. The second source is consumers who chose options over advance tickets. Some algebra shows that the total consumer surplus in terms of the arrival intensities, denoted by $S_o^D(\lambda_a,\lambda_o)$, is

$$S_o^D(\lambda_a,\lambda_o) = T(1-q)\ell s(\lambda_a) + Tqs(\lambda_a+\lambda_o).$$

Observe that the formula for consumer surplus is similar to the organizer's revenue with the exception that the value rate is replaced by the surplus rate.

Note that the derivative of the surplus rate w.r.t. λ_a is

$$\frac{ds}{d\lambda_a}(\lambda_a) = \frac{\lambda_a}{\Lambda}\frac{1}{f_v\left(\bar{F_v}^{-1}(\lambda_a/\Lambda)\right)}.$$

Composing the derivative with $\lambda_a(c) = \Lambda \bar{F}_v(c)$ we get

$$\left(\frac{ds}{d\lambda_a} \circ \lambda_a\right)(c) = \frac{ds}{d\lambda_a}\left(\Lambda \bar{F}_v(c)\right) = \frac{\bar{F}_v(c)}{f(c)} = \frac{1}{h(c)}.$$

Strict IFR implies that the composite function is decreasing in c. Because $\lambda_a(c)$ is decreasing, we conclude that original derivative is increasing and s is strictly convex.

Now, we are position to prove that offering options increases consumer surplus. First, let (λ_a, λ_o) be the optimal solution to the options pricing problem. Since seats are scarce, the capacity constraint (4.13b) is binding in the optimal solution. Then $\lambda_a^0 = C/T = \lambda_a + q\lambda_o = (1-q)\lambda_a + q(\lambda_a + \lambda_o)$, where we have written λ_a^0 as a convex combination of λ_a and $\lambda_a + \lambda_o$. Consider the convex combination of the same points, denoted by $\hat{\lambda}_a$, in which we multiply the first weight by ℓ and re-normalize. Hence, $\hat{\lambda}_a$ is given by

$$\hat{\lambda}_a = \frac{(1-q)\ell}{q + (1-q)\ell}\lambda_a + \frac{q}{q + (1-q)\ell}(\lambda_a + \lambda_o).$$

Notice that $\hat{\lambda}_a > \lambda_a^0$. This follows from $\lambda_o > 0$ implying that the second point is strictly greater than the first, and the weight of this larger point being larger in $\hat{\lambda}_a$ than in λ_a^0.

Finally, we have that

$$\begin{aligned} S_o^D = S_o^D(\lambda_a, \lambda_o) &= T(1-q)\ell s(\lambda_a) + Tqs(\lambda_a + \lambda_o) \\ &\geq T(q + (1-q)\ell)s(\hat{\lambda}_a) > T(q + (1-q)\ell)s(\lambda_a^0) = S_a^D(\lambda_a^0) = S_a^D, \end{aligned}$$

where the first inequality follows from the convexity of the surplus rate, the second inequality from the fact that the surplus rate is increasing and $\hat{\lambda}_a > \lambda_a^0$, and the last equality from λ_a^0 being the optimal solution to the advance selling problem when seats are scarce. Thus, the introduction of options increases consumer surplus. The proof for the sensitivity of options' benefits w.r.t ℓ is identical to the proof of Proposition 2 and is thus omitted. □

4.4 Numerical Results

In this section we describe a set of randomized experiments conducted to evaluate the improvements from offering options. The objective of these experiments is to study effect of introducing options on the event manager's revenue and consumer surplus, and to show that most of the results of Section 4.3 are robust to the heterogeneity of the tournament structure. In order to tackle instances of real-world size the analysis is based on the deterministic approximation of the problem.

The experiments were generated as follows. We assume that there were eight teams in a tournament; and similar to the FIFA World Cup, Rugby World Cup and the Superbowl, the tournament is of dyadic form. The probability vector q was drawn from the probability simplex for the two sets of teams in the tournament. The arrival rate λ_i and the love-of-the-game ℓ_i of each team i was sampled from a uniform distribution between $[0, 1]$. We assume that a fan's willingness to pay V is uniformly distributed between $[0, 4000]$, and that the stadium's capacity was of $C = 50,000$ seats. To asses the impact of scarcity on our model we consider different *load factors* across tournaments. The load factor is defined by $l_f = (T\Lambda)/C$ and measures the total demand relative to the size of the stadium: the higher the load factor, the scarcer the tickets. Load factors were sampled from a uniform distribution between $[2, 10]$, and the sales horizon T was scaled to match the load factor. We generated a total of 1000 different tournaments and used an interior point nonlinear optimization algorithm with multiple starting points to solve the first stage of the options pricing problem[3].

We start by analyzing the benefits of introducing options by comparing the event manager's revenue and consumer surplus with the baseline case of offering only advance tickets. Figure 4.4a shows a histogram of the distribution of the relative improvement of offering options across the different experiments. The average relative revenue improvement is 4.93% and its standard deviation is 5.19%. Figure 4.4b shows a similar histogram for the relative improvement in consumer surplus. The average relative consumer surplus improvement is 3.34% and the standard deviation is 4.45%.

[3]The experiment takes about 12 hours to run in MATLAB on a PC with a 8-core Xeon processor.

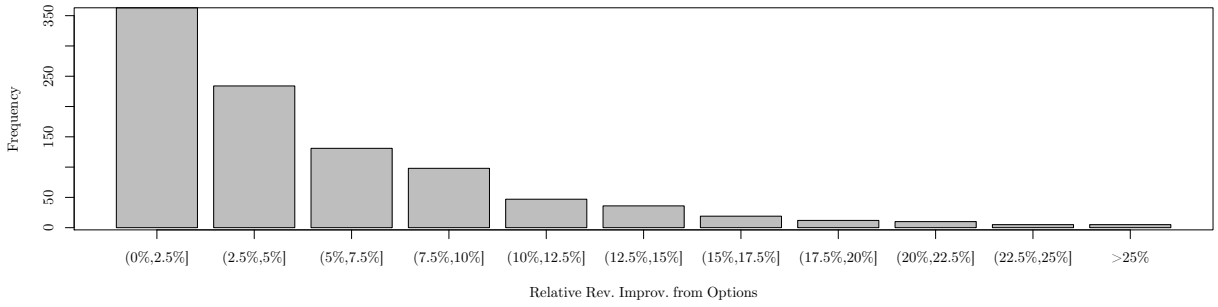

(a) Revenue

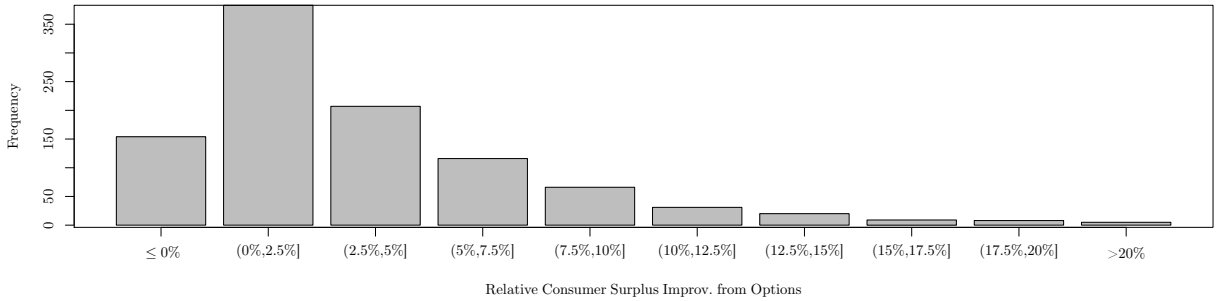

(b) Consumer surplus

Figure 4.4: Histograms of relative revenue and consumer surplus improvements from offering options.

Figure 4.5a plots the the average relative revenue improvement as a function of the load factors. The figure confirms that options are most beneficial when capacity is scarce, in agreement with the theoretical results obtained for symmetric tournaments in §4.3. Recall that the advantage of options over the advance tickets is that while each advance ticket consumes exactly one seat, options from different teams can be assigned to the same seat, which allows the organizer to effectively sell more tickets per unit of capacity. As more capacity is available, the relative benefit of selling options, in terms of a higher revenue per unit of capacity, dilutes. Thus, as the load factor is decreased, which is equivalent to increasing capacity, the benefit of introducing options decreases. Figure 4.5b shows that the impact of offering options on consumer surplus is also the greatest when capacity is scarce. Since the organizer has less incentive to sell options as capacity increases, the impact of

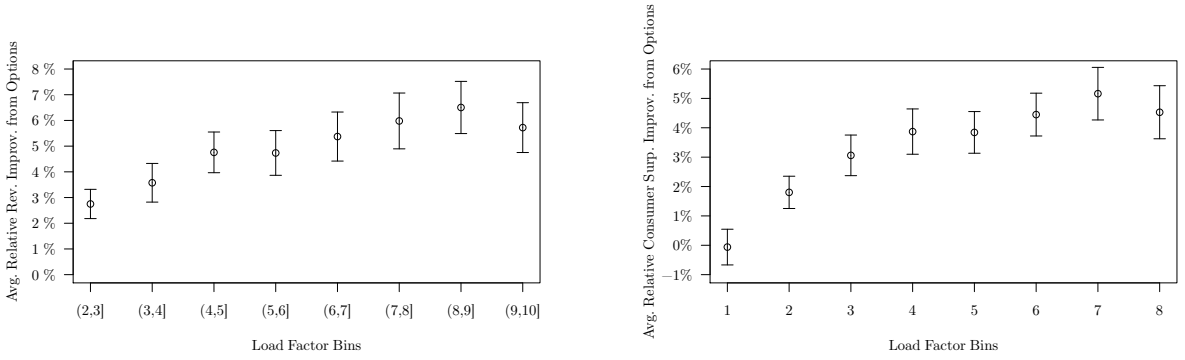

(a) Average relative revenue improvement for various load factors (with 95% conf. intervals).

(b) Average relative consumer surplus improvement for various load factors (with 95% conf. intervals).

Figure 4.5: Effect of l_f on revenues and consumer surplus.

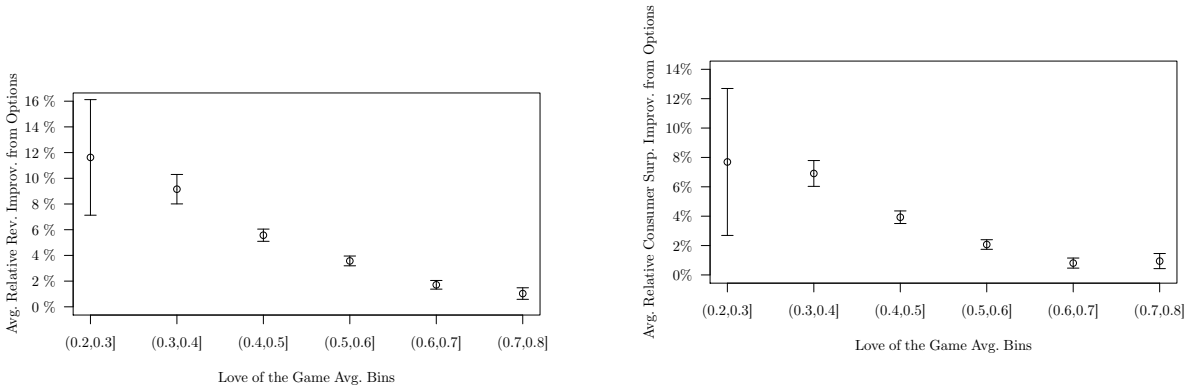

(a) Avg. relative revenue improvement by average ℓ across tournaments (with 95% conf. intervals).

(b) Avg. relative consumer surplus improvement by average ℓ across tournaments (with 95% conf. intervals).

Figure 4.6: Effect of ℓ on revenues and consumer surplus.

offering options on consumer surplus decreases.

Figure 4.6a depicts impact of the average love-of-the-game across all the teams in the tournament on the relative revenue improvement. As expected, offering options is most beneficial when ℓ is low since options target fans who care the most about their own teams playing in the finals. As ℓ increases, fans are less sensitive to the identity of the finalists, options become less attractive for them, and, consequently, the organizer does not benefit as much from offering options. Figure 4.6b confirms that the consumer surplus benefit of offering options also decreases as ℓ increases.

4.5 Conclusion

In this chapter we analyze consumer options that are contingent on a specific team reaching the tournament final. Offering options, in addition to advance tickets, allows an event manager to segment fans: advance tickets target fans with a higher willingness to pay who are less sensitive to the outcome, whereas options target fans who receive more value from attending a game when their favored team is in the finals. We address the problem of pricing and capacity control of such options and advance tickets under a stochastic and price-sensitive demand model, and propose a two-stage optimization approach to solve the problem. The first stage optimizes over the prices, while the second optimizes the expected revenue by controlling the subset of products that is offered at each point in time using a discrete choice revenue management model. To develop some insight, we provide a theoretical characterization of the problem in the symmetric case, i.e., when all teams are equal in terms of arrival rate and other characteristics. Under some mild assumptions we show that introducing options increases both the revenue of the organizer, and the surplus of the consumers. Numerical experiments confirm that most of these findings are robust to the heterogeneity of the tournament structure.

One promising line of future research involves relaxing the no-resale restriction, and allowing secondary markets and the selling of tickets after the tournament starts. In this case consumers decide wether to buy in the primary market, or wait for the resale market where brokers speculate on the resale price. The event manager, however, may exploit options as a mechanism to extract the consumer's surplus and potentially reduce the impact of the secondary market. Additionally, one may relax the single quality seat restriction by dividing the stadium according to seat quality, and considering instead a more sophisticated consumer choice model in which fans are offered a wider array of choices. Lastly, dynamic pricing of options is a natural future line of research. Dynamic pricing may provide higher revenues at the cost of substantially increased complexity.

Chapter 5

Small Modular Infrastructure

This chapter is based on the paper "Small Modular Infrastructure" which is joint work with Eric Dahlgren, Prof. Klaus Lackner and Prof. Garrett van Ryzin.

To develop the case for small modular infrastructure, one must examine existing examples of small-scale modular technologies, the determinants of economies of scale, the impact of manufacturing learning curves on capital costs and the effect of unit size on operating costs. It is also important to account for the many flexibility and diversification advantages of small modular units. Toward this end, in §5.1 we look at examples of small modular technology. §5.2 then provides a theoretical analysis on how economies of unit scale and learning affect capital costs, and how unit size affect operating costs. In §5.3 we use the U.S. electricity industry as a case study to validate the theoretical concepts. §5.4 looks at the flexibility advantages that come with employing small modular units, such as investment flexibility and diversification. In §5.5 we give examples of several technologies where the trend of ever increasing size has been observed but which could benefit from smaller unit scale. Lastly, §5.6 concludes with some general observations about how to make the transition to "thinking small".

5.1 Examples

Before analyzing the case for small unit scale in more depth, it is helpful to consider some examples from the industry. Small, modular nuclear reactors, chlorine plants, and biomass gasification systems are technologies that are either already commercially available or currently under development, and importantly, these technologies have taken advantage of small unit scale and the economies of mass manufacturing. The specific technologies are very different, and they face different impediments to a large unit scale; regulatory hurdles for nuclear power, safety hazards for the production and transportation of chlorine and the distributed nature of the inputs for biomass gasification. In each case, these idiosyncratic reasons were enough to make small unit scale a feasible option. Despite their differences, these examples hint at the common underlying potential of a radically new strategy for building infrastructure: modularize, automate and mass produce.

5.1.1 Small modular reactors (SMRs)

Small-scale nuclear power may seem counter-intuitive, but there is growing interest in a new generation of small, modular nuclear reactors (SMRs). Unlike existing generators with an average capacity close to 1 GWe, SMRs have capacities as small as 25 MWe (Nuclear Energy Institute, 2011; Adee and Guizzo, 2010). Because they are small, reactors can be manufactured off-site and transported to location semi- or fully-constructed; some are even small enough to be transported by truck. As a result, the time required to bring a new plant on line – one of the biggest obstacles for nuclear power – is shortened from an average of twelve to less than five years (Kadak *et al.*, 1998; Cohen, 1990). Along with long lead times, high capital costs have been a major impediment to nuclear power. A typical large-scale nuclear power plant requires a minimum investment of around $12 billion in capital (Wald, 2011). With SMRs, the upfront capital cost can be as low as $100 million. Moreover, investors can easily expand a plant in the future depending on market conditions (The Economist, 2010). Scalability of SMRs also makes nuclear power attractive for smaller projects, thereby increasing the market for such technology. For example, SMRs can be used as "drop-in replacements" in aging power plants since they can utilize the existing transmission capacity or

as power sources in remote applications like mining and oil and gas production where dependable baseload power is crucial (The Economist, 2010; Hyperion Power Generation, 2011).

While SMRs can be thought of as scaled down versions of classical reactors, they also share a common set of design characteristics that make them safer than classical reactors (Kuznetsov, 2004). Consequently, safety and support systems are less complex. In addition, due to their modularity, major maintenance tasks can be handled by shipping the entire reactor unit back to the factory. These factors can reduce the on-site staff size, per unit of power output fivefold compared to traditional nuclear power plants (Kadak *et al.*, 1998). Another operational advantage of SMRs is the reduced impact of maintenance down-time. Current nuclear power plants typically have one or two reactors, so during maintenance they lose most, if not all, of their generating capacity. With SMRs, a power plant would have 4-12 reactors, so if one reactor is taken off-line for maintenance, the impact on total generation capacity is much less (Kadak *et al.*, 1998).

There are numerous small modular reactors being designed around the world. Examples include Toshiba's 4S, Babcok & Wilcox's mPower, Hyperion's HPM, and Rosatom's KLT-40. Currently, most of the designs are being approved, and the first SMR plant is expected to be operational by 2018 (Smith, 2010). There are also plans to use SMRs in unconventional settings. For example, Rosatom, a Russian state corporation in charge of the nuclear complex, has ordered the construction of several floating nuclear power stations. The first, Akademik Lomosonov, was launched in 2010 and is expected to become operational by 2016 (World Nuclear News, 2012). Another example is the small offshore reactor Flexblue developed by DCNS, a French Naval shipyard company. Commercial production is scheduled to commence by 2016 (World Nuclear News, 2011).

Nascent SMRs provide a sense of how a radically smaller unit scale can fundamentally disrupt an industry accustomed to massive scale. Their designs are simplified and standardized; they are manufactured in the factory and not in the field; investment is significantly more flexible and less risky; and their small size opens entirely new domains of applications for nuclear power. All these are key advantages of the small modular approach to technology.

5.1.2 Small modular chlorine plants

Chlorine is widely used for the production of industrial and consumer products, disinfection and water purification. Being highly toxic, chlorine is dangerous to store and transport. For example, in a highly publicized train crash in 2005 in Graniteville, South Carolina, rail tank cars carrying chlorine ruptured resulting in the death of nine people and the evacuation of thousands of residents (Bogdanich and Drew, 2005). To avoid the costs and risks associated with chlorine storage and transportation, companies such as GE, MIOX and AkzoNobel have designed small skid-mounted modular chlorine plants which can be placed close to points of demand. Manufacturing these modular plants off-site reduces on-site construction requirements, shortening the time needed to bring a plant online. Modular design also enables efficient inspection and maintenance, reducing operational costs. All designs are highly automated, which decreases the requirement for on-site skilled personnel. Moreover, AkzoNobel's design aims to completely eliminate on-site personnel requirement by controlling the facilities remotely, thus realizing the scale benefits of traditional chlorine plants by providing centralized monitoring and control.

Small modular chlorine plants have been around for some time. GE's Cloromat has been in commercial use for over 35 years and, MIOX has been producing its own line of plants since 1994 (GE Power & Water, 2011; MIOX Corporation, 2011). AkzoNobel's solution is quite new, with the first plant targeted to come online in 2012 (Akzo Nobel N.V., 2011; UHDENORA, 2011).

This trend of small modular chlorine plants hints at what is possible more broadly with a strategy of small unit scale. Production is distributed and located close to points of demand, eliminating the need for transportation. Plant designs are standardized and mass produced to reduce capital costs. And on-site labor is minimized - or even eliminated - by utilizing advanced sensing, automation and communications technology that enable remote control of plant operations. The overall approach achieves many of the capital and labor savings of large unit scale yet provides benefits, such as distributed operation, that can only be achieved with small plants.

5.1.3 Small modular biomass gasification systems

Biomass, e.g. wood and agricultural waste, is a widely available resource that can be used to produce electricity and heat through gasification. Being abundant, biomass is a good candidate for use in distributed electricity production and accounts for approximately 1-2% of U.S. electricity production (EIA, 2010a).

Several companies such as AESI, Community Power Corporation(CPC) and Innovative Energy Inc.(IEI) have commercially available designs for small modular gasification devices. These devices convert biomass into synthesis gas to generate electricity and heat. AESI's and CPC's units have capacities in the range of 50-100 kWe and IEI produces standard 1-2 MWe units (Community Power Corporation, 2011b; AESI Inc., 2011; Innovative Energy Inc., 2011). Because of their small size, AESI and CPC ship their systems in a small number of shipping containers which are connected to each other on-site. This modular approach allows for easy integration and shortens the time required to get a system operational. IEI's system is larger, but it is also brought to the site semi-manufactured where it is connected to existing units and infrastructure. All designs are highly automated and CPC's design allows its equipment to be controlled remotely from a central location over the internet.

Like modular chlorine plants, small modular biomass gasification systems have already been deployed in numerous projects. IEI is constructing a 5 MWe waste-to-energy power plant in Missouri, and AESI has deployed its system at a pharmaceutical plant in North Carolina (Cure, 2011; Tomich, 2010). CPC lists numerous institutions, such as Kedco, Shell Solar, Idaho Power Corporation and Western Regional Biopower Energy Program, as its customers (Community Power Corporation, 2011a).

Again, this example of small modular biomass plants illustrates a broader strategy of combining mass manufacturing and highly automated operations to enable small unit scale plants to achieve economies of capital and operating costs comparable to their larger brethren, while creating entirely new benefits such as short lead times and distributed operation only achievable by small scale technology.

5.2 A theory of unit scale

We next look at the theory on the fundamental factors that drive the choice of unit size and how these factors are changing due to advances in technology. Our analysis considers capital costs, operating costs and the benefits of flexibility. Collectively, the theory points to significant advantages to radically reducing unit scale.

5.2.1 Capital costs

Given a prototype unit of known cost, one can follow two different strategies to scale up output. One option is to create a single large unit of sufficient capacity; in effect, simply scaling up the size of the prototype. The other option is to provide a large number of standardized units that aggregate to produce the total desired output. Such a massively parallel production strategy is possible as long as there is no significant cost to combining the separate outputs into a single stream.

Capital cost, regardless of strategy, is an important determinant of the economic viability of any project. The literature on cost engineering offers empirical relations between the cost of the required equipment and output for both strategies. In this section, we compare these costs and conclude that, based on established empirical relationships, the cost per unit of capacity approximately scales the same in both cases. Hence, capital cost considerations are not likely to determine the optimal size of the production equipment. In the following, we will refer to the cost reductions achievable in the two cases as the economies of unit scale and economies of mass production, respectively.

5.2.1.1 Economies of unit scale

A traditional method of estimating the cost k of a piece of equipment with capacity c uses a power law:

$$k(c) = k(c_0)\left(\frac{c}{c_0}\right)^{\alpha}, \tag{5.1}$$

where $k(c_0)$ is the cost of a reference unit of capacity c_0. If the exponent is less than unity ($\alpha < 1$), the cost per unit size is decreasing, ($d(k(c)/c)/dc < 0$), creating an impetus for building larger units. Numerical values for α have been estimated for a wide array of process equipment. Typically these

range from 0.6 to 0.8 (Humphreys and Katell, 1981; Jenkins, 1997; Euzen *et al.*, 1993), hence the so-called "0.7 rule," or sometimes "two-thirds rule." However, at very large sizes the structural integrity of materials becomes an issue. Consequently, pushing the boundaries on the large end of the spectrum has normally been accompanied by development in materials that are lighter and stronger, as for example in the use of carbon fibers in wind turbine construction (see (Levin, 1977)).

The observed decline in cost of equipment with increasing unit size can be attributed to several factors mentioned above. However, a frequently cited explanation for the appearance of the scaling law in (5.1), with the exponent α ranging from 0.6 to 0.8, relies on the geometric relationship between surface area and volume (Haldi and Whitcomb, 1967; Husan, 1997; Tribe and Alpine, 1986; van Mieghem, 2008). This explanation suggests that costs scale with the amount of material used in the structure, which in turn is supposed to scale with surface area. Often when considering a piece of industrial equipment like a pressure vessel, a chemical reactor or a truck bed, it is reasonable to assume that its capacity is proportional to its useful volume. If both assumptions apply, scaling the capacity with a factor λ results in costs scaling as $\lambda^{2/3}$. This offers a nice explanation for the often-observed value of $\alpha \approx 2/3$ in (5.1).

However, from the perspective of structural mechanics, this argument is flawed. In most situations, as the volume of a structure is increased, it is necessary to increase the wall thickness as well in order to preserve structural integrity. As a result, the mass of an optimally designed unit typically increases more rapidly than the 2/3 power of the enclosed volume. Indeed, in any situation in which the weight of the structure matters, it is usually not even possible to achieve uniform scaling, i.e. all linear dimensions increase by the same scaling factor, $\lambda^{1/3}$. Instead, wall thicknesses or diameters of structural members must grow faster than the linear size of the system. Therefore, the mass of the unit, and thereby costs, would scale faster than the capacity of the system.

In living systems, the break-down of uniform scaling can be seen by comparing a mouse to an elephant, where the latter has disproportionately thicker legs to support its weight; the same concept holds for industrial objects. A structure operating at its mechanical capacity (with appropriate safety factors) cannot be uniformly scaled up. The weight of the larger structure would exceed the limits of its structural integrity. A way around this problem is to use lighter materials, stronger

materials, or a combination of the two. Typically, advanced materials are not used at smaller scales because they are more expensive. However, even with the most advanced materials, physics imposes a boundary which can only be pushed so far. A detailed analysis of the scaling of solid structures can be found in (Dahlgren and Lackner, 2012). While we do not challenge the observed empirical relationship between cost and unit size, we submit that the conventional explanation, that the wall area to volume ratio drives scaling behavior, is overly simplistic and under more careful analysis proves incorrect. Instead, structural constraints tend to reduce cost advantages of larger units, and if these constraints were to dominate, they would result in diseconomies of unit scale.

5.2.1.2 Economies of mass production

Studies of the economies of mass production date back to Wright (1936) in the context of airplane production. Arrow (1962) provided a general analysis of the subject in which he argues that costs of manufactured goods decline with the cumulative number produced. There have since been various studies resulting in ample data on the cost reduction with cumulative production (see e.g. (Argote and Epple, 1990; Ferioli and van der Zwaan, 2009; McDonald and Schrattenholzer, 2001; Tsuchiya and Kobayashi, 2004)).

Costs decline as cumulative output increases because of specialization in the production process and improved process and product design. For example, when organizing a production process to manufacture a large number of identical units, one can justify high degrees of specialization in tools, layout and job design that can dramatically reduce per-unit manufacturing costs. Also, in high-volume manufacturing, it becomes justifiable to invest significantly in product design in order to make parts and subsystems more integrated, easier to assemble and hence less costly to make (*design for manufacturing*). The second benefit of producing in volume is learning. As a manufacturer gains cumulative experience producing a given product via a certain process, myriad improvements in design, materials and production methods are uncovered. Such a process of *continuous improvement* can lead to significant cost reductions as production volumes increase. Conversely, cost reductions attributed to learning can reverse themselves given extended breaks in production. This trend, akin to a "forgetting curve", can explain the relatively small cost reductions over time for larger

and more long-lived installations. Importantly, installations endowed with greater longevity also tend to be custom-made rather than mass-produced which further contributes to the comparably small reductions in cost from one investment to the next (McDonald and Schrattenholzer, 2001).

The effect of declining cost with the number of units produced is commonly formulated using learning curves, which state that the unit cost decreases by a fraction $\varepsilon < 1$ as the cumulative production doubles. That is, the cost, k_{2n}, of the $2n$-th unit is a fraction $\varepsilon < 1$ of the cost, k_n, of the n-th unit, or

$$\frac{k_{2n}}{k_n} = \varepsilon. \tag{5.2}$$

Sometimes this cost reduction is expressed by the learning rate, defined by $1 - \varepsilon$. Based on (5.2), a continuous approximation of k_n can be formulated as

$$k_n = k_1 \varepsilon^{\log_2 n} = k_1 n^{\log_2 \varepsilon},$$

where k_1 is the cost of the first unit produced. The aggregated cost, $K(N)$, of N mass-produced units following the given learning curve, can then be expressed as

$$K(N) \approx \int_1^N k_n dn = \frac{k_1}{1 + \log_2 \varepsilon} N^{\log_2 \varepsilon + 1}. \tag{5.3}$$

5.2.1.3 Comparing economies of unit scale with economies of mass production

The expressions in (5.1) and (5.3) offer cost estimates of the distinctly different strategies of producing systems of large total capacity. To compare the two, we consider the options of either scaling up a reference unit of capacity c_0 and cost k_0 by a factor N (economies of unit scale) or manufacturing N copies of the same reference unit (economies of mass production). Either way, the end result is a system of total capacity Nc_0. The two cost estimates yield

$$k(Nc_0) = k_0 \left(\frac{Nc_0}{c_0} \right)^{\alpha} = k_0 N^{\alpha}, \qquad \text{(Economies of unit scale)}, \tag{5.4}$$

$$K(N) = \frac{k_1}{1 + \log_2 \varepsilon} N^{\log_2 \varepsilon + 1}, \qquad \text{(Economies of mass production)}. \tag{5.5}$$

A statistical analysis based on a sample of 22 different mass-production-oriented industrial sectors found an average learning rate of 19% (Ferioli *et al.*, 2009), which corresponds to a value of the exponent in (5.5) of 0.7, i.e. $\log_2 \varepsilon + 1 = 0.7$. Since typical values for the exponent α in (5.4) range between 0.6 to 0.8 it is reasonable to conclude that $\log_2 \varepsilon + 1 \approx \alpha$ and hence, the reductions in production costs ensuing from economies of mass production are on par with those from economies of unit scale.

This comparison assumes that the total installed capacity is independent of the choice of unit size, which would be true, for example, in building a single factory. However, smaller unit sizes frequently opens up new domains of application for a given technology, and hence increase the overall market size. The increased volume of demand from an increased market, in turn, further reduces cost per unit capacity. For example, as noted in §5.1.1, current sizes of nuclear reactors make them infeasible for a wide range of applications. With the introduction of SMRs, nuclear energy is a viable option for much smaller projects such as powering remote mining operations.

5.2.2 Operating costs

As noted previously, high conversion and labor efficiencies are traditional benefits of large unit scale production. However, their impacts on cost have changed dramatically with advances in technology. Given these advances, one must take a closer look at the benefits of scale and how technology can capture these benefits without resorting to large unit scales.

5.2.2.1 Labor efficiency

When the amount of labor scales with the number of separate units employed, rather than with individual unit size, scaling up unit sizes naturally increases labor productivity. Arguably, this has been a common motivation in many energy and materials processing industries in the past century, thereby driving, at least in part, the trend of ever increasing unit size. Notable examples can be found in the electricity generation sector, see §5.3, and in the the mining industry, as detailed in §5.5.3. However, as remarked in section 5.2.1.1, such a strategy for increasing labor productivity will eventually run into physical barriers that are progressively harder to surmount.

An alternative strategy to reduce labor cost is to employ automation which can ultimately drive labor cost to zero, or at least decouple it from the number of individual units employed. Naturally, every process has its own characteristics and its amenability to automation needs to be evaluated on a case-by-case basis. However, progress in wireless communication, GPS technology, sensor technologies and computational processing power is fundamentally changing the economics of automation; the capabilities of these technologies are soaring while costs are plummeting, enabling unprecedented degrees of low-cost automation. To be specific, Nordhaus (2002) reports that the average price of computing power decreased by more than 40% per year between the years 1990-2002. The communication sector has also seen significant advances. International Telecommunication Union (ICT) reports that the average price for a high-speed Internet connection dropped by 52% in the world between the years 2008-2010, and Akamai reports that average global peak connection speed increased by 67% between 2010-2011 (International Telecommunication Union, 2011; Kaufmann, 2011). The result is that automation and remote sensing and control technologies now provide tremendous capability at very low cost.

Common instances of such automation include electronic toll collection, ATMs and electronic check-ins for flights. In the case of ATMs and car-sharing services such as ZipCar, automation has changed industry dynamics by making it possible to serve areas and markets that were previously too costly. While automation does not eliminate all the benefits of increasing unit scale, given the current state of technology, automation has often become cheaper than employing human workers, and this reduces the benefits of large unit scale significantly.

Two other strategies to decouple labor cost from unit scale and geography are remote operation and centralized maintenance. With appropriate instrumentation and automation technologies linked to the Internet, a central control center can monitor and operate units remotely, eliminating the need to have on-site personnel at every location and increasing utilization of operators due to pooling economies. As a result, labor costs become independent of the physical proximity of the units, and there is less incentive to keep units together geographically. Similarly, small units requiring maintenance can be shipped back to the manufacturer or to a local maintenance center for major repairs and upgrades. Again, this eliminates the need for a local maintenance staff and

creates pooling economies in maintenance and repair. The examples of SMRs and modular chlorine plants described in §5.1 illustrate these ideas in practice. When combined with automation technology, remote operation and centralized maintenance enable small-unit-scale technology to achieve levels of labor cost previously obtainable only by centralization and massive unit scale.

5.2.2.2 Conversion efficiency

Conversion efficiency is the ratio of inputs to outputs, for example how much energy or raw material is required to produce a unit of output. In some cases, the geometrical ratios of surface area to enclosed volume, might suggest a higher conversion efficiency, such as the reduction of thermal losses from working fluids discussed previously. In a similar way, geometry also influences the efficiency in turbines and compressors where the main frictional losses occur along the spinning structure's circumference, which scales linearly with the size of the turbine, while the power output scales proportional to the spinning structure's area, which grows like the square of the size. Hence, the output power grows faster with increasing size than the majority of frictional losses. Other scaling efficiencies arise from wasted materials in batch production processes of compounds (specialty chemicals, pharmaceuticals, cosmetics, etc.), since residue waste tends to grow like the area of a vessel, while the output capacity grows like the vessel's volume. So again, larger unit scale tends to improve conversion efficiency of these processes.

While one cannot disregard these geometrical arguments for conversion efficiency due to large unit scale, these arguments provide only a guideline and need to be evaluated on a case-by-case basis. For example, thermal power generation, previously discussed as a case for increasing unit size, does indeed seem to favor a larger size when considering constant operation. However, it is less clear how significant these size-dependent conversion efficiencies are in practical operation, see §5.3, Figure 5.2. Furthermore, a car engine operated under optimal conditions can exhibit conversion efficiencies in the range of 30-35% which is similar to those of large single-cycle power plants (White *et al.*, 2006). Another such example is water desalination using reverse osmosis explained in §5.5.2. Small-scale desalination systems intended to provide fresh water on board recreational sailboats exhibit specific power consumption on par with modern utility-scale plants. Moreover, conversion

efficiencies are primarily important when inputs are costly, such as fossil fuels or other purchased feed stocks. When inputs are sourced from the ambient environment, and hence effectively "free", as is the case for example with renewable energy technologies, the importance of efficiencies is greatly reduced.

In summary, conversion efficiency clearly plays a role in deciding between large and small scale unit production. However, one must take into account the variation exhibited under suboptimal operating conditions and the cost of the input sources rather than relying simply on accepted doctrine. Indeed, the next section illustrates this point for the U.S. electric power industry.

5.3 Case study: U.S. Electricity generating sector

In this section we analyze the size choice of the U.S. electricity generation industry and how it affects its operating cost structure. Figure 5.1 demonstrates that electricity generation is a prime example of the trend of building larger and larger units. (The surveyed capacity encompasses more than 80% of U.S. total installed capacity in 2011.) The average generator size for each technology is increasing over time as the total cumulative capacity goes up. The trend of increasing unit sizes is especially apparent during growth phases of a specific technology. For instance, during the primary growth phase of coal-fired generation between 1950 and 1980, the average generator size increased from 50 MW to almost 600 MW. Once the growth stagnates in a technology, niche and small installations are still built, explaining the apparent decrease in average unit sizes in coal and hydro power. The history of natural gas-fired generation is complicated by "The Powerplant and Industrial Fuel Use Act" enacted by the U.S. Congress in 1978 and later repealed in 1987. This law effectively banned new construction of natural gas-fired power plants, explaining the slump in average sizes during this period.

We can at least partially explain this trend of "bigger is better" by economies of unit scale across the entire electricity generating industry. Examples of numerical values for the scale factor, α, introduced in equation (5.1), used for engineering capital cost estimates for the various technologies can be found in Table 5.1. Decreasing capital costs by scaling up has clearly been a benefit to the

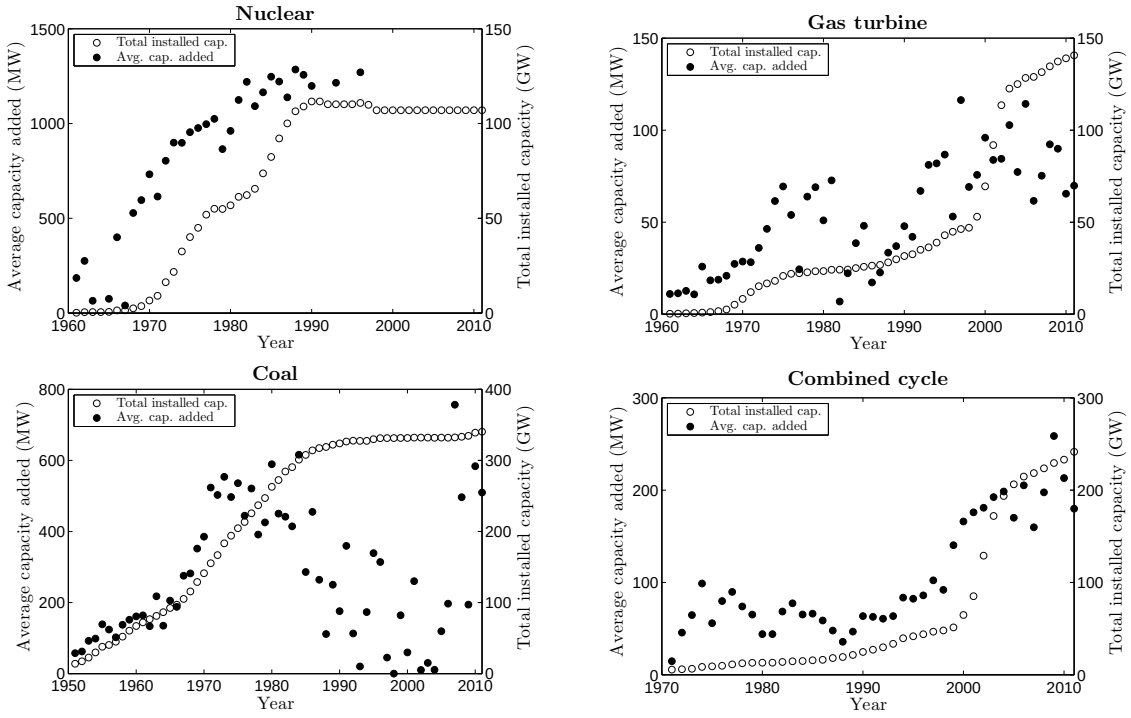

Figure 5.1: Average capacity of generators installed in the US and the total capacity of the same technology over time (EIA, 2011). The average generator size in 'Combined cycle' is the average size of the both the gas turbines and the steam turbines in one cluster. Furthermore, the year assigned to this class is the year the latest generator in a cluster was added.

industry.

To determine if, or to what extent, scaling up in size affects the operational costs of power plants, we analyzed plant-level operational cost data. In contrast to the data represented in Figure 5.1, operational data retrieved from the Federal Energy Regulatory Commission (FERC) covers only the major electric utilities that represent around 25% of total installed capacity in the U.S (FERC, 2010). This operational data from the year 2010 includes total production cost (minus capital charges), total fuel cost, total generation, capacity, efficiency and age. An employee head count is also reported but not salary levels. In order to find an estimate for labor costs, Census data on national average payroll levels for different electricity generating sectors was used (U.S. Census Bureau, 2007).

Two different log-linear regression models were tested on combined cycle, coal, natural gas (gas

Technology	α
Gas turbine + HRSG	0.7 (Hamelinck and Faaij, 2002)
Steam turbine + steam system	0.7 (Hamelinck and Faaij, 2002)
Nuclear power plant	0.619 (Locatelli and Mancini, 2010)
Hydroelectric plant	0.82 (Hreinsson, 1987)

Table 5.1: *Scale factors for various electricity generating technologies (HRSG – Heat recovery steam generator).*

turbine) and nuclear generation technologies to determine if the size of a generator significantly influences operating costs. These four technologies studied together represent more than 75% of U.S. electricity generating capacity. The remaining two main technologies not included in this study are hydroelectric generation and natural gas fired steam cycle plants. The former technology was excluded since is has no fuel cost and the latter since it is an outdated technology. The total sample size in this study represents around 270 GW of capacity, or almost 25% of total U.S. generation capacity. Each technology sample accounts for at least 20% of installed capacity in the U.S. for that technology.

In the first model the dependent variable is the total cost per kWh of electricity produced, whereas the second model analyzes only the non-labor portion of the costs. In both models the independent variables were the average generator size, capacity factor, fuel cost, efficiency and age. A complete result of the analysis, together with a more detailed description of the data can be found in Appendix D.

The analysis of the first model, examining total production costs, showed that increasing size significantly decreases operating costs for nuclear and gas turbine technologies. Neither coal nor combined cycle technologies exhibited any significant trend with respect to unit size. In the second model where labor costs are removed, none of the technologies show any residual reduction in cost with increasing unit size. Moreover, in this case coal even exhibits a significant increasing trend in cost with respect to size. The difference between the two regression analysis supports the argument presented in §5.2.2. Building larger units does, to a first approximation, decrease labor cost per unit output produced. But unit size has no discernible effect on the remaining operating costs.

Besides labor cost, the other variable cost factor discussed in §5.2.2 possibly acting to drive

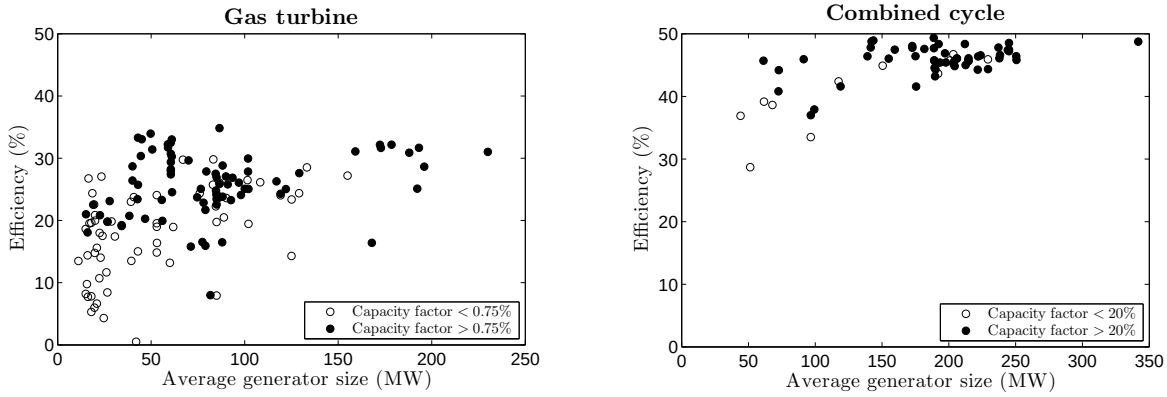

Figure 5.2: Relationship between efficiency and size (the segmentation is only meant to visually convey the significance of the capacity factor).

up unit size is efficiency. Figure 5.2, which plots efficiency against unit size, does indeed seem to support that claim at first glance.

However, when controlling for capacity factor, fuel costs and age, coal was the only technology where efficiency significantly increased with size. Non-negligible ramp-up times for all thermal power generation technologies mean that a low capacity factor, as is typically the case for peak generation technologies like gas turbines, will do more to influence efficiency than inherent size effects. Similarly, high fuel costs are just as likely to motivate stricter operational monitoring and more efficient operation.

In conclusion, the U.S. electric power sector has followed the trend of "bigger is better" over the last century. All technologies studied exhibit substantial economies of unit scale that lowers capital costs when installing larger units. Absent mass production, there is no other choice to reduce capital costs. Operationally, labor cost was found to generally influence total variable cost in favor of large unit scale. As predicted, per unit of output labor cost in general declines with unit size. Other than scale-related labor savings, there do not appear to be significant operating cost savings to large unit scale.

5.4 Flexibility and diversification

There are inherent flexibility and diversification benefits that can be attained only at a smaller unit scale. A careful examination of these benefits shows that they can be highly significant and may easily tip the scale in favor of small unit scale. Changes in cost functions, scaling relationships or scale-dependent flexibility and diversification benefits – like those driven by advances in technology – can lead to a "tipping point," at which the optimal scale switches discontinuously from large to small. The evolution of super computer technology discussed above illustrates a powerful real-world example of this tipping point phenomenon. The 'supercomputer market crash' of the mid 1990s occurred when mass-produced CPUs from the expanding personal computer industry, somewhat suddenly, reached a tipping point where it became less costly to achieve high computing capacity using large numbers of small-scale CPUs in parallel and demand for traditional super computers collapsed. This historical example underscores the point that shifts in optimal unit scale due to technological advances can occur rather suddenly and result in dramatic disruptions of entire industries.

5.4.1 Locational flexibility

Unlike large-unit-scale technologies, small unit scale offers the option of either centralization or decentralization. Multiple units can be aggregated at a single location to achieve economies of centralization in, for example, pooling the risk of demand variation. Alternatively, units can be distributed closer to sources of supply or points of demand and thereby reduce transport or transmission costs of either in- or out-bound goods.

An example that demonstrates the benefits of decentralization is distributed electricity generation as noted by Lovins *et al.* (2002). According to International Energy Agency (2002), on-site generation could result in 30% cost savings in transmission and distribution, which together account for above 40% of the cost of electricity for residential customers. Furthermore, distributed generation allows for the combined generation of heat and electricity which can result in energy savings from 10% to 30%, depending on the type and size of co-generation units (Pepermans *et al.*,

2005).

Decentralization also has safety and security implications. For example, while small nuclear reactors (SMRs) may increase the domain of applications for nuclear energy, dispersed nuclear generation offers a greater number of targets for individuals with disruptive motives. Another concern is nuclear proliferation. With widespread adoption of nuclear technology, it becomes more difficult to monitor nuclear fuel to ensure proper handling and secure distribution. Yet these security risks can be managed by other means. For example, most SMRs are designed for off-site refueling, which reduces the accessibility of the core by unauthorized personnel. In other cases, decentralization can have the potential of improving safety and increasing security. Chlorine production is a clear example where both storage and transportation carries significant safety risks due to the toxicity of the product. Decentralization enables the production of chlorine close to points of demand thus reducing the need to store and transport this hazardous substance. This results in a substantial decrease in the safety risks associated with the use of chlorine. More generally, by its sheer nature, a smaller scale of any technology reduces the local impact of possible catastrophic failure.

5.4.2 Investment flexibility

Unit scale affects the flexibility of an investment in several important ways. First, small-scale units can be used in multiples to better match the output requirements of a given project thus avoiding either capacity shortages or excess capital investment. Second, small units can be deployed more flexibly over time. They can be installed sequentially as uncertain demand evolves, avoiding excess investment in the early life of a project or investment errors later in the project life cycle. Also, mass-produced, standardized units can be built to stock and deployed more quickly than custom-built, large-scale units, reducing the lag between investment and revenue generation. Finally, while lifetimes of custom-built infrastructural investments tend to be very long, this need not be true for small-scale technologies. A shorter investment cycle for small-scale technologies would allow for disengagement if market conditions worsen without forsaking large sunk costs.

A full-fledged practical evaluation of these benefits would require detailed stochastic models

of the underlying variables, and a rigorous real option valuation. Such a valuation is made in (Dahlgren and Leung, 2013), where the value of consecutive investments, as a function of lifetime and lead-time, is treated as an optimal multiple stopping problem. The main finding in that study is that increasing lifetime does not greatly increase the value of an investment scenario where multiple consecutive investments can be made. We will here consider a couple of simple models that illustrate the advantages of shorter lead-time and of modularity individually. These two models are adapted from (Hoff, 1997).

5.4.2.1 Investment advantages of modularity

Being able to make investments in small increments over time provides significant economic advantages. The concept is best illustrated by an example: consider a firm, such as an electric utility, planning the future expansion of a plant to satisfy increasing demand. The firm has to satisfy all demand and has two options for investment: modular and non-modular. The modular investment involves increasing the capacity in increments of x and the non-modular investment involves a one-shot investment of nx units, where $n > 0$. For simplicity we assume that n is an integer.

The current capacity matches the demand, and demand each year either increases by x with probability p or stays the same with probability $1 - p$. The lead-time for both types of investments is zero and the total additional capacity to be installed is nx. With the first increase in demand, the firm can either choose to make a one-time capacity expansion of nx units or increase the capacity in increments of x every time the demand increases, for a total of n times.

The cost of a big (non-modular) and a small (modular) investment for each increment is denoted by K_{big} and K_{small}, respectively. With a constant discount rate, r, the expected discounted cost of the non-modular investment (occurring the first time demand increases from current level) is

$$I_{\text{big}} = \sum_{k=0}^{\infty} (1-p)^k p \frac{K_{\text{big}}}{(1+r)^k} = K_{\text{big}} \frac{p(1+r)}{r+p}.$$

For the modular investment scenario, we denote by I_i the expected discounted cost of the i-th investment. This investment occurs at the end of the k-th year ($k > i - 1$) when demand rises for

the i-th time. That is,

$$I_i = \sum_{k=i-1}^{\infty} \binom{k}{i-1} (1-p)^{k-i+1} p^i \frac{K_{\text{small}}}{(1+r)^k} = K_{\text{small}}(1+r)\left(\frac{p}{p+r}\right)^i.$$

Given the expected cost of each increment, we can calculate the total expected discounted cost, $I_{\text{small}} = \sum_{i=1}^{n} I_i$, of the modular scenario:

$$I_{\text{small}} = K_{\text{small}} \frac{p(1+r)}{r}\left(1 - \left(\frac{p}{p+r}\right)^n\right).$$

Taking the ratio of the total costs of the modular and the non-modular strategies we have

$$\frac{I_{\text{small}}}{I_{\text{big}}} = \frac{K_{\text{small}}}{K_{\text{big}}} \frac{(p+r)}{r}\left(1 - \left(\frac{p}{p+r}\right)^n\right) = \frac{K_{\text{small}}}{K_{\text{big}}}\left(1 + \frac{1}{\rho}\right)\left(1 - \left(\frac{1}{1+\rho}\right)^n\right), \tag{5.6}$$

where $\rho = r/p$. The ratio $I_{\text{small}}/I_{\text{big}}$ is strictly decreasing in ρ, corresponding to increasing attractiveness of the modular investment strategy as ρ increases. The reason for this is straightforward; increasing the discount rate, r, lowers the present value of future costs and decreasing the probability of demand increase p has the consequence of further deferring these costs into the future. Both reduce the present-value cost of the modular strategy.

Demanding that the two scenarios have the same total cost, $I_{\text{small}} = I_{\text{big}}$ and rearranging (5.6) reveals how much more one is willing to pay for capacity nx spread out over n separate investments, i.e. nK_{small} rather than incurring all the cost, K_{big}, at once. As can be seen in Figure 5.3, the ratio $nK_{\text{small}}/K_{\text{big}}$ increases almost linearly in n. For instance, with $\rho = 0.2$ as in Figure 5.3, considering 10 years of demand increase; the total investment cost $10K_{\text{small}}$ of the modular strategy is allowed to be over twice that of the one-off investment cost K_{big}; yet still produce an equivalent present-value of the total cost.

To give a sense of the potential benefit of modularity for a particular technology, consider the case of small modular reactors (SMRs); Westinghouse's conventional AP 1000 reactor (approximately 1,000 MW) and it's proposed SMR design (approximately 200MW) have comparable present-value capital costs of around $5,000 per kW (Ryan, 2012; Yurman, 2012). However, as-

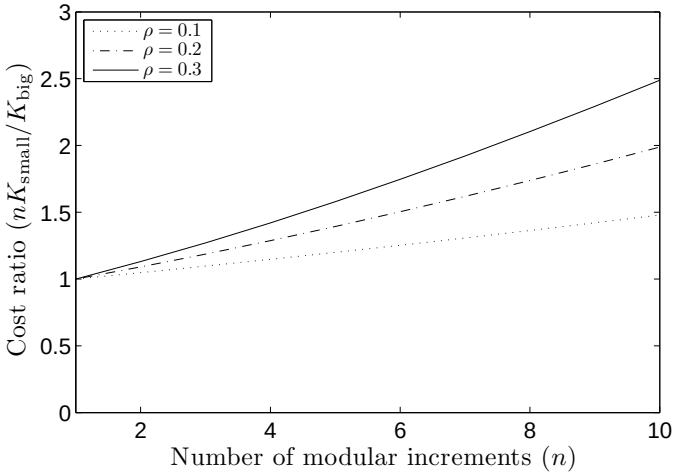

Figure 5.3: The ratio $nK_{\text{small}}/K_{\text{big}}$ evaluated at different n with equal total cost $I_{\text{small}} = I_{\text{big}}$ and with $\rho = r/p = \{0.1, 0.2, 0.3\}$.

suming a discount rate of 5% ($r = 5\%$) and that the probability that demand grows by 200MW in a given year is 20% ($p = 20\%$), the above model shows that the expected discounted total capital cost of the SMR plant is 30-35% lower than the corresponding conventional plant.

5.4.2.2 Investment advantages of shorter lead-time

Mass-produced modular technology that is manufactured to stock can significantly reduce the lead-time to deploy a new investment. We next examine how shorter lead-times can be beneficial in terms of total investment costs, again via a simple example. Similar to the previous section, assume a firm is planning the future expansion of a plant that has to satisfy increasing but uncertain demand. As above, the demand increases by x with probability p or it stays the same with probability $1 - p$. Let T denote the minimum number of years until the current excess capacity runs out; thus, the current excess capacity is Tx.

The firm has two options for investment. It can either invest in an expansion project with a long lead-time L_l or a short lead-time L_s. To compare these two investment options, we assume that $T \geq L_l > L_s$. Let K_l and K_s denote the costs of expansions with long and short lead-times

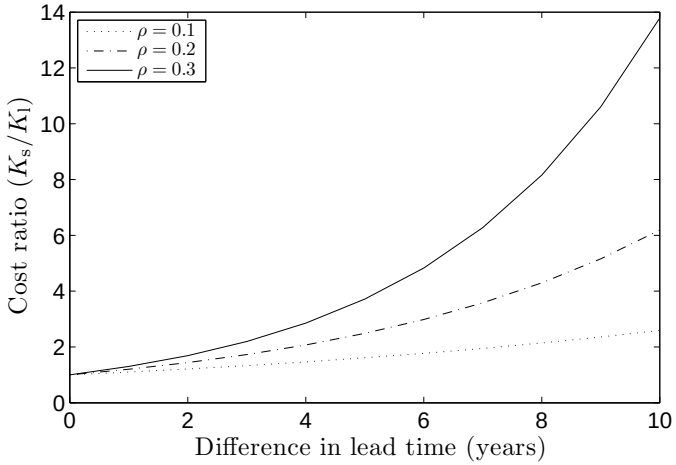

Figure 5.4: *The ratio of the immediate investment cost of the short lead-time option to the long lead-time option for $\rho = r/p = \{0.1, 0.2, 0.3\}$, for which their expected costs are equal.*

respectively. Then, the total expected cost of these expansions are obtained as follows:

$$I_i = \sum_{k=0}^{\infty} \overbrace{\binom{k+T-L_i-1}{T-L_i-1} p^{T-L_i}(1-p)^k}^{\text{probability of initiating construction in year } k+T-L_i} \underbrace{\left[\frac{K_i}{(1+r)^{(k+T-L_i)}}\right]}_{\text{discounted cost in year } k+T-L_i} = K_i \left(\frac{1}{1+\rho}\right)^{T-L_i}$$

where $i \in \{l, s\}$ and $\rho = r/p$. As the lead-time decreases, the expected present value of the cost decreases since it can be deferred further into the future. The value of shorter lead time can be visualized in a manner similar to the previous example. Equating the expected present value of the cost for the two lead-times, i.e. $I_l = I_s$ we see that

$$\frac{K_s}{K_l} = (1+\rho)^{L_l - L_s}$$

A difference in lead-time of only a few years can for reasonable values of ρ compensate for significant increases in capital cost. The effect is illustrated in Figure 5.4. For example, at $\rho = 0.2$ a difference in lead-time of four years can make up for a factor of two increase in the cost of the short lead-time technology. The attractiveness of the shorter lead time scenario is obviously compounded at greater values of ρ. The reasons are the same as in the preceding section; increasing the discount rate, r,

lowers the present value of future costs and decreasing the probability p of a demand increase has the consequence of further deferring these costs in the future.

As previously discussed, SMRs are expected to have much shorter lead-times compared to conventional nuclear reactors. By utilizing a methodology similar to the one in the previous section, we can demonstrate that this can lead to significant potential cost savings. Assuming the parameters stay the same, i.e. $p = 20\%$ and $r = 5\%$, if the lead-time for construction decreases by 3 years, this can lead to potential cost savings of 45-50%.

5.4.3 Operating flexibility

Small unit scale provides increased flexibility in terms of deploying partial capacity since it is possible to selectively run varying numbers of smaller units in order to achieve a targeted level of total output. Facilities consisting of a single large unit often have to be operated in an effectively binary, "on-off" mode, producing either nothing or at maximum capacity. A coal-fired power plant, for example, has a limited range of outputs for which it can operate efficiently. As a consequence, these plants are limited to providing steady, base-load power and cannot effectively serve variable peak-load demands or efficiently slow down to avoid waste during period of low demand.

To illustrate this idea, we rely on a model of a plant consisting of multiple units operated in an on-off fashion with total capacity C. The plant has to satisfy a random demand D. Let n denote the number of units in the plant, so $C_u = C/n$ denotes the unit capacity of the equipment in the plant. The excess operational capacity, X_C, can be written as

$$X_C = kC_u - D, \quad \text{where} \quad k = \left\lceil \frac{D}{C_u} \right\rceil.$$

The expected excess operational capacity, $\mathbb{E}[X_C]$ is

$$\mathbb{E}[X_C] = C_u \mathbb{E}[k] - \mathbb{E}[D] = C_u \sum_{k=1}^{n} kP\left[(k-1)C_u < D \leq kC_u\right] - \mu,$$

where μ is the mean demand.

Figure 5.5 depicts the average excess operational capacity for different unit capacities C_u using

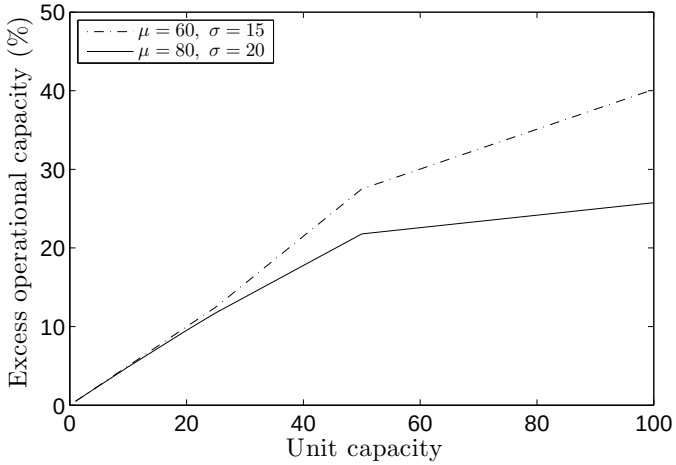

Figure 5.5: The figure shows the average excess operational capacity for different unit capacities where D is a normally distributed random variable with mean μ and standard deviation σ, truncated between 0 and 100.

two different normal distributions for D, defined by μ and σ, both truncated between 0 and 100. It can be seen from the figure that when the unit capacity is small, it is easier to satisfy the demand with little excess operational capacity since the plant's output can be adjusted in a flexible fashion. However, as the unit capacity increases, that flexibility is lost. For example, when the unit capacity is 100 there will only be one unit in the plant, and it will have to operate all the time whether the demand is 1 or 100. Another important factor to take into account is how far the mean demand is from the maximum possible demand. As the mean demand decreases, the impact of smaller unit size on excess capacity in operation increases especially for larger unit sizes.

In the above model we assumed that storing the output of the plant is not an option. With storage it is possible to achieve high utilization with large unit sizes by carrying inventory. For example, the plant may be turned on at full capacity when the inventory drops to a certain threshold and can be kept in operation until the inventory reaches a target level.

An example illustrating the benefit of this kind of operational flexibility is found in so-called "peaker plants" in electricity generation. At times, peak loads and rapidly varying demand requires a very quick generating response. The lower physical inertia of smaller units, such as combustion turbines or flywheels, allows them to quickly reach their optimum level of output. Moreover, these

small scale generators are typically deployed in multiples, which are activated in varying numbers to match peak load demands. The flexibility of these small generators combined with the high rates paid for peak generation mean they can be operated profitably at very low utilizations.

5.4.4 Diversification

Small unit scale also provides significant diversification benefits. By exploiting statistical independence of many small operating units rather than relying on a few large operating units, it is possible reduce unit reliability yet raise overall system reliability. If all output stems from one single large unit, a single failure can reduce output to zero, which makes it necessary to incur the costs of substantial redundancies. If, however, the same total output is provided by 10,000 units that are easily replaced, the impetus for built-in redundancies in any given unit are diminished. This reduced need for high unit-level reliability can both reduce capital costs and improve service reliability.

We illustrate this concept with the following simple example. Suppose a utility is to provide an output capacity D, available with a probability R in a given time period ($1 - R$ is the probability of failure). We assume that a single unit, with capacity C_u, can either be fully functioning with probability $p < R$ in a given time period or not at all. As a result, the utility will need redundancy to make up for the missing reliability. So, the utility has to decide on the minimum number of units to install, n^*, to ensure that the aggregate available capacity $C(n) = nC_u$ exceeds demand D with a probability of at least R. With the assumed independence of the individual units this problem can be formulated as

$$n^* = \min\left\{ n \geq \left\lceil \frac{D}{C_u} \right\rceil \middle| P(C(n) \geq D) \geq R \right\},$$
$$\text{where} \quad P(C(n) \geq D) = \sum_{s=\left\lceil \frac{D}{C_u} \right\rceil}^{n} \binom{n}{s} p^s (1-p)^{(n-s)}.$$

For different R and C_u, Figure 5.6 shows the total capacity the utility has to invest in when $D = 100$ and $p = 0.9$. The figure shows that as the size of the individual units increase, the excess capacity

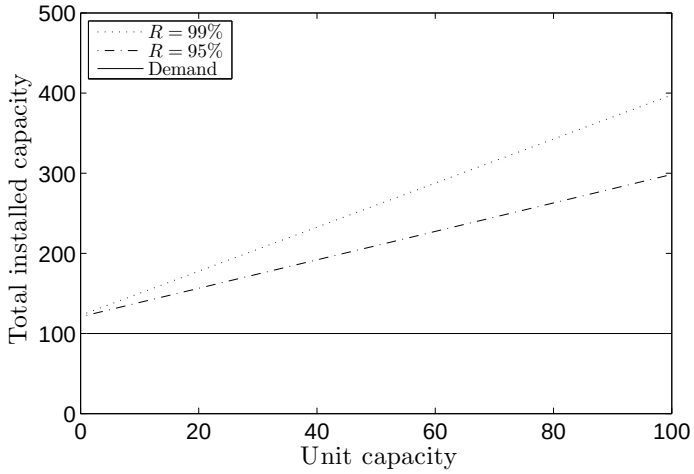

Figure 5.6: The total capacity investment required for different unit capacities and individual unit reliability $p = 0.9$.

that needs to be installed significantly increases. For example, when $R = 0.95$, the amount of excess capacity needed is five times more when the unit size is 50 compared to a unit size of 1. As the system reliability increases, this difference also increases, and the excess capacity for a unit size of 50 becomes 7-8 times the amount needed for a unit size of 1 in the case of $R = 0.99$.

Cloud computing is a good example of the benefits of diversification. For example, by utilizing statistical economies of scale, Google can guarantee 99.9% uptime (roughly 8 hours of down-time per year) for its cloud-based services. Such reliability would be prohibitively expensive for businesses that run applications on their own dedicated hardware due to the enormous amount of extra capacity investment that would be needed.

5.5 Existing technologies suited for a small scale

We next look at three technologies that appear ripe for a shift to radically smaller unit scale. While anecdotal, these examples point to the potential broader benefit of re-examining the orthodoxy of bigger-is-better in other infrastructure industries. We emphasize that a small-scale approach to physical capital should not be limited to the scaling down of existing technologies. Likely, the most significant benefits of small scale will be realized in novel technologies designed for highly modular

implementation. However, the sample technologies below exhibit either physical or economical features (or both) in their current incarnation that strongly support a smaller scale.

5.5.1 Ammonia synthesis

Except for minor alterations to the catalyst, ammonia synthesis looks very much the same throughout the $50 billion dollar industry of today (Erisman *et al.*, 2008; FERTECON, 2012) as it did during the early days of commercial implementation. One feature, however, has dramatically changed: unit size. The first commercial plant had a capacity of 30 metric tons per day (MTPD) (Jennings, 1991), which should be compared to the currently planned facility in Collie, Australia with a nominal capacity of 3,500 MTPD (Haldor Topsoe, 2009). An increase in unit capacity by two orders of magnitudes epitomizes the aforementioned trend in unit size.

As with most catalytic processes, ammonia synthesis requires careful control of temperatures throughout the reactor in order to maintain favorable reaction conditions. Maintaining such control requires sophisticated internal heat exchangers, which add cost. Additionally, dealing with explosive gases at elevated pressures exacerbates the consequences of a critical failure at larger reactor sizes.

Assuming sufficient capabilities of automation, a decrease in individual reactor size could potentially reduce overall costs. First, decreasing unit size to the point that no internal heat sinks are necessary would reduce the complexity of the individual reactor. Additionally, as explained in §5.2, the total amount of material used will, to a first approximation, remain constant or decrease when deploying multiple smaller units with the same aggregate capacity of a typical ammonia synthesis reactor. Furthermore, an array of parallel smaller units would substantially mitigate the impact of catastrophic failure of a single reactor. Also, catalytic processes, including the synthesis of ammonia, all suffer from catalyst deactivation. In a monolithic setting, regenerating or replacing catalysts requires a complete albeit temporary shutdown of the reactor. Referring to the operational flexibility arguments, a more modular plant consisting of parallel units would be less exposed to such complete but unavoidable outages. Instead of bringing the entire output to a standstill, individual units could be swapped out and repaired off-line. These factors all point to potential cost savings with a modular infrastructure approach.

Finally, it is worth mentioning that the main use of ammonia is in fertilizers. Serving mainly the agriculture industry, the demand for this end-product is extremely distributed. The case for distributed, and hence small-scale operation is further strengthened by the fact that all the inputs necessary for the process are found in the ambient environment.

5.5.2 Water desalination

One of the main engineering challenges of the coming century is to create large, stable and affordable supplies of fresh water from the earth's largest water reservoir, the oceans (National Academy of Engineering, 2012). Among the various desalination technologies available for this purpose, reverse osmosis (RO) has seen the largest growth in recent years and represents almost half of the $20 billion desalination market today (Greenlee *et al.*, 2009; Fritzmann *et al.*, 2007; Elimelech and Phillip, 2011). Some regions, notably the Middle East, parts of Australia and several island communities, have come to rely on reverse osmosis desalination as a base load source of fresh water.

Defining a unit scale in RO operations is less straightforward than in the previous examples because the membranes are currently manufactured and assembled in small units called modules. Regardless, the core process of separation in a modern RO-plant encompasses three components: a high-pressure pumping system, membrane modules housed in parallel pressure vessels, and an energy recovery system. One of the most modern and efficient RO desalination plants in the world is the Ashkelon plant in Israel with a capacity of 330,000 cubic meters of fresh water per day (Sauvet-Goichon, 2007). With eight high-pressure pumps, the 40,000 cubic meters of fresh water per day and per pumping system can serve as a benchmark for unit size in current RO desalination.

Almost half the cost of desalinated seawater through RO can be attributed to energy. Of the remaining cost components, capital costs dominate, leaving only a minor fraction to other variable costs (Wittholz *et al.*, 2008). With such a cost structure, the specific energy requirement (energy required per unit output) serves as a decent indicator of the total price of a given RO desalination operation. Conventional wisdom would suggest that to increase the physical efficiency of a process like RO, and hence lower the specific energy consumption, the strategy would be to scale up unit size. Indeed, the aforementioned plant in Ashkelon is not only one of the largest

plants in the world but also one of the most efficient with electricity requirements of 3-4 kWh/m^3 of produced water (Sauvet-Goichon, 2007). The notion that increased energy efficiency in RO has to be accompanied by increased unit size is, however, contradicted by examining desalination systems found on recreational boats. With a capacity of little more than one cubic meter per day, these small, modular systems consume only 3.8 kWh/m^3 (Spectra Watermakers, 2012), which is on par with the utility-sized operation. While based on the exact same technology, the tight on-board space constraints have resulted in process designs that have similar levels of energy consumption but with smaller footprints. This indicates that a truly modular design in RO desalination could lead to additional future cost savings as production of small units is scaled up to match large scale demand.

5.5.3 Mining

The value of U.S. domestic production of raw materials from mining was estimated at $64 billion dollars in 2010 (USGS, 2011). Including further downstream processing, the raw materials sector accounts for a substantial part of GDP and is the foundation of industrial economies. While mining operations differ substantially for different minerals in varying geologic formations, the task of hauling ore from the point of excavation to the initial processing site is worth examining from the perspective of unit scale. We focus here on operations in open pit, or surface mining, but the concepts apply more broadly to other mining operations.

The cost of one mining truck driver in remote areas of Australia amounts to $150,000 per year (quoted in Australian $, which has an exchange rate of roughly 1:1), of which more than $36,000 goes to auxiliary support such as transportation, accommodation and food (Bellamy and Pravica, 2011). Operating in three shifts, this translates into $450,000 per year per truck in labor costs. While truck prices are hard to ascertain exactly, assuming that the investment required is on the order of $5 million, the capital charges at 10% interest are almost on par with labor costs. Hence, labor productivity is a key metric in evaluating mining operations. The most natural way to increase profitability of a given mine has been to scale up the size of individual process equipment such as loaders and haulers. Indeed, the size of the largest available haulers has increased by a

factor ten over the past 50 years. A general consequence of this trend is that smaller mines, which preclude the use of larger equipment, become less profitable, and hence mining operations tend to be more concentrated on large mines (Bozorgebrahimi *et al.*, 2003; Bartos, 2007). It seems however that this trend has stagnated recently for several reasons. For instance, auxiliary civil works, e.g. roads and bridges, to accommodate larger trucks going in and out of a mine become more costly. Moreover, larger equipment diminishes the possibility of selective mining techniques, thus resulting in the transportation of lower grade ores for further processing. The complexity of larger machinery also increases markedly at the largest end of the spectrum and hence requires additional training of operators and repair crews as well as larger (and more expensive) maintenance facilities (Bozorgebrahimi *et al.*, 2003).

Even though tests have been performed recently on operating retro-fitted autonomous mining trucks in Australian mines, such technology has not yet caught on (Bellamy and Pravica, 2011). With non-stationary and interacting robotic systems making progress by the day, as manifested by Google's autonomous car (Folsom, 2011) and 'Junior', the driverless vehicle developed by Volkswagen and Stanford through DARPA (Stanek *et al.*, 2010), it is only a matter of time before such technology becomes viable in isolated areas such as a mine. There is little reason why automation should proceed with the ultra-large-size equipment of today and not with much smaller units, perhaps in the 1-10 ton class. In addition to the flexibility arguments raised in previous examples favoring small unit size, smaller automated units can make smaller mines economical alongside large ones, thus increasing the total resource base.

5.6 Conclusion: Learning to "think small"

When choosing from a palette of available technologies, the ultimate decision has historically been predicated on a positive response to the question: Does the technology "scale up?" Yet as we have argued here, our increased ability to automate and control processes without the presence of either the human hand or mind, the capability of mass production to drastically reduce capital costs, and a more enlightened view of the flexibility benefits of small unit scale, cast significant doubt on the

validity of the bigger-is-better mantra. As we have argued, scaling up in numbers – rather than in unit size – can provide many of the same benefits of large unit scale and offers entirely new benefits that can only be achieved with small unit scale. Consequently, the fundamental decision processes surrounding the choice of technologies and their implementation need to be revisited.

Doing so, however, requires an entirely new mind set. Educators, engineers, business leaders, financiers, standards bodies, regulators – the entire industrial ecosystem – must learn to "think small." In order to reap the benefits of small unit scale and achieve the needed paradigm shift, institutional biases towards large-scale must be purged and replaced by an ability to think small.

Engineers, for one, need revised training and new conceptual tools. In today's engineering schools, students are instilled with the notion that unit scale-up is a precondition for the viability of most technologies. So consequently, they focus on designing for scale economy. Instead, they must learn how to design small – *design for granularity* as it were. Small modular technologies designed to function in massively parallel configurations should not look like miniature versions of behemoth industrial plants; they require their own distinct approach to design – one that emphasizes off-loading control functions to central controllers, simplifies functionality to minimize the need for ongoing control and maintenance, and reduces part counts by creating more integrated components. Engineering small requires designs that aim to leverage the economies of mass production and exploit the power of automation and sensors to eliminate the need for human labor. Only by applying such design principles can the full benefits of small unit size be realized. Engineers must also be exposed to examples of designs that are optimized for granularity, so they can develop an instinct for how it is done.

Business leaders and financiers must likewise revise their approaches to project evaluation. Long-standing net present value (NPV) evaluations based on simplistic pro-forma projections of factors such as demand, cost, price, unit reliability and so on, must be replaced by the use of more sophisticated models (of the sort illustrated in this chapter) that accurately account for the many inherent flexibility and option-value benefits of small unit scale. Only then will their decisions be driven by the true economic costs and benefits of unit scale.

Lastly, a mass market for small unit scale technology will not flourish unless industry leaders

recognize the potential of thinking small and create the necessary standards and common interfaces needed to open their markets to small modular technology. Indeed, one of the reasons behind the astonishing developments of the computer industry in the past century was the abandonment of the mentality that every component had to be manufactured in-house. Opening up the black box that was the computer to outside parties allowed firms to focus on fewer parts and also forced the industry to adopt standards, resulting in the "plug-and-play" environment that eventually made the PC possible and so dramatically successful. In addition, down-sizing, standardizing and then proliferating technologies to a larger domain of applications further reduces costs by increasing the aggregate market size for each technology. It also increases the likelihood of applications not yet thought of; after all, the early pioneers of the computing industry could hardly have anticipated the multitude of applications that permeate virtually every part of our society today, like smart phones and video games.

These changes in mindset and industry norms will take time to develop; massively parallel plants will not suddenly appear overnight. Indeed, there is considerable inertia in most industries that may impede the transition to thinking small for many years to come. One explanation for this inertia is known as the "lock-in effect" in the economics literature. As in the case of the QWERTY keyboard, once a technology establishes dominance early on, a later superior technology may not be able to gain market share (David, 1985). In his seminal work, Arthur (1989) shows that this kind of a behavior is observed in industries with increasing returns to learning, as is the case with large-scale infrastructure. But two factors offer hope that this lock-in can be overcome. For one, as demonstrated in the preceding sections, once the flexibility and diversification benefits of small-scale technology are recognized, these may tip the scales toward adoption. Secondly, niche applications of small-scale technologies in areas where larger scales are infeasible or too costly may allow firms to accumulate the necessary experience to compete with large-scale technologies in conventional markets, as was the case with microcomputers. Once this transition happens and small scale thinking takes root, it has the potential to radically disrupt entire industries. Like the behemoth reptiles of the Cretaceous period, firms caught on the wrong side of such a meteoric transition will likely suffer.

Yet despite the great promise of thinking small, we are not arguing that small-scale technology is a panacea. Indeed, some enterprises adopting a small-scale strategy have had spectacular failures. Even though the reasons behind its failure are disputed, one example is the geothermal energy provider Raser Technologies that sought bankruptcy protection in 2011 (Madhani, 2011; MacFall and Engleston, 2011; Oberbeck, 2011). And, there will always be a role for large unit scale; massive rivers require massive hydroelectric dams, after all. Still, the concept that every industrial process with large aggregate output *requires* large unit scale technology to match is fundamentally flawed and inherently limiting. We will all benefit from a more enlightened world in which the ability to "scale up" does not dictate our choice of technology.

Bibliography

S. Adee and E. Guizzo. Nuclear redux. *IEEE Spectrum*, 47:25–32, 2010.

AESI Inc. Proven biomass gasification solutions by aesi. `http://www.aesintl.net/solutions/proven-biomass-gasification-solutions-by-aesi`, 2011. Accessed on 2011.10.21.

P. Afeche. Incentive-compatible revenue management in queueing systems: Capacity and optimal strategic delay. Technical report, University of Toronto, 2010.

Akzo Nobel N.V. Remote controlled chlorine production. `http://www.akzonobel.com/ic/products/remote_controlled_chlorine_production/`, 2011. Accessed on 2011.10.19.

L. Argote and D. Epple. Learning Curves in Manufacturing. *Science*, 247(4945):920–924, 1990.

K.J. Arrow. The economic implications of learning by doing. *The Review of Economic Studies*, 29(3):155–173, 1962.

W.B. Arthur. Competing technologies, increasing returns, and lock-in by historical events. *The Economic Journal*, 99(394):pp. 116–131, 1989.

T. Aven. Upper (lower) bounds on the mean of the maximum (minimum) of a number of random variables. *Journal of Applied Probability*, 22(3):723–728, 1985.

Yossi Aviv and Awi Federgruen. The value iteration method for countable state markov decision processes. *Operations research letters*, 24(5):223–234, 1999.

G. Barlow. *Yield Management Strategies for the Service Industries*, chapter Capacity Management in the Football Industry, pages 303–314. Continuum, New York, NY, 2000.

Paul J. Bartos. Is mining a high-tech industry? Investigations into innovation and productivity advance. *Resources Policy*, 32(4):149 – 158, 2007.

Hendrik Baumann and Werner Sandmann. Numerical solution of level dependent quasi-birth-and-death processes. *Procedia Computer Science*, 1(1):1561–1569, 2010.

D. Bellamy and L. Pravica. Assessing the impact of driverless haul trucks in Australian surface-mining. *Resources Policy*, 36(2):149 – 158, 2011.

Moshe Ben-Akiva and Steven Lerman. *Discrete choice analysis: theory and application to predict travel demand*. MIT press, 1985.

M. Ben-Akiva, M. Bierlaire, H. Koutsopoulos, and R. Mishalani. *Real Time Simulation of Traffic Demand-Supply Interactions Within DynaMIT*, chapter 2, pages 19–36. Kluwer Academic Publishers, 2002.

Moshe Ben-Akiva, Haris N Koutsopoulos, Constantinos Antoniou, and Ramachandran Balakrishna. *Traffic Simulation with DynaMIT*, chapter 10, pages 363–398. Springer, 2010.

Dimitri Bertsekas. *Dynamic programming and optimal control*, volume 2. Athena Scientific, 2007.

Julius R Blum. Multidimensional stochastic approximation methods. *The Annals of Mathematical Statistics*, 25(4):737–744, 1954.

W. Bogdanich and C. Drew. Deadly Leak Underscores Concerns About Rail Safety. *The New York Times*, January 9 2005. Accessed on 2011.10.19.

Stephen Boyd and Lieven Vandenberghe. *Convex Optimization*. Cambridge university press, 2004.

E. Bozorgebrahimi, R. A. Hall, and G. H. Blackwell. Sizing equipment for open pit mining - a review of critical parameters. *Mining Technology*, 112(3):171–179, 2003.

Richard P Brent. *Algorithms for minimization without derivatives*. Courier Dover Publications, 1973.

Richard P Brent. *Algorithms for minimization without derivatives*. Dover Publications, 2002.

Wilco Burghout. Mesoscopic simulation models for short-term prediction. Technical report, Royal Institute of Technology (KTH), 2005.

C. L. Chung and W. Recker. State-of-the-art assessment of toll rates for high-occupancy and toll lanes. In *Proceedings of the Transportation Research Board 90th Annual Meeting*, 2011.

B.L. Cohen. *The Nuclear Energy Option*. Plenum Press, 1990.

Community Power Corporation. About Us. `http://www.gocpc.com/about.html`, 2011. Accessed on 2011.10.21.

Community Power Corporation. Why Modular Biopower? `http://www.gocpc.com/biopower.html`, 2011. Accessed on 2011.10.21.

D. Cure. Pharmachem Invests in Green Energy in NC Facility with AESI System. `http://www.aesintl.net/blog/aesi-news/pharmachem-invests-in-green-energy-at-nc-facility-with-aesi-system`, October 10 2011. AESI Biomass Energy Blog. Accessed on 2011.10.21.

Carlos F Daganzo. The cell transmission model: A dynamic representation of highway traffic consistent with the hydrodynamic theory. *Transportation Research Part B: Methodological*, 28(4):269–287, 1994.

E Dahlgren and K.S. Lackner. Questioning a simple explanation to the two-thirds rule in scaling equipment cost. *Working paper*, 2012.

E. Dahlgren and T. Leung. An optimal multiple stopping approach to infrastructure investment decisions. *Working paper*, 2013.

P. A. David. Clio and the Economics of QWERTY. *The American Economic Review*, 75(2):pp. 332–337, 1985.

M. Drake, S. Duran, P. Griffin, and Swann J.. Optimal timing of switches between product sales for sports and entertainment tickets. *Naval Research Logistics*, 55(1):59–75, 2008.

S. Duran, J. Swann, and E. Yakici. Dynamic switching times for season and single tickets in sports and entertainment. To Appear in Optimization Letters, 2011.

EIA. Renewable & alternative fuels net summer capacity. `http://www.eia.gov/cneaf/alternate/page/renew_energy_consump/table4.html`, August 2010. Accessed on 2011.10.21.

EIA. Updated Capital Cost Estimates for Electricity Generation Plants. `eia.gov`, 2010. Table 1. p. 7.

EIA. Form 860, Annual Electric Generator Report 2011. `eia.gov`, 2011.

M. Elimelech and W.A. Phillip. The future of seawater desalination: Energy, technology, and the environment. *Science*, 333(6043):712–717, 2011.

J.W. Erisman, M.A. Sutton, J. Galloway, Z. Klimont, and W. Winiwarter. How a century of ammonia synthesis changed the world. *Nature Geoscience*, 1:636–639, 2008.

J. Euzen, P. Trambouze, and J. Wauquier. *Scale-up Methodology for Chemical Processes*. Gulf Publishing Company, 1993.

FERC. FERC Form No. 1 for the year 2010. `ferc.gov`, 2010. Accessed on 2012.10.5.

F. Ferioli and B. C. C. van der Zwaan. Learning in times of change: A dynamic explanation for technological progress. *Environmental Science & Technology*, 43:4002–4008, 2009.

F. Ferioli, K. Schoots, and B.C.C. van der Zwaan. Use and limitations of learning curves for energy technology policy: A component-learning hypothesis. *Energy Policy*, 37(7):2525 – 2535, 2009.

FERTECON. Fertecon ammonia report, weekly review of the ammonia market, 6 september 2012. `http://www.fertecon.com/latest_market_reports/FERTECON_latest_Ammonia_market_report.pdf`, 2012. Accessed on 2012.12.28.

T.C. Folsom. Social ramifications of autonomous urban land vehicles. In *IEEE International Symposium on Technology and Society, May 2011, Chicago*, 2011.

C. Fritzmann, J. Lwenberg, T. Wintgens, and T. Melin. State-of-the-art of Reverse Osmosis Desalination. *Desalination*, 216(1-3):1 – 76, 2007.

Jeffrey Fulmer. What in the world is infrastructure? *PEI Infrastructure investor*, pages 30–32, 2009.

G. Gallego and O. Sahin. Revenue management with partially refundable fares. *Operations Research*, 58(4):817–833, 2010.

G. Gallego and C. Stefanescu. Upgrades, upsells and pricing in revenue management. Working paper, Columbia University, New York, NY, 2009.

G. Gallego and C. Stefanescu. *Service engineering: Design and pricing of service features*, chapter Service engineering: Design and pricing of service features. Oxford University Press, 2012.

G. Gallego and G. J. van Ryzin. Optimal dynamic pricing of inventories with stochastic demand over finite horizons. *Management Science*, 40(8):999–1020, 1994.

G. Gallego, G. Iyengar, R. Phillips, and A. Dubey. Managing flexible products on a network. Technical report, Columbia University Computational Optimization Research Center, 2004.

GE Power & Water. Cloromat Fact Sheet. `http://www.gewater.com/pdf/Fact20Sheets_Cust/Americas/English/_FS1298EN.pdf`, 2011. Accessed on 2011.10.19.

Linda V Green, Peter J Kolesar, and Ward Whitt. Coping with time-varying demand when setting staffing requirements for a service system. *Production and Operations Management*, 16(1):13–39, 2009.

L.F. Greenlee, D.F. Lawler, B.D. Freeman, B.Marrot, and P.Moulin. Reverse osmosis desalination: Water sources, technology, and today's challenges. *Water Research*, 43(9):2317 – 2348, 2009.

J. Haldi and D. Whitcomb. Economies of scale in industrial plants. *Journal of Political Economy*, 75(4):pp. 373–385, 1967.

Haldor Topsoe. Press release: Topsoe contracts the world's largest ammonia plant. `http://www.topsoe.com/news/News/2009/020709.aspx`, 2009. Accessed in Dec 2010.

C.N. Hamelinck and A.P.C Faaij. Future prospects for production of methanol and hydrogen from biomass. *Journal of Power Sources*, 111(1):1 – 22, 2002.

Lee D Han, Fang Yuan, Shih-Miao Chin, and Holing Hwang. Global optimization of emergency evacuation assignments. *Interfaces*, 36(6):502–513, 2006.

R. Hassin and M. Haviv. *To Queue or Not to Queue: Equilibrium Behavior in Queueing Systems.* Kluwer Academic Publishers, 2003.

Highway capacity manual, 2010.

D. Heidemann. A queueing theory approach to speed-flow-density relationships. In *Proceedings of the 13th International Symposium on Transportation and Traffic Theory*, 1996.

T. Hoff. Integrating renewable energy technologies in the electric supply industry: A risk management approach. Technical report, NREL, 1997.

E.B. Hreinsson. Hydroelectric project sequencing using heuristic techniques and dynamic programming, 1987. Presented at the 9th. Power Systems Computation Conference.

K. Humphreys and S. Katell. *Basic cost engineering.* New York : M. Dekker, 1981.

R Husan. The continuing importance of economies of scale in the automotive industry. *European Business Review*, 97(1):38–42, 1997.

Hyperion Power Generation. Applications of HPM. `http://www.hyperionpowergeneration.com/applications/`, 2011. Accessed on 2011.10.19.

Innovative Energy Inc. Distributed generation: The use of biomass to create electricity. `http://tef.tulane.edu/pdfs/2011/jim-neumeier.pdf`, 2011. Accessed on 2011.10.21.

International Energy Agency. *Distributed Generation in Liberalised Electricity Markets.* 2002.

International Telecommunication Union. ICT Price Basket. `http://www.itu.int/ITU-D/ict/ipb/`, May 2011. Accessed on 2012.03.21.

S. Jasin and S. Kumar. A re-solving heuristic with bounded revenue loss for network revenue management with customer choice. Working paper, Stanford University, Stanford, CA., 2010.

R. Jayakrishnan, H. S. Mahmassani, and T. Hu. An evaluation tool for advanced traffic information and management systems in urban networks. *Transporation Research C*, 2:129–147, 1994.

B. M. Jenkins. A comment on the optimal sizing of a biomass utilization facility under constant and variable cost scaling. *Biomass and Bioenergy*, 13(1-2):1 – 9, 1997.

J.R Jennings. *Catalytic ammonia conversion.* Plenum Press, New York, 1991.

A.C. Kadak, R.G. Ballinger, T. Alvey, C.W. Kang, P. Owen, A. Smith, M. Wright, and X. Ya. Nuclear power plant design project: Phase 1 review of options and selection of technology of choice. Technical report, MIT, 1998.

C. Kaufmann. State of the Internet Report Q2 2011. Technical report, Akamai Technologies, Inc., 2011. Accessed on 2012.03.21.

Jack Kiefer and Jacob Wolfowitz. Stochastic estimation of the maximum of a regression function. *The Annals of Mathematical Statistics*, 23(3):462–466, 1952.

Sumit Kunnumkal and Huseyin Topaloglu. A new dynamic programming decomposition method for the network revenue management problem with customer choice behavior. *Production and Operations Management*, 19(5):575–590, 2010.

V. Kuznetsov. Innovative small and medium sized reactors: Design features, safety approaches and R&D trend. Technical report, IAEA, 2004.

Terence Lam and Kenneth Small. The value of time and reliability: measurement from a value pricing experiment. *Transportation Research Part E: Logistics and Transportation Review*, 37(2):231–251, 2001.

J. Larminie and A. Dick. *Fuel Cell Systems Explained*. John Wiley & Sons Ltd, 2003.

Guy Latouche and Vaidyanathan Ramaswami. *Introduction to matrix analytic methods in stochastic modeling*, volume 5. Society for Industrial and Applied Mathematics, 1987.

R. Levin. Technical Change and Optimal Scale: Some Evidence and Implications. *Southern Economic Journal*, 44:208–211, 1977.

Michael J Lighthill and Gerald Beresford Whitham. On kinematic waves. ii. a theory of traffic flow on long crowded roads. *Proceedings of the Royal Society of London. Series A. Mathematical and Physical Sciences*, 229(1178):317–345, 1955.

Q. Liu and G. J. van Ryzin. On the choice-based linear programming model for network revenue management. *Manufacturing Service Operations Management*, 10(2):288–310, 2008.

Henry X Liu, Will Recker, and Anthony Chen. Uncovering the contribution of travel time reliability to dynamic route choice using real-time loop data. *Transportation Research Part A: Policy and Practice*, 38(6):435–453, 2004.

Henry X Liu, Xiaozheng He, and Will Recker. Estimation of the time-dependency of values of travel time and its reliability from loop detector data. *Transportation Research Part B: Methodological*, 41(4):448–461, 2007.

G. Locatelli and M. Mancini. Small–medium sized nuclear coal and gas power plant: A probabilistic analysis of their financial performances and influence of CO2 cost. *Energy Policy*, 38(10):6360 – 6374, 2010.

A. B. Lovins, E. K. Datta, T. Feiler, K. R. Rabago, J. N. Swisher, A. Lehmann, and K. Wicker. *Small is Profitable*. Rocky Mountain Institute, 2002.

D. W. Low. Optimal dynamic pricing policies for an m/m/s queue. *Operation*, 22:545–561, 1974.

D. G. Luenberger. *Optimization by Vector Space Methods*. John Wiley & Sons, Inc., New York, NY, USA, 1st edition, 1969.

T. J. MacFall and G.M. Engleston. Rigrodsky & Long, P.A. and the Egleston Law Firm File Shareholder Class Action Lawsuit on Behalf of Raser Technologies, Inc. Shareholders. http://eon.businesswire.com/news/eon/20111129006954/en/Raser-Technologies/RZTIQ.PK/securities-fraud, November 29, 2011. Enhanced Online News. Accessed on 2012.06.12.

A. Madhani. Profits Elude Geothermal Companies. http://www.usatoday.com/news/washington/story/2011-10-05/profits-elude-clean-energy-companies/50674030/1, October 6, 2011. USA Today.

A. McDonald and L. Schrattenholzer. Learning rates for energy technologies. *Energy Policy*, 29(4):255–261, 2001.

MIOX Corporation. Miox at-a-glance. http://www.miox.com/about-miox/At-A-Glance.aspx, 2011. Accessed on 2011.10.19.

P. Naor. On the regulation of queue size by levying tolls. *Econometrica*, 37:15–24, 1969.

National Academy of Engineering. Grand Challenges of Engineering. engineeringchallenges.com, 2012. Accessed on 2012.12.28.

W. D. Nordhaus. The progress of computing. March 2002.

Nuclear Energy Institute. U.S. Nuclear Operating Plant Basic Information. http://nei.org/resourcesandstats/documentlibrary/reliableandaffordableenergy/graphicsandcharts/usnuclearoperatingplantbasicinformation/, 2011. Accessed on 2011.10.19.

S. Oberbeck. Raser Says It's Victim of $100 Million 'Joke'. http://www.sltrib.com/csp/cms/sites/sltrib/pages/printerfriendly.csp?id=52568877, September 27, 2011. The Salt Lake Tribune. Accessed on 2012.06.12.

Johan Janson Olstam and Andreas Tapani. *Comparison of Car-following models*. Swedish National Road and Transport Research Institute, 2004.

S. Peeta and A. Ziliaskopoulos. Foundations of dynamic traffic assignment: The past, the present and the future. *Networks and Spatial Economics*, 1:233–265, 2001.

G. Pepermans, J. Driesen, D. Haeseldonckx, R. Belmans, and W. D'haeseleer. Distributed generation: definition, benefits and issues. *Energy Policy*, 33(6):787 – 798, 2005.

R. Phillips, M. Eldredge, D. Levett, N. Pyron, J.S. Cohen, G. Cao, K. Holmquist, B. Buckalew, S. Ye, and R. Mace. Event revenue management system, 2006.

R. Phillips. *Pricing and Revenue Optimization*. Stanford University Press, Stanford, CA, 2005.

M. Puterman. *Markov Decision Processes: Discrete Stochastic Dynamic Programming*. John Wiley & Sons., 1994.

Paul Richards. Shock waves on the highway. *Operations Research*, 4(1):42–51, 1956.

Mark Roelofsen. Dynamic modelling of traffic management scenarios using dynasmart. Technical report, University of Twente, 2012.

Sheldon M Ross. *Stochastic Processes*. John Wiley & Sons, 1996.

Walter Rudin. *Principles of Mathematical Analysis (International Series in Pure & Applied Mathematics)*. McGraw-Hill Publishing Co., 1976.

M. Ryan. Summer Nuclear Unit Already Behind As It Gets Federal Green Light. `http://energy.aol.com/2012/04/03/summer-nuclear-unit-already-behind-as-it-gets-federal-green-ligh/`, April 2012. AOL Energy. Accessed on Jan. 7th, 2013.

P. Sainam, S. Balasubramanian, and B. Bayus. Consumer options: Theory and an empirical application to a sports market. *Journal of Marketing Research*, 47(3):401–414, 2009.

B. Sauvet-Goichon. Ashkelon desalination plant – a successful challenge. *Desalination*, 203(1-3):75 – 81, 2007. EuroMed 2006 - Conference on Desalination Strategies in South Mediterranean Countries.

Linn Sennott. *Stochastic dynamic programming and the control of queueing systems*. Wiley-Interscience, 1999.

R. Smith. Small Reactors Generate Big Hopes. `online.wsj.com`, February 18 2010. Wall Street Journal. Accessed on 2011.10.19.

James C Spall. *Introduction to stochastic search and optimization: estimation, simulation, and control*, volume 64. Wiley-Interscience, 2003.

Spectra Watermakers. Marine Products, Catalina 300 Mk II. `http://www.spectrawatermakers.com/`, 2012.

G. Stanek, D. Langer, B. Müller-Bessler, and B. Huhnke. Junior 3: A test platform for advanced driver assistance systems. In *Intelligent Vehicles Symposium (IV), 2010 IEEE*, pages 143 –149, june 2010.

Janakiram Subramanian, Shaler Stidham, and Conrad J Lautenbacher. The underlying markov decision process in the single-leg airline yield-management problem. *Transportation Science*, 33(2):136–146, 1999.

Edward Sullivan. Continuation study to evaluate the impacts of the sr 91 value-priced express lanes. Technical report, Cal Poly State University, 2000.

K. Talluri and G. J. van Ryzin. Revenue management under a general discrete choice model of consumer behavior. *Management Science*, 50(11):15–33, 2004.

The Apache Software Foundation. Apache commons math, release 3.2. Available from `http://commons.apache.org/math`, 2013.

The Economist. Thinking small. `http://www.economist.com/node/17647651`, December 2010. Accessed on 2011.10.19.

J. Tomich. Kirkwood utility is branching out with biomas. `stltoday.com`, December 10 2010. St. Louis Today. Accessed on 2011.10.21.

MA Tribe and RLW Alpine. Scale economies and the '0.6 rule'. *Engineering Costs and Production Economics*, 10(1):271–278, 1986.

H. Tsuchiya and O. Kobayashi. Mass production cost of PEM fuel cell by learning curve. *International Journal of Hydrogen Energy*, 29(10):985 – 990, 2004. Fuel Cells.

UHDENORA. UHDENORA to supply Uhde with skid-mounted chlor-alkali electrolysis modules for Leuna- Harze. `http://www.uhdenora.com/details.asp?id_news=73`, March 2011. Accessed on 2011.10.19.

U.S. Census Bureau. 2007 economic census. `http://www.census.gov/econ/census07/`, 2007. Accessed on 2012.10.12.

USGS. Mineral Commodities Summaries 2011. `http://minerals.usgs.gov/minerals/pubs/mcs/2011/mcs2011.pdf`, 2011. Accessed on 2012.03.01.

J. A. van Mieghem. *Operations Strategy: Principles and Practice*. Dynamic Ideas, Llc, 2008.

M.L. Wald. Administration to Push for Small Modular Reactors. `nytimes.com`, February 12 2011. New York Times. Accessed on 2011.10.19.

C.M. White, R.R. Steeper, and A.E. Lutz. The hydrogen-fueled internal combustion engine: a technical review. *International Journal of Hydrogen Energy*, 31(10):1292 – 1305, 2006.

M. K. Wittholz, B. K. O'Neill, C. B. Colby, and D. Lewis. Estimating the cost of desalination plants using a cost database. *Desalination*, 229(1-3):10 – 20, 2008.

World Nuclear News. Deep Sea Fission. `http://www.world-nuclear-news.org/NN_Deep_sea_fission_2001111.html`, January 2011. Accessed on 2011.10.19.

World Nuclear News. Delivery of floating plant set for 2016. `http://www.world-nuclear-news.org/NN-Delivery_of_floating_plant_set_for_2016-1212124.html`, December 2012. Accessed on 2013.1.2.

T.P Wright. Factors affecting the cost of airplanes. *Journal of the Aeronautical Sciences*, 3:122 – 128, 1936.

Shunan Xu. Development and test of dynamic congestion pricing model. Master's thesis, Massachusets Institute of Technology, 2009.

Y. Yin and Y. Lou. Dynamic tolling strategies for managed lanes. *Journal of Transportation Engineering*, 135:45–52, 2009.

D. Yurman. Competition heats up for DOE SMR funding. `http://ansnuclearcafe.org/2012/04/20/competition-heats-up-for-doe-smr-funding/`, April 2012. American Nuclear Society. Accessed on January 7th, 2013.

D. Zhang and D. Adelman. An approximate dynamic programming approach to network revenue management with customer choice. *Transportation Science*, 43(3):381–394, 2006.

Appendix A

Chapter 3 Demand Model Parameters

t	β_t	α_t^1	α_t^2	α_t^3	Std. Dev. of Residual (ε_t)
0	116.94	0.67	-0.01	-0.03	180.51
1	152.92	0.73	-0.19	0.04	159.63
2	259.67	0.73	-0.09	0.00	83.25
3	303.68	0.71	-0.20	0.06	62.11
4	379.54	1.67	-0.38	-0.12	130.38
5	288.02	2.35	-0.20	-0.44	165.62
6	792.27	1.59	-0.11	-0.23	204.16
7	1091.10	0.77	0.35	-0.05	195.74
8	1540.70	0.47	0.37	-0.06	220.13
9	1818.52	0.56	0.04	0.01	354.20
10	197.21	1.37	-0.14	-0.22	270.91
11	810.85	1.01	-0.02	-0.05	287.93
12	452.39	0.95	-0.12	0.20	315.61
13	2122.24	1.10	-0.24	-0.10	388.58
14	4729.05	1.13	-0.28	-0.49	519.94
15	6479.56	1.14	-0.25	-0.89	734.43
16	2618.14	0.87	-0.11	-0.20	644.00
17	1599.20	0.78	0.00	-0.04	538.35
18	1371.06	0.69	-0.01	0.12	513.08
19	3602.23	0.73	-0.27	0.01	528.49
20	4118.83	0.78	-0.29	-0.15	505.42
21	1082.86	1.00	-0.12	-0.11	424.01
22	212.01	1.09	0.00	-0.26	565.98
23	-280.13	0.90	-0.16	0.01	442.78

Table A.1: Hourly demand model parameters for the Eastbound direction.

	Eastbound		Westbound	
	Mean	Std. Dev.	Mean	Std. Dev.
Hour 21	5887.20	862.36	2958.30	529.14
Hour 22	4940.18	1142.69	2339.71	506.18
Hour 23	3351.17	1103.87	1633.21	356.85

Table A.2: Mean and standard deviation of traffic volume for the hours used to start the demand generation module.

	Eastbound	Westbound
Hours 21 & 22	0.78	0.93
Hours 21 & 23	0.62	0.77

Table A.3: Correlations between hours used to start the demand generation module.

t	β_t	α_t^1	α_t^2	α_t^3	Std. Dev. of Residual (ε_t)
0	692.42	0.10	0.09	0.01	180.51
1	218.53	0.69	0.11	-0.12	159.63
2	310.82	0.89	-0.13	-0.02	83.25
3	881.90	1.12	-0.44	-0.11	62.11
4	1626.93	3.23	-1.71	-1.00	130.38
5	1565.48	1.85	0.33	-1.65	165.62
6	2309.88	0.96	0.21	-1.52	204.16
7	856.04	0.63	0.21	0.05	195.74
8	1339.35	0.66	-0.11	0.23	220.13
9	2555.56	0.43	0.06	0.08	354.20
10	2736.31	0.50	-0.02	0.04	270.91
11	1855.47	0.83	-0.10	-0.07	287.93
12	1030.70	0.85	0.10	-0.14	315.61
13	30.46	0.80	0.14	0.07	388.58
14	-350.95	0.98	-0.12	0.27	519.94
15	813.96	1.07	-0.04	-0.09	734.43
16	323.55	1.03	0.04	-0.12	644.00
17	73.59	0.65	0.36	-0.03	538.35
18	-277.89	0.60	-0.03	0.33	513.08
19	282.95	0.94	-0.37	0.14	528.49
20	417.60	1.03	-0.18	-0.05	505.42
21	295.30	0.94	-0.07	-0.03	424.01
22	-216.51	0.90	0.07	-0.07	565.98
23	390.16	0.97	-0.26	-0.08	442.78

Table A.4: Hourly demand model parameters for the Westbound direction.

Min.	Hour 0	Hour 1	Hour 2	Hour 3	Hour 4	Hour 5
0	0.1003	0.1020	0.0883	0.0762	0.0553	0.0555
5	0.0982	0.0921	0.0850	0.0738	0.0568	0.0584
10	0.0964	0.0923	0.0934	0.0762	0.0612	0.0625
15	0.0939	0.0948	0.0914	0.0784	0.0706	0.0688
20	0.0907	0.0863	0.0861	0.0861	0.0769	0.0794
25	0.0838	0.0853	0.0855	0.0876	0.0847	0.0848
30	0.0810	0.0800	0.0777	0.0876	0.0916	0.0896
35	0.0769	0.0765	0.0798	0.0838	0.0978	0.0975
40	0.0753	0.0729	0.0765	0.0854	0.0984	0.1019
45	0.0711	0.0734	0.0827	0.0843	0.0967	0.0993
50	0.0693	0.0748	0.0818	0.0892	0.1021	0.0994
55	0.0630	0.0695	0.0718	0.0914	0.1077	0.1028

Min.	Hour 6	Hour 7	Hour 8	Hour 9	Hour 10	Hour 11
0	0.0614	0.0770	0.0878	0.0872	0.0824	0.0822
5	0.0629	0.0758	0.0826	0.0805	0.0768	0.0810
10	0.0672	0.0759	0.0774	0.0820	0.0831	0.0815
15	0.0724	0.0806	0.0823	0.0845	0.0804	0.0822
20	0.0790	0.0830	0.0855	0.0830	0.0817	0.0828
25	0.0859	0.0822	0.0871	0.0826	0.0830	0.0812
30	0.0886	0.0872	0.0830	0.0801	0.0838	0.0850
35	0.0924	0.0879	0.0835	0.0864	0.0844	0.0837
40	0.1001	0.0909	0.0845	0.0838	0.0847	0.0832
45	0.1000	0.0886	0.0848	0.0843	0.0872	0.0858
50	0.0959	0.0857	0.0813	0.0838	0.0864	0.0856
55	0.0941	0.0852	0.0801	0.0818	0.0861	0.0860

Table A.5: Proportion of hourly demand for each five-minute interval for the Eastbound direction.

Min.	Hour 12	Hour 13	Hour 14	Hour 15	Hour 16	Hour 17
0	0.0792	0.0776	0.0812	0.0871	0.0925	0.0878
5	0.0784	0.0775	0.0793	0.0829	0.0864	0.0902
10	0.0800	0.0788	0.0807	0.0832	0.0866	0.0851
15	0.0822	0.0821	0.0824	0.0849	0.0831	0.0858
20	0.0834	0.0831	0.0833	0.0827	0.0873	0.0842
25	0.0842	0.0829	0.0844	0.0818	0.0829	0.0818
30	0.0853	0.0816	0.0829	0.0802	0.0818	0.0841
35	0.0859	0.0822	0.0834	0.0806	0.0818	0.0820
40	0.0859	0.0881	0.0864	0.0833	0.0790	0.0806
45	0.0850	0.0891	0.0871	0.0847	0.0774	0.0827
50	0.0852	0.0891	0.0859	0.0845	0.0798	0.0785
55	0.0853	0.0877	0.0831	0.0842	0.0814	0.0773

Min.	Hour 18	Hour 19	Hour 20	Hour 21	Hour 22	Hour 23
0	0.0769	0.0840	0.0838	0.0865	0.0874	0.1019
5	0.0830	0.0810	0.0811	0.0816	0.0853	0.0975
10	0.0773	0.0869	0.0853	0.0848	0.0882	0.0943
15	0.0815	0.0853	0.0853	0.0860	0.0862	0.0908
20	0.0877	0.0870	0.0859	0.0879	0.0888	0.0908
25	0.0865	0.0873	0.0861	0.0865	0.0847	0.0860
30	0.0860	0.0844	0.0858	0.0855	0.0839	0.0821
35	0.0853	0.0826	0.0843	0.0828	0.0822	0.0780
40	0.0842	0.0816	0.0812	0.0827	0.0830	0.0741
45	0.0839	0.0802	0.0814	0.0807	0.0780	0.0698
50	0.0840	0.0810	0.0814	0.0782	0.0776	0.0680
55	0.0837	0.0787	0.0784	0.0768	0.0746	0.0666

Table A.5: Proportion of hourly demand for each five-minute interval for the Eastbound direction (continued).

Min.	Hour 0	Hour 1	Hour 2	Hour 3	Hour 4	Hour 5
0	0.0960	0.0921	0.0798	0.0637	0.0431	0.0709
5	0.0949	0.0863	0.0738	0.0627	0.0490	0.0721
10	0.0910	0.0837	0.0804	0.0685	0.0554	0.0763
15	0.0883	0.0885	0.0784	0.0728	0.0628	0.0825
20	0.0814	0.0847	0.0775	0.0751	0.0753	0.0857
25	0.0832	0.0819	0.0876	0.0834	0.0798	0.0854
30	0.0870	0.0811	0.0866	0.0886	0.0906	0.0864
35	0.0818	0.0789	0.0861	0.0968	0.1012	0.0874
40	0.0758	0.0767	0.0872	0.0950	0.1035	0.0880
45	0.0767	0.0807	0.0853	0.0960	0.1117	0.0878
50	0.0735	0.0892	0.0853	0.0971	0.1116	0.0900
55	0.0705	0.0763	0.0920	0.1003	0.1160	0.0875

Min.	Hour 6	Hour 7	Hour 8	Hour 9	Hour 10	Hour 11
0	0.0862	0.0870	0.0866	0.0837	0.0850	0.0873
5	0.0841	0.0848	0.0847	0.0839	0.0833	0.0859
10	0.0853	0.0851	0.0823	0.0832	0.0835	0.0835
15	0.0869	0.0861	0.0847	0.0841	0.0815	0.0835
20	0.0854	0.0815	0.0861	0.0834	0.0847	0.0835
25	0.0842	0.0840	0.0853	0.0851	0.0841	0.0839
30	0.0857	0.0829	0.0844	0.0838	0.0867	0.0833
35	0.0833	0.0815	0.0825	0.0843	0.0822	0.0831
40	0.0828	0.0828	0.0819	0.0833	0.0836	0.0814
45	0.0789	0.0829	0.0825	0.0841	0.0833	0.0813
50	0.0784	0.0793	0.0810	0.0818	0.0801	0.0821
55	0.0786	0.0820	0.0780	0.0794	0.0820	0.0812

Table A.6: Proportion of hourly demand for each five-minute interval for the Westbound direction.

Min.	Hour 12	Hour 13	Hour 14	Hour 15	Hour 16	Hour 17
0	0.0854	0.0846	0.0796	0.0842	0.0860	0.0843
5	0.0813	0.0814	0.0790	0.0791	0.0821	0.0850
10	0.0842	0.0826	0.0795	0.0802	0.0817	0.0863
15	0.0823	0.0832	0.0821	0.0815	0.0839	0.0874
20	0.0839	0.0838	0.0829	0.0841	0.0845	0.0880
25	0.0834	0.0829	0.0828	0.0813	0.0830	0.0865
30	0.0820	0.0816	0.0822	0.0807	0.0815	0.0855
35	0.0829	0.0823	0.0810	0.0846	0.0840	0.0832
40	0.0839	0.0847	0.0846	0.0847	0.0846	0.0821
45	0.0850	0.0853	0.0863	0.0858	0.0833	0.0783
50	0.0830	0.0838	0.0895	0.0873	0.0831	0.0765
55	0.0828	0.0836	0.0905	0.0865	0.0823	0.0768

Min.	Hour 18	Hour 19	Hour 20	Hour 21	Hour 22	Hour 23
0	0.0876	0.0914	0.0892	0.0879	0.0916	0.0964
5	0.0889	0.0896	0.0884	0.0858	0.0908	0.0974
10	0.0911	0.0888	0.0869	0.0860	0.0910	0.0930
15	0.0881	0.0879	0.0827	0.0854	0.0891	0.0903
20	0.0895	0.0867	0.0840	0.0889	0.0882	0.0866
25	0.0886	0.0855	0.0813	0.0870	0.0825	0.0838
30	0.0846	0.0812	0.0809	0.0827	0.0835	0.0812
35	0.0808	0.0799	0.0849	0.0843	0.0814	0.0780
40	0.0794	0.0814	0.0802	0.0827	0.0798	0.0761
45	0.0782	0.0769	0.0804	0.0772	0.0766	0.0712
50	0.0725	0.0759	0.0812	0.0787	0.0747	0.0738
55	0.0707	0.0748	0.0800	0.0734	0.0707	0.0722

Table A.6: Proportion of hourly demand for each five-minute interval for the Westbound direction (continued).

Appendix B

Chapter 3 Consumer Choice Models

Variable	Model 1-1	Model 1-2	Model 1-3	Model 1-4
Toll	-0.2460^{***}		-0.2253^{***}	
	(0.0011)		(0.0012)	
Toll - Hour 14		-0.4781^{***}		-0.3999^{***}
		(0.004)		(0.0067)
Toll - Hour 15		-0.2352^{***}		-0.3156^{***}
		(0.0022)		(0.0043)
Toll - Hour 16		-0.1595^{***}		-0.1611^{***}
		(0.0018)		(0.0028)
Toll - Hour 17		-0.1444^{***}		-0.1670^{***}
		(0.0018)		(0.0034)
Toll - Hour 18		-0.1770^{***}		-0.1495^{***}
		(0.0022)		(0.0040)
Toll - Hour 19		-0.3354^{***}		-0.2958^{***}
		(0.003)		(0.0048)
Toll - Hour 20		-0.4520^{***}		-0.3999^{***}
		(0.0051)		(0.0074)
Time Savings	0.0567^{***}	0.0357^{***}		
	(5e-04)	(5e-04)		
Time Savings - Hour 14			-0.1969^{***}	-0.0453^{***}
			(0.0041)	(0.0065)
Time Savings - Hour 15			0.0534^{***}	0.0922^{***}
			(0.0014)	(0.0025)
Time Savings - Hour 16			0.0588^{***}	0.0348^{***}
			(8e-04)	(0.0013)
Time Savings - Hour 17			0.0690^{***}	0.0462^{***}
			(8e-04)	(0.0014)
Time Savings - Hour 18			0.0503^{***}	0.0241^{***}
			(8e-04)	(0.0016)
Time Savings - Hour 19			-0.0092^{***}	0.0155^{***}
			(0.0014)	(0.0023)
Time Savings - Hour 20			-0.1217^{***}	-0.0201^{***}
			(0.0038)	(0.0051)
Log Likelihood	-16294.6593	-7443.8744	-9295.4047	-6943.2609

$^{***}p < 0.01$

Table B.1: Parameter estimates for models with untransformed variables.

Variable	Model 2-1	Model 2-2	Model 2-3	Model 2-4
Toll	-0.1874^{***}		-0.2488^{***}	
	(0.0016)		(0.0019)	
Toll - Hour 14		-0.4792^{***}		-0.5423^{***}
		(0.0042)		(0.0081)
Toll - Hour 15		-0.2186^{***}		-0.1438^{***}
		(0.0027)		(0.0060)
Toll - Hour 16		-0.1237^{***}		-0.1528^{***}
		(0.0021)		(0.0057)
Toll - Hour 17		-0.1000^{***}		-0.2540^{***}
		(0.0021)		(0.0074)
Toll - Hour 18		-0.1340^{***}		-0.1128^{***}
		(0.0027)		(0.0055)
Toll - Hour 19		-0.3128^{***}		-0.3009^{***}
		(0.0036)		(0.0061)
Toll - Hour 20		-0.4491^{***}		-0.3859^{***}
		(0.0052)		(0.0096)
log(Time Savings)	0.1395^{***}	0.0988^{***}		
	(0.0044)	(0.0050)		
log(Time Savings) - Hour 14			-0.5207^{***}	0.3300^{***}
			(0.0141)	(0.0260)
log(Time Savings) - Hour 15			0.1559^{***}	-0.1408^{***}
			(0.0077)	(0.0176)
log(Time Savings) - Hour 16			0.4856^{***}	0.2072^{***}
			(0.0073)	(0.0175)
log(Time Savings) - Hour 17			0.5443^{***}	0.5396^{***}
			(0.0067)	(0.0207)
log(Time Savings) - Hour 18			0.3453^{***}	0.0456^{***}
			(0.0060)	(0.0131)
log(Time Savings) - Hour 19			-0.0380^{***}	0.0779^{***}
			(0.0072)	(0.0137)
log(Time Savings) - Hour 20			-0.4543^{***}	-0.1193^{***}
			(0.0154)	(0.0270)
Log Likelihood	-22175.6920	-9437.6691	-10465.0480	-9022.4410
Num. obs.	720	720	720	720

$^{***}p < 0.01$

Table B.2: Parameter estimates for models with log. of time savings.

Variable	Model 3-1	Model 3-2	Model 3-3	Model 3-4
Toll	-0.1954^{***}		-0.1882^{***}	
	(8e-04)		(8e-04)	
Toll - Hour 14		-0.4547^{***}		-0.4153^{***}
		(0.004)		(0.0045)
Toll - Hour 15		-0.1994^{***}		-0.2700^{***}
		(0.0021)		(0.0028)
Toll - Hour 16		-0.1360^{***}		-0.1307^{***}
		(0.0016)		(0.0019)
Toll - Hour 17		-0.1136^{***}		-0.1083^{***}
		(0.0015)		(0.0020)
Toll - Hour 18		-0.1340^{***}		-0.1345^{***}
		(0.0019)		(0.0027)
Toll - Hour 19		-0.2859^{***}		-0.2887^{***}
		(0.0028)		(0.0037)
Toll - Hour 20		-0.4290^{***}		-0.4110^{***}
		(0.0050)		(0.0056)
$(\text{Time Savings})^2$	0.0016^{***}	0.0010^{***}		
	(1e-04)	(1e-05)		
$(\text{Time Savings})^2$ - Hour 14			-0.0235^{***}	-0.0029^{***}
			(6e-04)	(6e-04)
$(\text{Time Savings})^2$ - Hour 15			0.0033^{***}	0.0045^{***}
			(1e-04)	(1e-04)
$(\text{Time Savings})^2$ - Hour 16			0.0011^{***}	$6e-04^{***}$
			(2e-05)	(0.0000)
$(\text{Time Savings})^2$ - Hour 17			0.0018^{***}	$9e-04^{***}$
			(3e-05)	(0.0000)
$(\text{Time Savings})^2$ - Hour 18			0.0018^{***}	$9e-04^{***}$
			(4e-05)	(0.0000)
$(\text{Time Savings})^2$ - Hour 19			$-9e-04^{***}$	0.0012^{***}
			(1e-04)	(1e-04)
$(\text{Time Savings})^2$ - Hour 20			-0.0082^{***}	-0.0014^{***}
			(3e-04)	(3e-04)
Log Likelihood	-15642.3036	-7174.4661	-12972.6198	-6309.6336
Num. obs.	720	720	720	720

$^{***}p < 0.01$

Table B.3: Parameters estimates for models with time savings squared.

Appendix C

Chapter 3 Numerical Study Data

Hour	Certainty Eqv. (CE)	Sample Avg. Appx. (SAA)
0	$ 5.06	$ 3.35
1	$ 4.37	$ 4.81
2	$ 4.36	$ 1.88
3	$ 4.32	$ 1.80
4	$ 3.31	$ 4.23
5	$ 2.71	$ 2.42
6	$ 2.80	$ 3.25
7	$ 3.74	$ 2.82
8	$ 3.01	$ 3.21
9	$ 4.25	$ 3.57
10	$ 4.04	$ 2.56
11	$ 4.91	$ 2.57
12	$ 2.46	$ 3.09
13	$ 2.52	$ 14.68
14	$ 11.59	$ 30.58
15	$ 14.43	$ 33.19
16	$ 16.85	$ 32.57
17	$ 12.14	$ 32.22
18	$ 9.85	$ 19.95
19	$ 5.76	$ 9.35
20	$ 3.39	$ 3.68
21	$ 3.68	$ 3.64
22	$ 3.29	$ 3.40
23	$ 4.46	$ 2.74

Table C.1: Starting points for the time-of-use policy.

	α^+				α^-			
	Hour 16	Hour 17	Hour 18	Hour 19	Hour 16	Hour 17	Hour 18	Hour 19
a	0.5	0.5	0.5	1	5	2	5	10
A	100	100	100	100	100	100	100	100
α	1.5	1.8	1.5	1.5	1.8	1.5	1.5	1.5

Table C.2: Parameters of a_k used in the calibration of LinTD for the Eastbound example.

Tolling Interval	1 min.	5 min.	10 min.	15 min.	20 min.	30 min.	60 min.
Hour 16	(0.44,1.36)	(0.35,1.17)	(0.36,1.26)	(0.22,1.11)	(0.34,1.13)	(0.48,1.04)	(0.44,1.25)
Hour 17	(0.62,1.60)	(0.52,1.39)	(0.53,1.37)	(0.47,1.53)	(0.52,1.94)	(0.58,1.81)	(0.51,1.91)
Hour 18	(0.54,1.59)	(0.44,1.05)	(0.45,1.67)	(0.39,1.46)	(0.47,2.61)	(0.41,2.29)	(0.37,2.58)
Hour 19	(0.24,1.57)	(0.3,4.60)	(0.01,1.43)	(0.20,3.44)	(0.14,3.73)	(0.34,3.94)	(0.10,1.41)

Table C.3: Stochastic approximation procedure results for the (α^+, α^-) pairs for the Eastbound example.

Tolling Interval	1 min.	60 min.
Hour 5	(0.15,3.5)	(1.38,3.45)
Hour 6	(0.18,2.58)	(1.35,1.89)
Hour 7	(0.25,2.50)	(0.77,4.17)
Hour 8	(0.42,4.88)	(0.57,3.76)
Hour 9	(0.28,2.49)	(0.38,4.70)
Hour 10	(0.25,1.63)	(0.28,1.95)
Hour 11	(0.23,1.53)	(0.18,2.19)
Hour 12	(0.38,1.47)	(0.39,2.71)
Hour 13	(0.28,1.67)	(0.36,3.00)
Hour 14	(0.29,1.76)	(0.23,3.44)
Hour 15	(0.35,1.37)	(0.24,2.53)
Hour 16	(0.41,2.45)	(0.57,2.56)
Hour 17	(0.28,1.57)	(0.59,0.45)
Hour 18	(0.17,1.74)	(0.23,1.42)

Table C.4: Stochastic approximation procedure results for the (α^+, α^-) pairs for the Westbound example.

Appendix D

Statistical analysis of U.S. electricity generation

In order to test whether unit size significantly affects the operational cost of a plant we analyzed the following regression models:

$$\begin{aligned} \text{avgUnitCost} &= \beta_0 \times \text{avgGenSize}^{\beta_1} \times \text{capFactor}^{\beta_2} \times \text{adjFuelCost}^{\beta_3} \times \text{Eff}^{\beta_4} \\ &\quad \times \prod_{i=1}^{N} \text{yearDummy}_i^{\beta_i^{\text{year}}} \qquad \text{(D.1)} \\ \text{avgUnitCost} - \text{avgLaborCost} &= \gamma_0 \times \text{avgGenSize}^{\gamma_1} \times \text{capFactor}^{\gamma_2} \times \text{adjFuelCost}^{\gamma_3} \times \text{Eff}^{\gamma_4} \\ &\quad \times \prod_{i=1}^{N} \text{yearDummy}_i^{\gamma_i^{\text{year}}} \qquad \text{(D.2)} \end{aligned}$$

The definition of the variables used in the regression model above can be found in Table D.1. The first model is used to analyze the total unit operating cost of power plants, whereas the second model only looks at the non-labor portion of a plant's operating costs. These two models were tested for four different generation technologies: combined cycle, coal, gas turbines and nuclear.

The operational data on electric generating facilities was found in the annual filings to the Federal Energy Regulatory Commission (FERC) by the major utilities (FERC, 2010) for the year 2010. A data point includes information regarding employee count, capacity, age of the generator, fuel

Variable	Definition
avgUnitCost	Average cost of production for a power plant.
avgLaborCost	Average cost of labor for a power plant.
avgGenSize	Average size of the generators in the power plant.
capFactor	Fraction of the total capacity used for net generation.
adjFuelCost	Normalized fuel cost of a power plant.
Eff	The average efficiency of the power plant.
yearDummy	Dummy variables for the year the last generator was added to the power plant.

Table D.1: *Definitions of variables used in the analysis.*

cost, total production cost, net generation and heat rate. With the data sometimes being reported on a generator level and sometimes on a plant level information from the Energy Information Energy (EIA, 2011) was used to augment or verify the FERC data. Also, the FERC data only includes a head count of employees and not labor cost. In order to estimate this cost U.S. Census data on average annual payroll amount per employee and sector was used, (U.S. Census Bureau, 2007).

A data point reported on plant level, rather than single generator level, had to meet the following three criteria to be used in the analysis; a) the plant can only comprise generators of the same technology, b) the difference in age between any two generators in a plant is at most 10 years and c) the difference between the largest and the smallest generator is at most a factor two. Since we are controlling for age and generator size in the statistical analysis conditions b and c are imposed to make the averages more meaningful.

The output of the regression analysis for the first model (D.1) can be found in Table D.2. Apart from natural gas and nuclear technologies, size doesn't appear to be a significant variable. Table D.3 reports the output of the regression for the second model (D.2). It is easily seen that for all technologies other than coal, the average size of the generators was not a significant variable. In the case of coal, the value of the coefficient is positive indicating that, everything else held constant, the average costs increase as the average generator size increases. Thus, after controlling for all other factors present in our dataset, we can conclude that increasing the average generator size in a plant does not result in statistically significant operational cost savings once the labor cost is taken out of the picture.

In order to test for multicollinearity we calculated the variance inflation factors for all the

	Combined Cycle	Coal	Natural Gas (Gas Turbine)	Nuclear
(Intercept)	-4.72^{***}	-4.93^{***}	-4.46^{***}	-1.58
	(0.33)	(0.42)	(0.40)	(1.60)
log(avgGenSize)	-0.04	-0.02	-0.14^{*}	-0.33^{*}
	(0.04)	(0.03)	(0.08)	(0.16)
log(eff)	-0.56^{***}	-1.12^{***}	-0.72^{***}	0.00
	(0.17)	(0.23)	(0.10)	(0.96)
log(capFactor)	-0.15^{***}	-0.18^{***}	-0.29^{***}	-1.50^{***}
	(0.02)	(0.03)	(0.03)	(0.30)
log(adjFuelCost)	0.81^{***}	0.76^{***}	0.52^{***}	0.63^{***}
	(0.05)	(0.03)	(0.09)	(0.17)
yearDummy(1950,1960]		-0.33^{**}		
		(0.15)		
yearDummy(1960,1970]		-0.32^{**}		
		(0.15)		
yearDummy(1970,1980]		-0.37^{**}	-0.12	
		(0.15)	(0.15)	
yearDummy(1980,1990]	0.05	-0.38^{**}	0.15	0.11
	(0.13)	(0.15)	(0.20)	(0.09)
yearDummy(1990,2000]	-0.06	-0.25	-0.18	
	(0.08)	(0.16)	(0.19)	
yearDummy(2000,2010]	-0.09	-0.11	0.03	
	(0.08)	(0.18)	(0.18)	
R^2	0.90	0.91	0.80	0.65
Adj. R^2	0.89	0.90	0.79	0.58
Num. obs.	68	149	140	30

$^{***}p < 0.01$, $^{**}p < 0.05$, $^{*}p < 0.1$

Table D.2: Statistical output for the first model (D.1).

	Combined Cycle	Coal	Natural Gas (Gas Turbine)	Nuclear
(Intercept)	-4.73^{***}	-5.97^{***}	-4.84^{***}	-4.83^{*}
	(0.34)	(0.51)	(0.64)	(2.42)
log(avgGenSize)	-0.02	0.06^{*}	0.00	0.06
	(0.04)	(0.03)	(0.12)	(0.25)
log(eff)	-0.47^{**}	-1.52^{***}	-0.78^{***}	-0.22
	(0.18)	(0.27)	(0.16)	(1.45)
log(capFactor)	-0.12^{***}	-0.07^{*}	-0.22^{***}	-1.71^{***}
	(0.02)	(0.04)	(0.05)	(0.45)
log(adjFuelCost)	0.81^{***}	0.87^{***}	0.62^{***}	0.77^{***}
	(0.06)	(0.04)	(0.14)	(0.26)
yearDummy(1950,1960]		-0.34^{*}		
		(0.18)		
yearDummy(1960,1970]		-0.34^{*}		
		(0.18)		
yearDummy(1970,1980]		-0.42^{**}	-0.42^{*}	
		(0.18)	(0.24)	
yearDummy(1980,1990]	0.00	-0.46^{**}	-0.11	-0.03
	(0.14)	(0.18)	(0.32)	(0.13)
yearDummy(1990,2000]	-0.09	-0.26	-0.54^{*}	
	(0.08)	(0.19)	(0.29)	
yearDummy(2000,2010]	-0.12	-0.16	-0.41	
	(0.08)	(0.21)	(0.29)	
R^2	0.88	0.87	0.59	0.51
Adj. R^2	0.87	0.86	0.57	0.40
Num. obs.	68	149	140	30

$^{***}p < 0.01$, $^{**}p < 0.05$, $^{*}p < 0.1$

Table D.3: Statistical output for the second model (D.2).

Variable Name	Combined Cycle	Coal	Natural Gas (GT)	Nuclear
log(avgGenSize)	2.26	4.76	2.10	1.72
log(eff)	2.42	3.95	1.86	1.34
log(capFactor)	1.92	2.05	1.79	1.21
log(adjFuelCost)	1.11	1.76	1.16	1.11
yearDummy	2.03	3.31	2.60	1.72

Table D.4: Variance inflation factors.

variables. Table D.4 reports variance inflation factors for all variables in all datasets. As it can be seen from the table, multicollinearity does not appear to be a significant issue in our model.